# The Role of the Ubiquitin-Proteasome System in the Regulation of Nuclear Hormone Receptor-Dependent Transcription

Dissertation

for the award of the degree

“Doctor rerum naturalium (Dr. rer. nat.)“

Division of Mathematics and Natural Sciences

of the Georg-August-Universität Göttingen

submitted by

Tanja Prenzel

born in Königs Wusterhausen

Göttingen, 2010

Members of the Thesis Committee:

Prof. Dr. Steven A. Johnsen (Reviewer)

Molecular Oncology,

University of Göttingen Medical School, Göttingen

Prof. Dr. Holger Reichardt (Reviewer)

Cellular and Molecular Immunology,

University of Göttingen Medical School, Göttingen

Dr. Tobias Pukrop

Hematology/Oncology,

University of Göttingen Medical School, Göttingen

Date of the oral examination: 22th October 2010

# Affidavit

I hereby declare that the PhD thesis entitled “The role of the ubiquitin-proteasome system in the regulation of nuclear hormone receptor-dependent transcription” has been written independently and with no other sources and aids than quoted.

_____

Tanja Prenzel

September, 2010
Göttingen

# Table of Contents

# Abbreviations

| | |
|---|---|
| α | alpha |
| A | ampere |
| 7-AAD | 7-amino-actinomycin D |
| ACH | active chromatin hub |
| AF | transactivation function |
| AI | aromatase inhibitor |
| AP-1 | activator protein 1 |
| APS | ammonium persulfate |
| AR | androgen receptor |
| AREG | amphiregulin |
| ATP | adenosine triphosphate |
| ß | beta |
| BAC | bacterial artificial chromosome |
| BGP | ß-glycerolphosphate |
| BHQ | black hole quencher |
| Bort | Bortezomib |
| BSA | bovine serum albumin |
| °C | degree Celsius / centrigrade |
| 3C | chromosome conformation capture |
| CARM1 | coactivator-associated arginine methyltransferase 1 |
| CBP | CREB-binding protein |
| cDNA | complementary DNA |
| ChIA-PET | chromatin interaction analysis by paired-end tag sequencing |
| ChIP | chromatin immunoprecipitation |
| ChIP-Seq | ChIP followed by high-throughput sequencing |
| CIA | chloroform : isoamylalcohol (24 : 1) |
| CLIM | cofactor of LIM-homeodomain proteins |
| $CO_2$ | carbon dioxide |
| Cont | control |
| CSS | charcoal-dextran treated FBS |
| CTCF | CCCTC-binding factor |
| CTD | carboxy-terminal domain |
| CT-L | chymotrypsin-like activity |
| CXCL12 | chemokine (C-X-C motif) ligand 12 |
| CYP1B1 | cytochrome P450, family 1, subfamily B, polypeptide 1 |
| δ | delta |
| Da | Dalton (g/mol) |
| DBD | DNA binding domain |
| $ddH_2O$ | double distilled water |
| DEPC | diethylpyrocarbonate |
| DMEM | Dulbecco's modified eagle's medium |
| DMSO | dimethyl sulfoxide |
| DNA | deoxyribonucleic acid |
| dNTP | deoxyribonucleotide |
| DTT | dithiothreitol |
| DUB | deubiquitinating enzyme |

| | |
|---|---|
| ε | epsilon |
| E | glutamic acid residue |
| E2 | 17ß-Estradiol |
| E1 enzyme | ubiquitin-activating enzyme |
| E2 enzyme | ubiquitin-conjugating enzyme |
| E3 enzyme | ubiquitin-ligase |
| E6-AP | E6-associated protein |
| EDTA | ethylenediaminetetraacetic acid |
| e.g. | exempli gratia = for example |
| EGF | epidermal growth factor |
| EGFP | enhanced green fluorescent protein |
| EGFR | epidermal growth factor receptor |
| eNOS | endothelial nitric oxide synthase |
| EPAS | endothelial PAS domain protein 1 |
| ER | estrogen receptor |
| ERE | estrogen responsive element |
| *et al.* | *et alii* = and others |
| EtOH | ethanol |
| F | forward |
| FACS | fluorescence-activated cell sorting |
| FAM | fluorescein |
| FBS | fetal bovine serum |
| FC | fold-change |
| FDR | false discovery rate |
| FKBP5 | FK506 binding protein 5 |
| FRAP | fluorescence recovery after photobleaching |
| FRK | fyn-related kinase |
| γ | gamma |
| *g* | gravity (9.81 $m/s^2$) |
| GATA-1 | globin transcription factor 1 |
| GDF15 | growth differentiation factor 15 |
| GILZ | glucocorticoid-induced leucine zipper |
| GR | glucocorticoid receptor |
| GRE | glucocorticoid responsive element |
| GREB1 | growth regulation by estrogen in breast cancer 1 |
| GRIP | glutamate receptor interacting protein 1 |
| HAT | histone acetyltransferase |
| HDAC | histone deacetylases |
| HECT | homologous to E6-AP C-terminus |
| HMT | histone methyltransferase |
| HSC70 | heat shock 70kDa protein |
| hnRNA | heterogeneous nuclear RNA |
| h | hour |
| HRE | hormone responsive element |
| HRP | horseradish peroxidase |
| i.e. | id est = that is |
| IGF | insulin-like growth factor |
| IGF-1R | insulin-like growth factor 1 receptor |
| IgG | immunoglobulin G |

| | |
|---|---|
| IVT | *in vitro* transcription |
| K | lysine residue |
| kDa | kilo Dalton |
| KRT13 | keratin 13 |
| L | leucine residue or liter |
| LB | Luria broth |
| LBD | ligand binding domain |
| LCR | locus control region |
| LIPH | lipase, member H |
| m | milli ($10^{-3}$) |
| M | methionine residue or molar, mol/L |
| MAPK | mitogen-activated protein kinase |
| µ | micro ($10^{-6}$) |
| min | minute |
| mRNA | messenger RNA |
| *n* | number of individual values |
| n | nano ($10^{-9}$) |
| N-CoR | nuclear receptor corepressor |
| NEM | N-ethylmaleimide |
| NF-κB | nuclear factor of kappa B cells |
| NHR | nuclear hormone receptor |
| NP-40 | Nonidet P-40 |
| NPY1R | neuropeptide Y receptor Y1 |
| n.s. | non-significant |
| NuRD | nucleosome remodelling and deacetylating complex |
| OD | optical density |
| p | probability |
| PE | phycoerythrin |
| pH | measurement of acidity or alkalinity of a solution |
| PI | propidium iodide |
| PBS | phosphate buffered saline |
| PBS-T | phosphate buffered saline with Tween-20 |
| p/CAF | p300/CBP-associated factor |
| PCIA | Phenol : CIA (1 : 1) |
| PCR | polymerase chain reaction |
| PGPH | peptidylglutamyl peptide hydrolyzing activity |
| PGR | progesterone receptor |
| PIAS | protein inhibitor of activated signal transducer and activator of transcription |
| PKIB | protein kinase (cAMP-dependent, catalytic) inhibitor beta |
| PML | promyelocytic leukemia protein |
| PRMT1 | protein arginine methyltransferase 1 |
| P/S | penicillin/streptomycin |
| PSMB3 | proteasome subunit, beta type, 3 |
| PSMB5 | proteasome subunit, beta type, 5 |
| qPCR | quantitative real-time PCR |
| R | arginine residue or reverse |
| RAB31 | RAB31, member RAS oncogene family |
| RIN | RNA integrity number |

| | |
|---|---|
| RING | really interesting new gene |
| RLIM | RING finger LIM domain-interacting protein |
| RNA | ribonucleic acid |
| RNAPII | RNA polymerase II |
| rpm | rotations per minute |
| Rpn | regulatory particle of non- ATPase |
| Rpt | regulatory particle of triple-ATPase |
| RT | room temperature |
| RT-PCR | reverse transcription PCR |
| s | second |
| S | serine residue |
| s.d. | standard deviation |
| SDS | sodium dodecylsulfate |
| SDS-PAGE | sodium dodecylsulfate polyacrylamide gel electrophoresis |
| SEM | standard error of the mean |
| SERM | selective estrogen receptor modulator |
| SGK | serum/glucocorticoid regulated kinase |
| Shc | Src homolog and collagen homolog |
| siRNA | small inhibitory ribonucleic acid |
| SLC/CCL21 | chemokine (C-C motif) ligand 21 |
| SMRT | silencing mediator for retinoid and thyroid hormone receptors |
| snRNA | non-coding small nuclear RNA |
| SRC | steroid receptor coactivator |
| SWI/SNF | SWItch/Sucrose NonFermentable |
| Tam | Tamoxifen |
| *Taq* | *Thermus aquaticus* |
| TBP | TATA-binding protein |
| TdT | terminal deoxynucleotidyl transferase |
| TEMED | N,N,N’,N’-tetramethylethylenediamine |
| TFIIA/B | transcription factor A/B |
| TFF1 | trefoil factor 1 |
| T-L | trypsin-like activity |
| Tris | Tris(hydroxymethyl)aminomethane |
| U | unit (enzyme activity) |
| $Ub_n$ | higher molecular weight polyubiquitinated proteins |
| UPS | ubiquitin proteasome system |
| V | voltage |
| v/v | volume per volume |
| *vs.* | versus |
| WB | Western blot |
| WISP2 | WNT1 inducible signaling pathway 2 |
| WT | whole transcript |
| w/v | weight per volume |

# List of Figures

# Summary

Nuclear hormone receptors (NHRs) are ligand-dependent transcription factors which exert a broad range of functions in physiology and disease. Molecular therapies directed against the NHRs represent an ideal treatment for some human diseases. For example the estrogen receptor is the primary therapeutic target in a large portion of breast cancers.

Upon ligand binding, transcriptional regulation by the NHRs occurs in an ordered manner which involves binding to corresponding target sequences and recruitment of transcriptional cofactors. NHRs also recruit specific ubiquitin-proteasome components to the target gene during each cycle of binding. The ubiquitin-proteasome system (UPS) is the cell's primary mechanism of controlling the half-life of intracellular proteins and is the target of cancer therapy (Bortezomib). Several lines of evidence suggest that the UPS plays an integral role in steroid hormone receptor-mediated transcription regulation.

This work aimed to study the role of the UPS in the regulation of glucocorticoid receptor (GR) and more comprehensively of estrogen receptor-alpha (ERα)-mediated transcription. Proteasomal activity was inhibited either with the proteasome inhibitor Bortezomib or via transient siRNA-mediated knockdown of 20S proteasomal subunits.

Transcriptome-wide gene expression analysis revealed that the expression of the bulk of estrogen-activated genes is negatively influenced by proteasome inhibition. Subsequent time course analyses showed that the effect on the regulation of target gene expression as well as receptor recruitment is dependent on gene and time. Proteasome inhibition using Bortezomib appears to be specific since similar effects, albeit weaker, were observed following knockdown of 20S subunits. Further, inhibition of proteasomal activity decreases proliferative capacity of breast cancer cells by inducing cell cycle arrest at the G2/M transition.

Elucidating the mechanism by which the UPS influences transcription was one major goal of this study, thus the effects of proteasome inhibition on ERα mobility and its ability to induce long-range chromosomal interactions was investigated. Fluorescence recovery after photobleaching (FRAP) studies showed that Bortezomib decreases ERα nuclear mobility. Furthermore, spatial chromosomal organization analysis on two ERα target genes revealed that proteasome inhibition impairs the estrogen-induced long-range intrachromosomal interactions. The data obtained in this study demonstrate the complexity by which the UPS functions in NHR-regulated transcription and provide an important basis for the further exploration of proteasome inhibitors in the treatment of diseases such as breast cancer.

# Zusammenfassung

Nukleare Hormonrezeptoren (NHRs) sind Liganden-abhängige Transkriptionsfaktoren mit breitem physiologischem sowie pathophysiologischem Funktionsspektrum. Molekulare Therapien die sich gegen NHRs richten, stellen eine optimale Behandlung einiger humaner Krankheiten dar. Der Östrogenrezeptor ist beispielsweise das primäre, therapeutische Ziel in einem Großteil von Brustkrebsvarianten. Nach Ligandenbindung erfolgt die NHR-regulierte Transkription, welche die Bindung an korrespondierende Zielsequenzen und Rekrutierung von Transkriptionsfaktoren einschließt. Während jedem Bindungzyklus rekrutieren NHRs auch Komponenten des Ubiquitin-Proteasom-Systems an die Zielgene. Das Ubiquitin-Proteasom-System (UPS) ist das wichtigste intrazelluläre Proteinabbausystem und ist Ziel in der Krebstherapie (Bortezomib). Verschiedene Indizien sprechen für eine wesentliche Rolle des UPS in Steroidhormonrezeptor-vermittelter Transkriptionskontrolle.

Das Ziel dieser Arbeit war die Untersuchung der UPS-Funktion in Glucocorticoidrezeptor- (GR-) und im Besonderen in Östrogenrezeptor alpha- (ERα-) vermittelter Transkription. Die Proteasomaktivität wurde entweder durch den Proteasominhibitor Bortezomib oder mittels transientem siRNA-vermittelten Knockdown von 20S Proteasomuntereinheiten inhibiert.

Eine transkriptomweite Genexpressionsanalyse verdeutlichte, dass die Expression vom Großteil der Östrogen-aktivierten Gene durch Proteasominhibition negativ beeinflusst wird. Anschließende Zeitreihen-Analysen zeigten einen gen- und zeitabhängigen Effekt auf die Regulation von Gentranskription sowie Rezeptorbindung. Die Proteasominhibition mittels Bortezomib erscheint spezifisch, da ähnliche, wenn auch schwächere Effekte nach dem Knockdown von 20S Untereinheiten beobachtet wurden. Weiterhin vermindert die Inhibition der proteasomalen Aktivität die Proliferationskapazität von Brustkrebszellen durch einen induzierten Zellzyklus-Arrest im G2/M-Übergang.

Ein Hauptziel war die Aufdeckung des Mechanismus, durch welchen das UPS die Transkription beeinflusst. Daher wurden ERα-Mobilität und chromosomale Interaktionen nach Proteasominhibition untersucht. FRAP-Analysen zeigten, dass Bortezomib die nukleare ERα-Mobilität verringert. Die räumliche Organisationsanalyse zweier ERα-Zielgene deckte auf, dass durch Proteasominhibition die Östrogen-induzierten intrachromosomalen Interaktionen beeinträchtigt werden. Die Ergebnisse der Arbeit verdeutlichen die komplexe Funktion des UPS in NHR-regulierter Transkription und liefern die Grundlage für die weitere Erforschung von Proteasominhibitoren in der Krankheitstherapie, wie z.B. Brustkrebs.

# 1 Introduction

## 1.1 Nuclear receptors

The large family of nuclear receptors includes 48 members which can be classified into six evolutionary groups (Committee, 1999; Germain *et al.*, 2006). Nuclear receptors are transcription factors which can activate or repress transcription in a ligand-dependent or -independent way. Although the actions of nuclear receptors are very diverse, they all share a highly conserved structural organization. The typical nuclear receptor encloses a variable amino-terminal domain (A/B) bearing an important transactivation function 1 (AF1); a conserved DNA binding domain (C) composed of two zinc fingers; a variable hinge region (D) containing the nuclear localization signal; a conserved ligand binding domain (E) with an additional transactivation function 2 (AF2); and a variable carboxy-terminal domain (F) (Figure 1). Based on their ligand and DNA binding properties, nuclear receptors can be roughly divided into four groups. Class I receptors comprise steroid hormone receptors which upon ligand binding dimerize and bind to specific DNA sequences. The vitamin D receptor (VDR), thyroid hormone receptor (TR), retinoic acid receptor (RARα, ß, γ) and peroxisome proliferator-activated receptor (PPARα, ß, γ) belong to the class II receptors which heterodimerize with the retinoic X receptor (RxR). Class III and IV receptors are so-called orphan receptors for which the natural ligands have not been identified. Orphan receptors can bind as homodimers (class III) or as monomers (class IV) (Mangelsdorf *et al.*, 1995).

## 1.2 Nuclear hormone receptor family

The steroid hormone receptors regulate transcription of target genes by binding to specific DNA sequences, termed hormone-responsive elements (HREs) in a ligand-dependent manner. This receptor family includes the estrogen receptor (ER), glucocorticoid receptor (GR), mineralocorticoid receptor (MR), progesterone receptor (PR) and androgen receptor (AR).

Their ligands, the steroid hormones, are small lipophilic compounds derived from a common precursor, cholesterol. Steroids regulate various metabolic, reproductive, immune and neuroendocrine responses both under physiological and pathophysiological conditions. There are four main classes of steroids: androgens, corticoids (which include mineralcorticoids and glucocorticoids), estrogens and progestins.

## 1.3 Estrogen and estrogen receptor

The ovarian steroid hormone estrogen is produced in ovary, placenta and in marginal amounts also in adrenal cortex, testis, liver and adipose tissue. It exhibits a broad spectrum of physiological functions, such as establishment and maintenance of female reproduction, modulation of bone density, influence on the cardiovascular system and brain function. Estrogen is also implicated in the initiation or progression of several diseases, like breast or endometrial cancer (Henderson *et al.*, 1988), osteoporosis (Horowitz, 1993), neurodegenerative (Pike *et al.*, 2009) and cardiovascular diseases (Bakir *et al.*, 2000; Xing *et al.*, 2009).

Most of the actions of estrogen are exerted through the estrogen receptor (ER). The ER has two subtypes, ERα and ERß which are encoded by separate genes, *ESR1* on chromosome 6 and *ESR2* on chromosome 14, respectively. These two receptor isoforms display important structural (Figure 1) and functional differences which are crucial for temporal and tissue-specific actions of estrogen. As depicted in Figure 1, the amino-terminal A/B domain which contains the activation function 1 is the least conserved domain between ERα and ERß, with only 30% identity (Pearce and Jordan, 2004). It was also shown that the ERß contains a non-active AF1 (Hall and McDonnell, 1999).

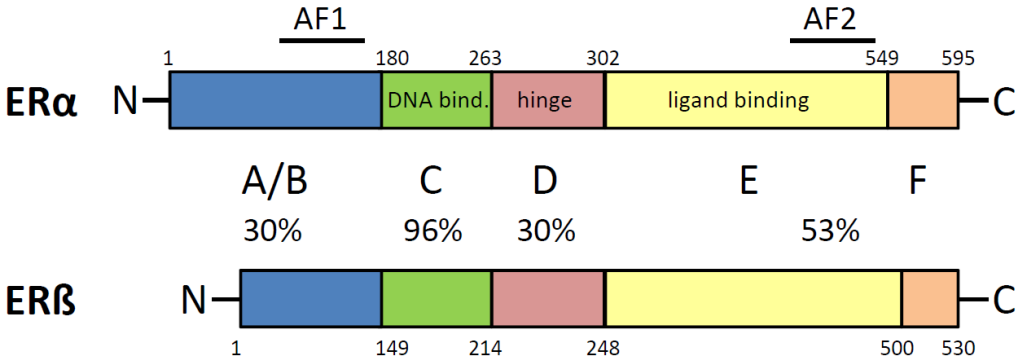


**Figure 1: Structure and homology between human ERα and ERß.** The domains A-F are depicted and the percent identity between the individual domains of ERα and ERß at the amino acid level are shown. Activation functions 1 (AF1) and 2 (AF2) are also indicated. A/B, variable N-terminal domain that modulates transcription in a gene- and cell-specific manner through AF1; C, highly conserved DNA binding domain, comprised of two zinc fingers through which the ER interacts directly with the DNA helix; D, variable hinge region containing the nuclear localization signal; E, conserved ligand binding domain that contains AF2; F, variable C-terminal domain; N, amino-terminus; C, carboxy-terminus. Adapted from (Pearce and Jordan, 2004) and modified according to (Klinge, 2000).

ERα and ERß also differ in distribution and abundance in organs and tissues. Both receptors are localized in breast, brain, cardiovascular system, bone and urogenital tract. In liver and uterus, ERα is the main subtype whereas ERß is dominant in colon and prostate. And even if both receptors are found in the same tissue, they can localize to distinct cellular subtypes. For

example within the ovary, ERα is mostly present in thecal and interstitial cells while ERß is mainly in the granulosa cells (Pearce and Jordan, 2004; Taylor and Al-Azzawi, 2000).
Differences in localization and in ligand affinities partly determine the effect of a specific ligand. For example the selective estrogen receptor modulator (SERM) Tamoxifen acts as a cell- and tissue specific agonist/antagonist for ERα but as pure antagonist for ERß (Barkhem *et al.*, 1998; Watanabe *et al.*, 1997).
Furthermore it was shown that ERα and ERß can form homo- or heterodimers when co-expressed. In the latter case the ERα seems to be the functionally dominant part (Hall and McDonnell, 1999; Li *et al.*, 2004). Since the ratio of ERα:ERß changes during osteoblast differentiation (Arts *et al.*, 1997), these cells exhibit an appropriate model to compare the transactivation capacity of ERα or ERß homodimers as well as ERα/ß heterodimers. Using a canonical ERE upstream of luciferase (ERE-TK-Luc) system it could be shown that the coexpression of ERα and ERß decreases the transcriptional capacity compared to both ERα and ERß alone in osteoblasts but not in non-osteoblastic cells (Monroe *et al.*, 2003b). Further, by generating U2OS-ERα, U2OS-ERß and U2OS-ERα/ß cell lines, genes were identified which are uniquely regulated by either ERα or ERß homodimer or by the ERα/ß heterodimer (Monroe *et al.*, 2003a; Monroe *et al.*, 2005).
Even more complexity to estrogen actions is added by the estrogen receptor-related receptors (ERR α, ß and γ) which are orphan nuclear hormone receptors. These receptors are closely related to ERα and ERß, e.g. in terms of sequence identity, there is a 68% identity in the DNA binding domain and 36% in the ligand binding domain between the ERRα and the ERα (Giguere *et al.*, 1988). Further, these orphan receptors share target genes (Lu *et al.*, 2001), EREs, and regulatory proteins with the ERα and ERß and interfere with estrogen- as well as other steroid-signaling pathways (Teyssier *et al.*, 2008).

The generation of ERα knockout (αERKO), ERß knockout (ßERKO) as well as ERα and ERß knockout (αßERKO) mice has proved useful in understanding the role and mechanisms of estrogen and of each receptor in reproduction as well as in skeletal and cardiovascular tissue. Most pronounced phenotypes were detected in the reproductive tissues and the mammary gland. The ERα loss in αERKO mice leads to infertile females because they are anovulatory, have estrogen-insensitive uteri and display little sexual behavior. Further, the mammary glands of adult αERKO females are severely underdeveloped. The αERKO male mice are also infertile, due to impairments in spermatogenesis. The ßERKO females are subfertile defined

as producing fewer litters and significant fewer pups per litter and show normal mammary gland structure. The ßERKO male fertility appears unaffected (Couse *et al.*, 2000; Curtis Hewitt *et al.*, 2000; Emmen and Korach, 2003; Hewitt and Korach, 2003). Both sexes of the αßERKO mice are infertile and unexpectedly, the ovaries of adult αßERKO females exhibit structures reminiscent of male seminiferous tubules of the testis (Couse *et al.*, 1999).

Due to the fact that the αERKO phenotype shows the greatest effects in most tissues; the ERα is widely used to decipher the molecular mechanisms of estrogen signaling; and further this receptor is already well-characterized in terms of e.g. transcriptome-wide target gene expression profiling and transcription factor recruitment, the ERα was the estrogen receptor of choice for analyzing the transcriptional effects caused by the ubiquitin-proteasome system in this study.

## 1.4 Glucocorticoid and glucocorticoid receptor

Endogenous glucocorticoids include corticosterone and cortisol, the latter being the principal hormone in humans. Glucocorticoids, synthesized from cholesterol in the adrenal cortex, exert a wide range of actions in the body. They are involved primarily in homeostasis, metabolism, stress response, regulation of the immunity and inflammation (Buckingham, 2006; Sapolsky *et al.*, 2000). But the action of glucocorticoids can also contribute to a number of diseases like osteoporosis, hypertension, insulin resistance, type II diabetes, obesity, autoimmune inflammatory disease and depression (Buckingham, 2006).

Glucocorticoids can diffuse through the cell membrane and bind to their cytoplasmic receptor. The glucocorticoid receptor (GR) exists in the cytoplasm in an inactivated form (Picard and Yamamoto, 1987) as part of a complex with heat shock proteins, including heat shock protein 90 (HSP90) and immunophilins (Galigniana *et al.*, 1998; Pratt and Toft, 1997; Sanchez *et al.*, 1985). The GR is structurally similar to other nuclear hormone receptors consisting of the N-terminal A/B domain which includes the activation function domain 1 (AF1), the DNA binding and receptor dimerization domain C, the hinge domain D and the C-terminal E region including the AF2 domain (Kumar and Thompson, 1999).

Also in case of the GR, two isoforms GRα and GRß exist (Hollenberg *et al.*, 1985) which result from alternative splicing of the same gene (Encio and Detera-Wadleigh, 1991). While GRα is the ligand-activated transcription factor, GRß is defective in hormone binding and is transcriptionally inactive. The GRß can act as dominant negative inhibitor of GRα

(Bamberger *et al.*, 1995; Oakley *et al.*, 1999). Upon interaction with glucocorticoids, the GR undergoes a conformational change, dissociates from the inactive complex and translocates to the nucleus.

## 1.5 Post-translational modifications of steroid receptors

Transcriptional activity of hormone receptors is primarily governed by ligand binding. But the activity has been shown to also be controlled and fine-tuned by a number of post-translational modifications such as phosphorylation, acetylation, ubiquitination, methylation and sumoylation. These modifications affect receptor stability, subcellular localization, dimerization and DNA and cofactor binding (Faus and Haendler, 2006) and can be mutually exclusive.

### 1.5.1 Post-translational modifications of ERα

**Phosphorylation**

The ERα can be phosphorylated in response to estrogen (Denton *et al.*, 1992) and second messengers, preferential on serine residues which reside in the N-terminal region of the receptor (Lannigan, 2003). S118 is the major residue which is phosphorylated upon estrogen activation (Joel *et al.*, 1995) or activation of mitogen activated protein kinase (MAPK) pathway (Bunone *et al.*, 1996). In addition, serine residues S104 and S106 are phosphorylated in response to estrogen and S167 can also be phosphorylated upon MAPK pathway activation. Due to the fact that the serine residues which are prone to be phosphorylated are located within the AF1 domain, their phosphorylation affects coactivator recruitment which in turn leads to increased ERα-mediated target gene transcription (Lannigan, 2003). For example, it was shown that MAPK-mediated phosphorylated S118 potentiates the association of coactivator p68 RNA helicase and ERα leading to enhanced ERα AF-1 activity (Endoh *et al.*, 1999). Also the ligand-independent activation of ERα by insulin-like growth factor (IGF) or epidermal growth factor (EGF) is mediated through the phosphorylation of ERα at S118 via the Ras-Raf-MAPK cascade (Bunone *et al.*, 1996; Kato *et al.*, 1995).

**Acetylation**

Various ERα coregulatory proteins, including p300, CBP, SRC-1, SRC-3 and p/CAF possess intrinsic histone acetyltransferase activity and upon recruitment, these cofactors modulate chromatin structure through histone acetylation. ERα is also directly acetylated by the coactivator p300 at five lysine residues (K266, K268, K299, K302 and K303) within the

ERα hinge region. Stimulation of DNA-binding and transcriptional activity of the ERα is induced by acetylation of K266 and K268 (Kim *et al.*, 2006; Wang *et al.*, 2001).

**Methylation**

During rapid estrogen signaling, the coactivator arginine methyltransferase 1 (PRMT1) (Koh *et al.*, 2001) methylates ERα in the DNA-binding domain at R260 in ligand-dependent manner. This transient methylated form of ERα is exclusively localized in the cytoplasm where this post-translational modification triggers the interaction of ERα and factors involved in cytosolic signaling pathways such as Src and PI-3 kinase (Le Romancer *et al.*, 2008). Further, the ERα is also methylated at K302 by SET7 methyltransferase which is required for efficient ERα binding to target genes but also regulates ERα turnover, probably via direct competition between methylation, acetylation and ubiquitination (Subramanian *et al.*, 2008).

**Ubiquitination**

The estrogen receptor turnover is mediated mainly through the ubiquitin-proteasome pathway (Alarid *et al.*, 1999; El Khissiin and Leclercq, 1999; Nawaz *et al.*, 1999a; Nirmala and Thampan, 1995). The ERα has a protein half-life from about 5 days (Nirmala and Thampan, 1995) but ERα stability is affected by ligand binding. Upon estrogen binding the half-life reduces to approximately 3-5 h while the selective estrogen receptor modulator Tamoxifen inhibits ubiquitination and proteasomal degradation. The pure anti-estrogen ICI 182,780 decreases ERα half-life even stronger by increasing the ubiquitin-proteasome-mediated turnover (Wijayaratne and McDonnell, 2001). The recruitment of the ubiquitin ligases E6-AP (Nawaz *et al.*, 1999b) and MDM2 as well as Rpt6/Trip1, a subunit of the 19S proteasomal regulatory particle, to ERα occupied gene promoters seems to be dependent on the phosphorylation of S118 within in the amino-terminal AF1 domain (Valley *et al.*, 2005).

**Sumoylation**

Sumoylation is the covalent attachment of the small ubiquitin-like modifier (SUMO) to lysine residues of target proteins via a pathway similar to, but distinct from the ubiquitin enzymatic cascade. Sumoylation functions in various cellular processes such as nuclear trafficking, signal transduction and transcriptional regulation (Seeler and Dejean, 2003).

The ERα hinge region can be sumoylated by the SUMO-E3 ligases PIAS1 and PIAS3 at K266 and K268. This post-translational modification is strictly ligand-dependent and seems to regulate transcriptional activity of ERα (Sentis *et al.*, 2005).

### 1.5.2 Post-translational modifications of GR

**Phosphorylation**

The GR can be phosphorylated at three major serine residues in the N-terminal A/B domain, namely S203, S211 and S226. In the absence of hormone, the GR phosphorylation is kept at a steady-state level. After ligand binding LBD-linked phosphatases dissociate which then lead to an increase in GR phosphorylation (Wang *et al.*, 2007). The phosphorylation status seems to play a role in GR turnover (Webster *et al.*, 1997), subcellular trafficking (Wang *et al.*, 2002), non-genomic signaling, transcriptional activity and GR-coactivator (GRIP1) interaction (Avenant *et al.*, 2010).

**Acetylation**

Upon hormone binding, the glucocorticoid receptor is acetylated at K494 and K495 and HDAC2-mediated deacetylation enables GR binding to the NF-κB complex (Ito *et al.*, 2006).

**Ubiquitination**

The GR is also a substrate for the ubiquitin-proteasome degradation pathway and the ligand-dependent downregulation of the receptor was shown to be proteasome-dependent (Deroo *et al.*, 2002; Wallace and Cidlowski, 2001). Upon proteasome inhibition using MG-132 the glucocorticoid-dependent GR downregulation is blocked which in turn was shown to lead to an enhanced GR transactivation (Wallace and Cidlowski, 2001), an effect which was suggested to be mediated by alterations in chromatin modification and an increase in global phosphorylated RNA polymerase II levels (Kinyamu and Archer, 2007).

**Sumoylation**

Sumoylation of GR can occur in the presence or absence of ligand and regulates receptor stability and GR-mediated transcription. Three sumoylation sites have been identified, two N-terminal residues K277, K293 and one residue, K703 in the ligand-binding domain (Le Drean *et al.*, 2002; Tian *et al.*, 2002).

## 1.6 Nuclear hormone receptors and disease

### 1.6.1 The role of estrogen receptor in breast cancer

The growth of the mammary gland and uterine endometrium is dependent on estrogen. But in addition to these physiological proliferative effects, estrogen is also a risk factor for the initiation and promotion of tumors in these tissues. It is well-established that prolonged exposure to estrogen, e.g. early menarche, late menopause and estrogen replacement therapy can be potential risk factors in breast (Kelsey *et al.*, 1993) and uterine (Rose, 1996) cancers. In contrast, factors which induce differentiation in the mammary gland, such as pregnancy and lactation are likely to reduce the risk of breast cancer (Russo *et al.*, 2005).

Breast cancer is, in accordance with various other cancer types, a complex and heterogeneous disease. An early diagnosis as well as the molecular characterization of tumors are therefore important factors for determining an individualized treatment. A broad selection of new commercialized multigene assays for the identification of prognostic and predictive molecular factors were recently developed (Ross, 2009). But so far only a small number of biomarkers are established and routinely used such as ERα, progesterone receptor (PGR) and human epidermal growth factor receptor-2 (EGFR-2/HER2) (Weigel and Dowsett, 2010). Gene expression analyses have defined five different breast cancer subtypes: 1) luminal A (ER+ and/or PGR+, HER2-), 2) luminal B (ER+ and/or PGR+, HER2+), 3) basal-like (ER-, PGR-, HER2-, cytokeratin 5/6+ and/or HER1+), 4) HER2+/ER- (ER-, PGR-, and HER2+), and 5) unclassified (negative for all markers) (Carey *et al.*, 2006).

One of the most important markers is the expression of ER. Approximately two-thirds of human breast tumors express higher concentrations of ERs than normal mammary tissue and display estrogen-dependent growth. ERα expression is associated with more differentiated tumors and a more favorable prognosis since these tumors are susceptible to anti-estrogen treatment and/or hormone reduction therapy using aromatase inhibitors which block the conversion of androgens to estrogens. In contrast, breast tumors which lack any ER expression display a more aggressive phenotype and poorer prognosis (Sorlie *et al.*, 2001).

Until recently, the ER is the primary target of breast cancer therapy. Thereby the basic principle is blocking the interaction between estrogen and the ER. Synthetic analogs of estrogen called selective estrogen receptor modulators (SERMs) such as Tamoxifen or Raloxifene are competitive inhibitors of estrogen which display agonist behavior in some

tissues while antagonizing estrogen in other tissues (Jordan, 2001; Park and Jordan, 2002). Tamoxifen is currently the most widely used therapy for hormone-dependent breast cancer. Tamoxifen counteracts the proliferative effects of estrogen in mammary tissue while it manifests estrogenic activities in the uterus (Gottardis *et al.*, 1988; Satyaswaroop *et al.*, 1984) and bone (Fisher *et al.*, 2005; Love *et al.*, 1992). The drawbacks of treating ERα-positive breast cancers with Tamoxifen are the incidence of endometrial cancers (Fisher *et al.*, 2005) and especially after long-term treatment, the development of resistance (Clarke *et al.*, 2001) which was proposed to be mediated by the epidermal growth factor receptor (EGFR)/HER2 pathway (Massarweh *et al.*, 2008).

Pure antiestrogens such as Fulvestrant (ICI 182,780) (Wakeling *et al.*, 1991) only display antagonistic effects and are therefore useful in the treatment of advanced breast cancer. Upon binding of Fulvestrant, ERα dimerization as well as nuclear localization are prevented (Dauvois *et al.*, 1993). Furthermore, cellular ERα levels are reduced (Wijayaratne *et al.*, 1999) and due to the fact that Fulvestrant blocks both AF1 and AF2 on ERα, target gene transcription is prevented.

Crystal structure analysis revealed that depending on the nature of the bound ligand: agonist (estrogen) or antagonist (e.g., Tamoxifen), the conformation of the ERα is modulated which in turn leads to the binding of opposing cofactors and subsequently different transcriptional outcomes. Estrogen and Tamoxifen bind to the same α helical pocket within the LBD, but binding modulates the orientation of helix 12 in this binding pocket. In the estrogen-bound LBD, helix 12 is positioned over the ligand-binding cavity (Brzozowski *et al.*, 1997). This proper positioning generates a functional AF2 which interacts via a hydrophobic groove (Feng *et al.*, 1998) with coactivators such as p160 factors containing the NR-box (nuclear receptor interacting box) comprised of an amphipathic α-helical LxxLL motif (where L is leucine and x is any amino acid) (Heery *et al.*, 1997). In contrast, when bound to Tamoxifen, helix 12 is displaced and, via its LLEML sequence which mimics the LxxLL coactivator motif, it binds to the coactivator binding site, thereby blocking coactivator recruitment (Shiau *et al.*, 1998). Further, Tamoxifen binding leads to an altered ERα structure which preferentially interacts with corepressors such as nuclear receptor corepressor (N-CoR) (Horlein *et al.*, 1995) and silencing mediator for retinoid and thyroid hormone receptors (SMRT) (Chen and Evans, 1995; Keeton and Brown, 2005).

The hormone reduction therapy with aromatase inhibitors (AIs, e.g. Letrozole, Anastrozole) exerts a different mechanism of antiproliferative action by targeting the P450 enzyme complex aromatase which is critical for estrogen biosynthesis (Brueggemeier *et al.*, 2005).

## 1.7 Mechanisms of NHR-mediated transcriptional regulation

Various genome-wide transcriptome analyses in a variety of cell types revealed a large number of genes whose expression alters upon steroid exposure, such as estrogen (Carroll *et al.*, 2006; Coser *et al.*, 2003; Frasor *et al.*, 2003; Fullwood *et al.*, 2009; Stender *et al.*, 2007) or glucocorticoid (Galon *et al.*, 2002; Rogatsky *et al.*, 2003; Yoshikawa *et al.*, 2009). Steroid-induced cellular changes can be induced through different mechanisms which will be explained here in more detail for ERα and briefly for GR.

### 1.7.1 "Classical", cyclic transcriptional regulation through estrogen responsive elements

In the "classical" or "genomic" pathway, estrogen exerts its effects through binding to the ligand binding domain (LBD or E in Figure 1) of nuclear ERα which in turn dimerizes, binds via the DNA binding domain (DBD or C in Figure 1) to estrogen responsive element (ERE) target gene sequences and thereby regulates target gene expression. The ERE element is an inverted repeat of two 6 bp consensus half sites with three intervening base pairs (n): 5'-AGGTCAnnnTGACCT-3' (Beato, 1989) but most estrogen-regulated genes contain imperfect EREs which are modifications of the consensus ERE (Driscoll *et al.*, 1998).

The estrogen-induced "genomic" transcriptional regulation is a highly ordered process which involves a cyclical association of the ERα on target genes promoters. Upon estrogen binding, the ERα undergoes structural rearrangements (Brzozowski *et al.*, 1997), forms stable dimers and binds to ERE sequences on target genes. As shown for different ERα target genes, e.g. *TFF1* (Metivier *et al.*, 2003; Reid *et al.*, 2003), *Cyclin D1* (Park *et al.*, 2005) and *Cathepsin D* (Shang *et al.*, 2000) the ERα associates with target gene promoters with a periodicity of 40-60 min in the presence of ligand.

In addition to binding to gene promoters, upon estrogen-induced structural rearrangements the ERα also exposes binding platforms to coordinately recruit various coregulatory proteins in a sequential manner. These cofactors include p160 factors (SRC-1, SRC-2/GRIP1 and SRC-3/AIB1); histone acetyltransferases (HATs), e.g. p300, CBP, p/CAF, SRC-1 and SRC-3; histone methyl transferases (HMTs), e.g. CARM1, PRMT1 and ATP-dependent chromatin remodeling SWI/SNF factors. In order to ensure efficient transcription, during each cycle

these cofactors are recruited sequentially into six different ERα-containing protein complexes (Metivier *et al.*, 2003). Subsequently, RNA polymerase II (RNAPII) is either recruited to target gene promoters or in the case of "preloaded" RNAPII, its phosphorylation is induced and thereby transcription elongation is promoted (Kininis *et al.*, 2009). Furthermore, it was shown that also E3 ligases like MDM2 and E6-AP as well as the 19S regulatory subunit component Rpt6 are cyclically recruited to the *TFF1* promoter and inhibiting proteasomal activity abolishes ERα transcriptional activity (Reid *et al.*, 2003). It was indicated, that at the end of each cycle ERα and transcription factors have to be removed from gene promoters in order to allow a new cycle to begin. In this model, the "clearance" is accomplished by ubiquitin ligases and histone deacetylases (HDACs), SWI/SNF factors and NuRD remodel the chromatin context (Metivier *et al.*, 2003; Metivier *et al.*, 2006). These results point to a central role of the proteasome in ERα and transcriptional complex turnover.

### 1.7.2 "Tethered", indirect transactivation through protein-protein interactions

The estrogen receptor can also regulate expression of genes which do not contain a classical ERE. In that indirect transactivation pathway, the ERα regulates transcription without interacting directly with DNA but through protein-protein interactions with other transcription factors such as activator protein-1 (AP-1) or Sp1 in a way that stabilizes the DNA binding of these transcription factors and/or recruits coactivators. At AP-1 sites the ligand-bound ERα triggers transcriptional regulation via the Jun/Fos transcription factors (Jakacka *et al.*, 2001; Kushner *et al.*, 2000). And for the transactivation of e.g. *Cathepsin D* gene, ERα interacts with Sp1 at Sp1 - ERE half-site, an imperfect palindromic ERE or at Sp1-dioxin-responsive element (DRE) core motifs (Wang *et al.*, 1998).

### 1.7.3 "Non-genomic activity" of ERα

In addition to transcriptional responses which occur over the course of hours, estrogens also induce very rapid responses within seconds or minutes through "non-genomic" mechanisms. These signaling pathways can be initiated by the interaction of estrogen-bound ERα with cytosolic or cell membrane associated regulatory proteins or by membrane-bound ERα. Although the ERα has no transmembrane domain, several studies provide evidence that a subpopulation of the receptor translocates to or close to the plasma membrane in order to conduct the non-genomic effects of estrogen. A transporter function for Shc was proposed in which Shc is phosphorylated in response to estrogen, binds to ERα and delivers the receptor to the phosphorylated insulin-like growth factor receptor IGF-1R (Song *et al.*, 2004). Also

striatin, a calveolin-binding protein (Lu *et al.*, 2004), was reported to play an anchoring role in ERα translocation to membrane caveolae (Razandi *et al.*, 2002). In addition, the palmitoylation of ERα, the attachment of fatty acids on Cys447, was shown to enhance cell membrane association (Acconcia *et al.*, 2005). A recent study revealed that the G protein-coupled receptor (GPR30) induces the expression of the truncated ERα variant ERα36 which in turn mediates non-genomic estrogen signaling (Kang *et al.*, 2010).

Non-genomic actions of estrogen include, e.g. rapid activation of the Ras/Raf/MAPK transduction pathway; increase in active form of $p21^{ras}$, tyrosine phosphorylation of Shc and p190, activation of insulin-like growth factor 1 receptor (IGF-1R) and epidermal growth factor receptor (EGFR), activation of endothelial nitric oxide synthase (eNOS) and NO secretion via the phosphatidylinositol 3-kinase (PI3K)/Akt signaling pathway (Cheskis *et al.*, 2007; Song *et al.*, 2006). Further, it was shown, that non-genotropic estrogen signaling leads to the prevention of apoptosis in murine osteoblasts and osteocytes through the activation of the Src/Shc/ERK signaling pathway (Kousteni *et al.*, 2001).

Due to the fact that the ERα itself has no intrinsic kinase domain, the receptor has to activate a kinase which in turn mediates the induction of signal transduction pathways via phosphorylation of other signaling molecules. A kinase candidate for inducing these rapid estrogen effects is the tyrosine kinase c-Src (Migliaccio *et al.*, 1996) which e.g. phosphorylates Shc and IGF-1R (Peterson *et al.*, 1996; Song *et al.*, 2006) and thereby induces successive signal transductions.

### 1.7.4 Mechanisms of GR-regulated transcription

Glucocorticoids can also exert their effects through binding to the glucocorticoid receptor which in turn binds to glucocorticoid responsive elements (GREs) on target gene promoters. There, the activated GR binds as a homodimer and can bind an imperfect palindrome DNA consensus sequence of hexameric half sites separated by a three-base spacer: 5'-GGTACAnnnTGTTCT-3', where n is any nucleotide (Beato, 1989). Upon binding of coactivators or corepressors the GR regulates target gene expression in a manner analogous to ERα with most of the same coregulators.

Like ERα, the activated GR can also activate or repress transcriptional activity indirectly by binding to other transcription factors. The interaction of GR with activator protein 1 (AP-1) (Jonat *et al.*, 1990; Schule *et al.*, 1990) or NF-κB (McKay and Cidlowski, 1998; Ray and Prefontaine, 1994; Scheinman *et al.*, 1995) leads to mutual repression. While GR dimerization

is a prerequisite for the "classical" transcription pathway, including DNA binding and induction of GR target genes, GR monomers can mediate the repression of e.g. AP-1 (Heck *et al.*, 1994; Reichardt *et al.*, 1998).

Furthermore, GR can also induce rapid non-genomic responses such as activation of eNOS through PI3K and protein kinase Akt phosphorylation which leads to vasorelaxation (Hafezi-Moghadam *et al.*, 2002). These non-genomic actions are probably exerted through G-protein-coupled membrane glucocorticoid receptors which are distinct from the intracellular receptors (Maier *et al.*, 2005).

## 1.8 Three-dimensional structural organization of genomes

### 1.8.1 Nuclear architecture

The view of the cell nucleus being a static compartment has long been discarded and at present the nucleus is considered to be a highly complex, spatially and functionally compartmentalized organelle. Chromatin is one example of non-random nuclear organization since chromosomes have preferential positions in respect to the center or periphery of the nucleus and in respect to each other (Bolzer *et al.*, 2005; Parada and Misteli, 2002). Further, the dynamic interactions of chromatin with other nuclear components give rise to a highly ordered nuclear architecture with functional and specialized non-randomly positioned domains such as the nuclear matrix, interchromatin granules, splicing speckles, Cajal and PML bodies (Nunez *et al.*, 2009), (Figure 2).

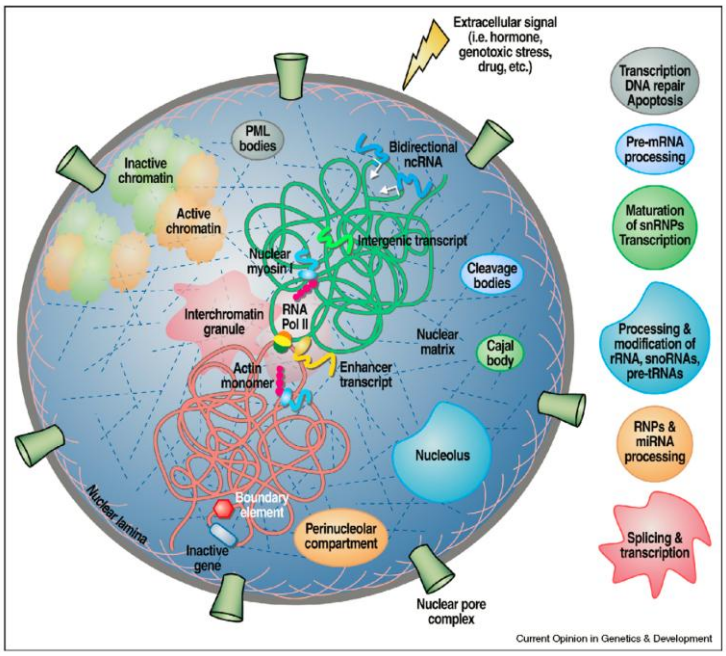


**Figure 2: Graphical presentation of the mammalian cell nucleus depicting a number of compartments and their respective functions.** In the center the formation of interchromosomal interactions between specific genes (depicted in green and red) in response to extracellular signals (e.g. hormones, genotoxic stress) is shown (Nunez *et al.*, 2009).

Altogether it is now well-established that although the genomic information is a linear series of bases, the dynamic three-dimensional interactions and subnuclear structures play important roles in highly-regulated gene expression.

Importantly, the nuclear organization is highly dynamic and the spatial and temporal genomic organization is a prerequisite for the adequate response to external stimuli. Moreover, long-range inter- (trans) (Osborne *et al.*, 2004; Spilianakis *et al.*, 2005) and intra- (cis) (Simonis *et al.*, 2006; Sun *et al.*, 2007) chromosomal interactions via chromatin folding events result in specific gene networks. These folding events are essential for high-level expression since distal enhancers and respective promoters have to communicate via long-distance interactions. The direct interaction between the remote enhancer and the gene leads to a "looping" of the intervening sequences.

The *ß-globin* locus is an intensively studied gene locus and an example of an important enhancer-gene interaction. The human *ß-globin* locus contains five genes: embryonic $\varepsilon$, fetal $^{G}\gamma$ and $^{A}\gamma$, and adult $\delta$ and *ß* arranged on the chromosome in order of their differential developmental expression; an upstream regulatory element, termed the locus control region (LCR) consisting of five DNase I hypersensitive sites (HSs); as well as two remote 5'HSs (-110/-107) and a 3'HS1 (Noordermeer and de Laat, 2008). The LCR and activated globin genes interact via DNA looping formation and thereby form a specific spatial chromatin

structure named the active chromatin hub (ACH) (Palstra *et al.*, 2003; Tolhuis *et al.*, 2002). Different erythroid activators were identified to be involved in the looping formation at the *ß-globin* locus such as GATA-1, its cofactor FOG-1 (Vakoc *et al.*, 2005) and EKLF (Drissen *et al.*, 2004). But also the nuclear protein LDB1/CLIM, a transcriptional coregulatory LIM domain-binding protein (Agulnick *et al.*, 1996), was shown to bind in a complex with GATA-1/SCL/LMO2 to the LCR and facilitate the anchoring of chromatin loops between the LCR and the active *ß-globin* gene. CLIM is a non-DNA-binding protein and therefore, its proposed functions are the formation of multiprotein complexes on the LCR and *ß-globin* genes as well as triggering the loop formation via its self-interacting domain (Song *et al.*, 2007).

### 1.8.2 ERα-bound chromatin network

In recent years several studies revealed that the majority of estrogen receptor binding sites are distal to the transcription start sites of target genes (Carroll *et al.*, 2005; Carroll *et al.*, 2006; Fullwood *et al.*, 2009; Lin *et al.*, 2007; Welboren *et al.*, 2009). These findings imply extensive chromatin looping for coordinated transcriptional regulation. Various studies have described inter- and intrachromosomal interactions between ERα target genes and their biological effects.

It could be shown for the *TFF1* (Pan *et al.*, 2008), the *GREB1* (Sun *et al.*, 2007) and the *Cathepsin D* (Bretschneider *et al.*, 2008) loci that distal ERα binding sites can function as transcriptional enhancers, communicate with the proximal ERα binding sites via long range interactions and are even critical for maximum transcriptional activity. In a recent genome-wide study, Fullwood and co-workers addressed the question which of the thousands of ERα-binding events to distal elements are functional and actually regulate gene expression. They applied a method called ChIA-PET (chromatin interaction analysis by paired-end tag sequencing) and revealed 689 ERα-bound chromatin interaction clusters which are made up of complex interactions and looping structures (Fullwood *et al.*, 2009).

Further, interchromosomal nuclear Myosin-I (NMI)-dependent interaction was shown between the two estrogen responsive genes, *TFF1* and *GREB1* in “transcriptional hubs” or “factories”. This interaction seems to be required for coordinated gene expression (Hu *et al.*, 2008).

## 1.9 Ubiquitin-proteasome system

The proteolytic degradation of cellular proteins through the ubiquitin-proteasome system is a highly complex and controlled process which plays important roles in several cellular pathways.

### 1.9.1 Ubiquitin

Ubiquitin is a small 76-amino acid protein which is a ubiquitously expressed in all eukaryotic cells and which is involved in many cellular processes. The protein contains seven lysine residues (K6, K11, K27, K29, K33, K48 and K63) and through different linkages various polyubiquitin chains can be formed. Most prominently K48 (Chau *et al.*, 1989; Finley *et al.*, 1994) but also K11 and K29-linked polyubiquitin chains target proteins for proteasomal degradation while K63-linked polyubiquitin is a signal for endocytosis (Galan and Haguenauer-Tsapis, 1997), signal transduction, DNA repair (Spence *et al.*, 1995) and ribosome function. But also monoubiquitination of proteins can play a role in histone modifications and thus in transcription (Kim *et al.*, 2005) as well as in receptor endocytosis (Shih *et al.*, 2000; Terrell *et al.*, 1998) and membrane trafficking.

Ubiquitin chains are highly dynamic as ubiquitin is removed from substrate proteins by deubiquitinating (DUB) enzymes, namely cysteine and metalloproteases (Nijman *et al.*, 2005).

### 1.9.2 Proteasome

The proteasome is a cylindrical, multicatalytic protease which is present in the cytoplasm and nucleus of eukaryotic cells. The 26S proteasome is composed of a proteolytic active 20S core particle capped on the ends by 19S regulatory complexes (Figure 3). The remarkable self-compartmentalization of the proteasome permits highly regulated protein degradation (Baumeister *et al.*, 1998).

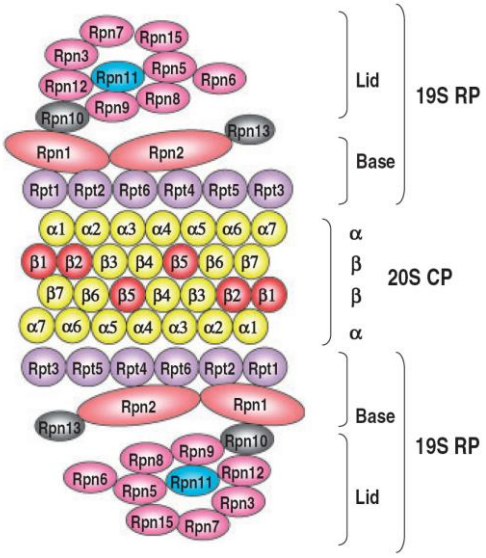


**Figure 3: Schematic drawing of the proteasome subunit structure.** 20S core particle (CP) consists of four stacked heptameric ring structures, two outer α subunits and two inner ß subunits rings. The three red marked ß-type subunits of the inner rings contain catalytically active threonine residues. 19S regulatory particles (RP) consist of base and lid subcomplexes which are composed of regulatory particle of triple-ATPase (Rpt) and regulatory particle of non-ATPase (Rpn) subunits; nomenclature in yeast (Tanaka, 2009).

### 1.9.2.1 19S regulatory particle

The 19S regulatory particles play a role in recognition of polyubiquitinated substrates, removing polyubiquitin chains, protein unfolding and translocation into the catalytic core particle. Each 19S complex is composed of approximately 20 subunits which can be grouped as follows: Regulatory particle of triple-ATPase (Rpt) and Regulatory particle of non-ATPase (Rpn) subunits. The lid subcomplex is formed by nine Rpn subunits (Rpn3, Rpn5, Rpn6, Rpn7, Rpn8, Rpn9, Rpn11, Rpn12 and Rpn15), while the base subcomplex consists of six AAA-ATPase subunits (Rpt1-Rpt6) and four non-ATPase subunits (Rpn1, Rpn2, Rpn10 and Rpn13) (Tanaka, 2009).

### 1.9.2.2 20S core particle

The 20S core proteinase complex is a stack of four heptameric rings, two outer structural α- and two inner catalytic β-rings, each comprised of seven α or β subunits, respectively. These ring-structures give rise to an enclosed cavity where substrate protein degradation takes place. This central chamber is only accessible through a narrow pore at either end (Hochstrasser, 1996; Tanaka, 2009). Proteins selected for degradation must be at least partially unfolded before they can be translocated through these pores and enter the proteolytic hollow. The three main catalytic activities, peptidylglutamyl peptide hydrolyzing (PGPH), trypsin-like (T-L) and chymotrypsin-like (CT-L) activity, are mediated by the ß-type subunits ß1, ß2 and ß5, respectively (Tanaka, 2009).

### 1.9.3 Proteasomal protein degradation

Protein degradation by the ubiquitin proteasome system is composed of two distinct phases: (1) the covalent attachment of polyubiquitin chains to the substrate protein and (2) the subsequent degradation of the tagged protein by the 26S proteasome (Figure 4).

The ubiquitination process is divided into three steps. Initially, the ubiquitin molecule is linked through an ATP-dependent formation of a thiolester bond to the cysteine residue of the ubiquitin-activating enzyme (E1). Then, the activated ubiquitin is transferred from E1 to the cysteine residue of an ubiquitin-conjugating enzyme (E2). The last step in the cascade is the ubiquitin-ligase (E3)-catalyzed covalent attachment of the ubiquitin molecule to target lysines of a substrate protein. E3 ubiquitin ligases include the two main enzyme families: Homologous to E6-Associated Protein (E6-AP) C-Terminus (HECT) E3 ligases and Really Interesting New Gene (RING) E3 ligases. In case of the HECT E3 ligases the E2-bound ubiquitin is transferred and bound via a thioester linkage to the cysteine residue of the HECT E3 prior to the transfer of ubiquitin to the substrate protein (Scheffner *et al.*, 1995). RING E3 ligases act as scaffolds that bind the ubiquitin-charged E2 and the substrate protein and thereby mediate the direct transfer of ubiquitin to the substrate (Zheng *et al.*, 2000).

In consecutive ubiquitination reactions in which additional ubiquitin molecules are attached to K48 residues of the previously conjugated molecule, a polyubiquitin chain is generated either by the same E3 ubiquitin ligase or by another "E4" enzyme that is specifically involved in polyubiqutination (Hatakeyama *et al.*, 2001; Koegl *et al.*, 1999). In order to be recognized and degraded by the proteasome, a substrate protein must be tagged with a polyubiquitin chain of at least four ubiquitin molecules (Thrower *et al.*, 2000). Polyubiquitinated substrate proteins can be directly recognized and tethered by the 19S regulatory particle subunits Rpn10 (Deveraux *et al.*, 1994), Rpn13 (Husnjak *et al.*, 2008) and most likely Rpt5 (Lam *et al.*, 2002) or ubiquitin-tagged proteins may first be bound to adaptor proteins which in turn transfer the substrate proteins to the proteasome (Elsasser *et al.*, 2004; Kim *et al.*, 2004). Adaptor proteins contain an ubiquitin-like (UBL) domain for interaction with the proteasome as well as one or two ubiquitin-associated (UBA) domains that specifically bind polyubiquitin chains (Wilkinson *et al.*, 2001). Upon binding, the polyubiquitin chain is hydrolyzed by the DUBs Rpn8 and Rpn11 (Finley, 2009; Yao and Cohen, 2002) and ubiquitin molecules are recycled. The substrate protein is unfolded and the chaperone-like activity of the 19S base subcomplex inhibits refolding (Braun *et al.*, 1999). Subsequently, the target protein is translocated into the

proteolytic active chamber where it is degraded into small polypeptides of 3-22 residues in length (Kisselev *et al.*, 1999) that are further digested to amino acids by other peptidases.

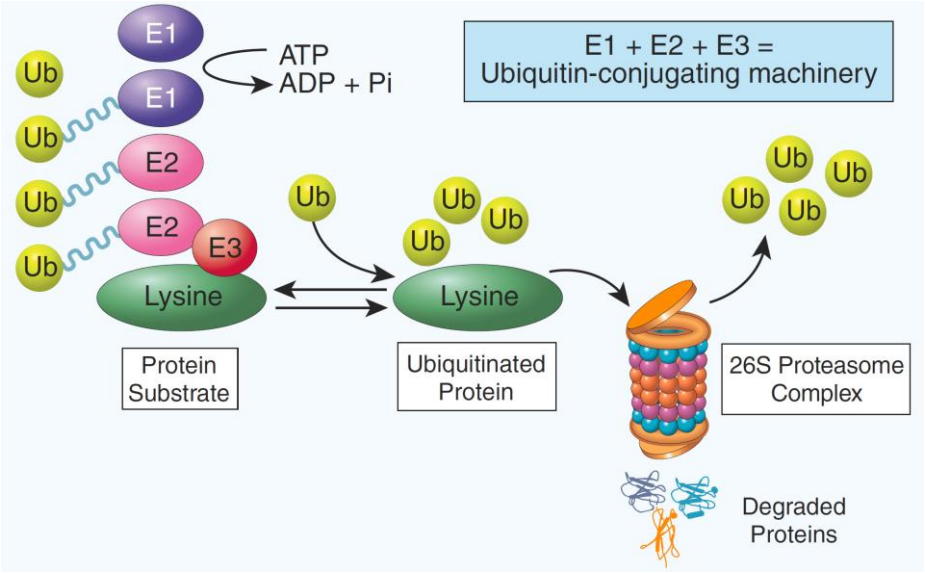


**Figure 4: Protein degradation through the ubiquitin-proteasome system.** Protein degradation is initiated by the covalent attachment of a polyubiquitin chain to specific lysine residues of the substrate protein. Ubiquitin molecules are added to target proteins by an enzyme cascade, including the ubiquitin-activating (E1), ubiquitin-conjugating (E2) and ubiquitin-ligating (E3) enzymes. Several cycles through this E1-E2-E3 cascade generate the polyubiquitin chain which acts as signal that shuttles the substrate protein to the proteasome. Before the proteolytic degradation of the target protein, ubiquitin molecules are recycled (Cardoso *et al.*, 2004).

### 1.9.4 The UPS as a potential chemotherapeutic target

The described highly ordered and controlled proteasomal degradation of cellular proteins is crucial for cell viability. The ubiquitin-proteasome pathway plays an important role in various pathways and cell responses such as degradation of short-lived and misfolded proteins, cell cycle progression, signal transduction, transcriptional regulation (Collins and Tansey, 2006), antigen presentation (Rock *et al.*, 1994) and activation of the transcription factor NF-κB (Palombella *et al.*, 1994).

Many of the UPS-controlled cellular processes, such as activation of transcription factors, cell cycle progression and apoptosis, can contribute to the growth and survival of cancer cells. The critical role of the UPS in cancer growth has led to a great interest in targeting the ubiquitin-proteasome system in cancer therapy. Potential targets of the UPS are the E1 enzyme (Yang *et al.*, 2007), specific E3 ligases such as MDM2 (Arya *et al.*, 2010; Vassilev, 2007) or the proteasome itself (Orlowski and Kuhn, 2008), the latter being the most common approach.

There are various mechanisms by which proteasome inhibitors can lower tumor growth, e.g. by cell cycle regulator stabilization, inducing p53 accumulation, induction of apoptosis and activation of bone morphogenetic protein (BMP) signaling (Wu *et al.*, 2010).

### 1.9.5 Proteasome inhibitors

There are several classes of chemical inhibitors which selectively inhibit the proteasome either reversibly or irreversibly (Moore *et al.*, 2008). Peptide aldehydes are the best characterized proteasome inhibitors. The most widely used agent is MG-132 which reversibly inhibits all three ß subunits of the 20S proteasome (Berkers *et al.*, 2005). A drawback of this class of inhibitors is the blockage of calpains and other lysosomal cathepsins in addition to the proteasome (Tsubuki *et al.*, 1996).

Furthermore, there are non-aldehyde peptide inhibitors, such as Epoxomicin, an irreversible proteasome inhibitor (Meng *et al.*, 1999) and natural products such as the *Streptomyces* metabolite Lactacystin (Fenteany *et al.*, 1995; Ostrowska *et al.*, 1997).

Lastly, there are highly selective and potent boronic acid inhibitors. One of the most prominent inhibitor of this class is Bortezomib (Velcade®, formerly known as PS-341; Millennium Pharmaceuticals, Inc., Cambridge, MA, and Johnson &Johnson Pharmaceutical Research & Development, L.L.C.). Bortezomib is the first proteasome inhibitor which has been approved by the United States Food and Drug Administration (FDA) for the treatment of relapsed/refractory multiple myeloma and mantle cell lymphoma (Bross *et al.*, 2004; Kane *et al.*, 2006; Orlowski and Kuhn, 2008). The antineoplastic agent is a dipeptidyl boronic acid which reversibly inhibits the PGPH (ß1 subunit) and the CT-L activity (ß5 subunit) of the 20S proteasome (Altun *et al.*, 2005; Berkers *et al.*, 2005; Lightcap *et al.*, 2000). Bortezomib exerts several mechanisms of action in various cell types such as preventing the degradation of cell cycle-regulatory cyclins leading to a cell cycle arrest at the G2/M transition (Ling *et al.*, 2003) or inhibition of NF-κB, (Sunwoo *et al.*, 2001) thus decreasing the expression of growth and angiogenic factors, cytokines and adhesion molecules. Further, Bortezomib induces anti-angiogenic effects by downregulating the expression of growth-signaling pathway components such as insulin-like growth factor 1 (IGF-1) and its receptor (IGF-1R) and by activating apoptosis pathways such as the c-Jun N-terminal kinase (JNK) and Fas/caspase-8-dependent pathway in multiple myeloma cells (Mitsiades *et al.*, 2002).

Although Bortezomib showed no clinical activity as a single anticancer agent in metastatic breast cancer (Yang *et al.*, 2006), the combined treatment of Bortezomib and Trastuzumab

(Herceptin), a clinical used antibody against the growth factor receptor HER2 in treating metastatic breast cancer, displayed an increased Trastuzumab efficacy *in vitro* (Cardoso *et al.*, 2006). Further, also in a mouse mammary carcinoma xenograft model Bortezomib was shown to increase the efficacy of other chemotherapeutic agents (Teicher *et al.*, 1999).

### 1.9.6 Involvement of the UPS in NHR-regulated gene transcription

The ubiquitin-proteasome system has been suggested to play an essential role in transcription and promote transcription through proteolytic and non-proteolytic functions. Proteolytic functions such as the ubiquitination and degradation of coactivator proteins as well as the ligand-dependent proteasome-mediated proteolysis of NHRs may result in the disassembly of transcription complexes after RNA polymerase II release and thereby facilitate multiple rounds of transcription. Non-proteolytic functions were shown in yeast where e.g. the monoubiquitination of histone H2B (H2Bub1) leads to the recruitment of 19S subunits (Rpt4 and 6) to the chromatin. The 19S binding was proposed to link H2Bub1 to histone H3 methylation (Ezhkova and Tansey, 2004).

But also the proteasome itself can be closely involved in transcription at various stages. There are several evidences which imply that not the whole proteasome but rather the non-proteolytic 19S sub-complex is recruited to an activated promoter in yeast (Gonzalez *et al.*, 2002). Further it was shown in yeast that independently of proteolysis the 19S particle is capable of activating RNAPII transcription elongation (Ferdous *et al.*, 2001). In addition, both proteolytic as well as non-proteolytic proteasomal actions were shown to regulate the human immunodeficiency virus type 1 (HIV-1) transcription. In the absence of the transactivator protein Tat, both 19S and 20S subunits associate with the promoter and coding regions and negatively regulate transcription. Tat switches the proteolytic to a non-proteolytic activity and only 19S subunits are recruited to the promoter-proximal region and a 19S-like complex facilitates transcriptional elongation (Lassot *et al.*, 2007).

Nuclear hormone receptors not only interact with “classical”, already stated transcription factors such as HATs, HMTs and p160 factors but also with components of the UPS. This association can directly or indirectly affect the transcriptional regulatory activity of NHRs and there is significant evidence that proteasome-mediated protein degradation plays a crucial role in transcriptional regulation.

#### 1.9.6.1 The UPS in ERα-mediated gene transcription

The ubiquitin-proteasome system is the major proteolytic pathway controlling ERα turnover (Nawaz *et al.*, 1999a) and has been implicated in the periodic binding of the ERα and coregulatory complexes to the promoters of target genes (Reid *et al.*, 2003). It was shown that both unliganded as well as ERα-bound receptors are degraded via the proteasomal pathway (Tateishi *et al.*, 2004).

The ubiquitin-proteasome system further controls ERα transcriptional activity (Fan *et al.*, 2004; Lonard *et al.*, 2000; Reid *et al.*, 2003). But interestingly, proteasome inhibitor studies revealed different roles for the UPS in ERα-regulated target gene expression. While two of these studies concluded that ubiquitin-proteasome function is required for proper ERα transcriptional activity (Lonard *et al.*, 2000; Reid *et al.*, 2003), a third study claimed a rather limited function on ERα-mediated transcriptional activity (Fan *et al.*, 2004).

It was further shown that proteasome inhibition using MG-132 leads to an immobilization of the ERα in the nucleus (Reid *et al.*, 2003; Stenoien *et al.*, 2001). In addition, after binding to EREs on target gene promoters and regulating gene transcription, the ERα also recruits and interacts with proteins possessing ubiquitin ligase activity such as E6-AP (Nawaz *et al.*, 1999b), MDM2 (Saji *et al.*, 2001) and RLIM (Johnsen *et al.*, 2009). These ubiquitin ligases were shown to coactivate ERα-mediated transcription. Also the 20S proteasome subunit low molecular mass polypeptide 2 (LMP2) was shown to be involved in the entire process of ERα-regulated transcription (Zhang *et al.*, 2006).

Due to the remarkable impact of the ubiquitin-proteasome on NHR-mediated transcriptional regulation, the estrogen-induced transcription was suggested to be a therapeutic target of proteasome inhibitors in breast cancer (Sato *et al.*, 2008).

### 1.9.6.2 The UPS in GR-mediated gene transcription

Similar to ERα, the ligand-dependent GR downregulation is dependent on the ubiquitin-proteasome system (Wallace and Cidlowski, 2001). However, in contrast to ERα, proteasome inhibition was shown to enhance GR-mediated transcriptional activity (Deroo *et al.*, 2002; Kinyamu and Archer, 2007; Wallace and Cidlowski, 2001).

Since it was shown that blocking proteasomal activity also reduced the mobility of the GR in the nucleus (Deroo *et al.*, 2002), an additional mechanism other than subnuclear trafficking of the receptor must be involved. One such proposed mechanism by which proteasome inhibition enhances GR-regulated gene transcription is the modification of chromatin structure and transcription machinery (Kinyamu and Archer, 2007).

These cited studies indicate that proteasome inhibition increases transcriptional activity of the GR but decreases ERα-regulated gene expression. The caveat of most of these studies was that they were either based on reporter gene constructs or only a very limited number of target genes (Deroo *et al.*, 2002; Kinyamu and Archer, 2007; Lonard *et al.*, 2000; Reid *et al.*, 2003; Wallace and Cidlowski, 2001).

Recently, a genome-wide transcriptional profiling study in MCF-7 breast cancer cells stably expressing the GR and endogenous ERα examined the impact of proteasome activity on these two receptors. This genomic approach revealed that proteasome inhibition influenced the ERα and GR transcriptional activity in a gene-specific rather than receptor-specific manner. Further, the results implied that proteasome activity affects NHR-mediated transcription through changes in chromatin modifying enzymes (Kinyamu *et al.*, 2008).

## 1.10 Aims of study

There are controversial reports concerning the influence of the ubiquitin-proteasome on the nuclear hormone receptor-mediated transcription regulation. The inhibition of the ubiquitin-proteasome activity has been reported by different groups to either increase (Kinyamu and Archer, 2007; Wallace and Cidlowski, 2001) or block (Lin *et al.*, 2002; Lonard *et al.*, 2000; Reid *et al.*, 2003) the NHR-mediated activation of target gene expression. The reasons for these differences begun to be resolved (Kinyamu *et al.*, 2008) but the precise mechanism by which the UPS influences NHR-regulated gene transcription remains unknown.

Therefore, one goal of this study was to elucidate the impact of proteasomal activity on the transcriptional activity of two selected NHRs, namely estrogen receptor-alpha (ERα) and glucocorticoid receptor (GR).
In order to accomplish this goal, the effects of proteasome inhibition using Bortezomib and siRNA-mediated knockdown were examined on gene expression levels for selected endogenous GR target genes and for 807 ERα target genes via DNA microarray analysis. Further, the effects of proteasome blockage were analyzed on receptor recruitment to the promoters of representative target genes. Thereby, particular attention was placed on the comparison of the effects induced by either proteasome inhibition or proteasome knockdown.

The second goal was to decipher the molecular mechanism(s) by which the ubiquitin-proteasome system influences NHR-regulated transcription. To shed light on this mechanism in ERα-positive cells, the nuclear ERα mobility as well as the chromosomal organization of two ERα target genes were analyzed in dependence of proteasomal activity via FRAP and 3C experiments, respectively.

# 2 Material

## 2.1 Technical equipment

| | |
|---|---|
| Agarose gel chamber | Harnischmacher Labortechnik, Kassel |
| Balance | Sartorius AG, Göttingen |
| Bandelin Sonoplus Sonicator | Bandelin electr. GmbH & Co. KG, Berlin |
| Biological Safety Cabinet “Hera Safe” | Thermo Fisher Scientific, Waltham, USA |
| Bioruptor | Diagenode SA, Liège, Belgium |
| Centrifuge (Megafuge 1.OR) | Thermo Fisher Scientific, Waltham, USA |
| Centrifuge 4 °C (5417R) | Eppendorf AG, Hamburg |
| C1000™ Thermal Cycler | Bio-Rad Laboratories GmbH, München |
| CFX96™ Optical Reaction Module | Bio-Rad Laboratories GmbH, München |
| Confocal microscope (TCS SP2 AOBS) | Leica Microsystems GmbH, Wetzlar |
| Counting chamber (Neubauer) | Brand GmbH & Co. KG, Wertheim |
| 5100 Cryo 1 °C Freezing Container | Thermo Fisher Scientific |
| Electrophoresis & Electrotransfer Unit | GE Healthcare Europe GmbH, München |
| Freezer -20 °C | Liebherr GmbH, Biberach |
| Freezer -80 °C “Hera freeze” | Thermo Fisher Scientific, Waltham, USA |
| Gel Imager “Gel iX imager” | Intas Science Imaging GmbH, Göttingen |
| Incubator (bacteria) | Memmert GmbH & Co. KG, Schwabach |
| Incubator (bacteria culture) | Infors AG, Bottmingen |
| Incubator (cell culture) “Hera cell 150“ | Thermo Fisher Scientific, Waltham, USA |
| Inverse Microscope “Axiovert 40 CFL” | Carl Zeiss MicroImaging GmbH, Göttingen |
| Magnet stirrer “MR3001” | Heidolph GmbH & Co. KG, Schwabach |
| Microscope “Axiovert 40 C“ | Carl Zeiss MicroImaging GmbH, Göttingen |
| Microwave | Clatronic International GmbH, Kempen |
| Nano Drop® ND-1000 Spectrophotometer | Peqlab Biotechnology GmbH, Erlangen |
| Pestle | Sartorius AG, Göttingen |
| pH meter inoLab® | WTW GmbH, Weilheim |
| Pipette Aid® portable XP | Drummond Scientific Co., Broomall, USA |
| Pipettes “Research” Series | Eppendorf AG, Hamburg |
| Power supply “Power Pack P25T” | Biometra GmbH, Göttingen |

| | |
|---|---|
| Refrigerator | Liebherr GmbH, Biberach |
| Repeat Pipette | Gilson Inc., Middleton, USA |
| Scanner (CanoScan 8600F) | Canon GmbH, Krefeld |
| Shaker “Rocky” | Schütt Labortechnik GmbH, Göttingen |
| Table centrifuge (GMC-060) | LMS Co., Ltd., Tokyo, Japan |
| Test tube rotator | Schütt Labortechnik GmbH, Göttingen |
| Ultrapure Water System “Aquintus” | membraPure GmbH, Bodenheim |
| Vacuum pump | Integra Bioscienc. AG, Zizers, Switzerland |
| Vortex mixer | Scientific Industries, Inc., Bohemia, USA |
| Water bath “TW 20” | JULABO Labortechnik GmbH, Seelbach |
| X-Ray Cassettes | Rego X-ray GmbH, Augsburg |

## 2.2 Consumable materials

| | |
|---|---|
| Cellstar 6- and 12-well cell culture plate | Greiner Bio-One GmbH, Frickenhausen |
| Cellstar PP-tube 15 and 50 ml | Greiner Bio-One GmbH, Frickenhausen |
| Cellstar tissue culture dish 100×20 mm | Greiner Bio-One GmbH, Frickenhausen |
| Cellstar tissue culture dish 145×20 mm | Greiner Bio-One GmbH, Frickenhausen |
| Cell scraper (16 cm) | Sarstedt AG & Co., Nümbrecht |
| Cryo Tube™ Vial (1.8 ml) | Thermo Fisher Scientific, Waltham, USA |
| Falcon® assay plate, 96 well | VWR Int., LLC, West Chester, USA |
| Gel blotting paper (Whatman paper) | Sartorius AG, Göttingen |
| Glass coverslips (18 mm) | Gebr. Rettberg GmbH, Göttingen |
| Hybond™-PVDF Transfer Membrane | GE Healthcare Europe GmbH, München |
| Microtube 1.5 ml | Sarstedt AG & Co., Nümbrecht |
| Microtube 1.5 ml, conical | VWR International GmbH, Darmstadt |
| Microtube 2 ml | Sarstedt AG & Co., Nümbrecht |
| 96 Multiply® PCR plate white | Sarstedt AG & Co., Nümbrecht |
| 96-well Multiplate® PCR plate white (low) | Bio-Rad Laboratories GmbH, München |
| Parafilm® “M” | Pechiney Plastic Packaging, Chicago, USA |
| Petri dish 92×16 mm | Sarstedt AG & Co., Nümbrecht |
| Pipette tips | Greiner Bio-One GmbH, Frickenhausen |
| Pipette filter tips | Sarstedt AG & Co., Nümbrecht |
| Protan® Nitrocellulose transfer membrane | Whatman GmbH, Dassel |

| | |
|---|---|
| X-ray films “Super RX” | Fujifilm Corp., Tokyo, Japan |

## 2.3 Chemicals

| | |
|---|---|
| Acetic acid | Carl Roth GmbH & Co. KG, Karlsruhe |
| Adefodur WB developing concentrate | Adefo-Chemie GmbH, Dietzenbach |
| Adefodur WB fixing concentrate | Adefo-Chemie GmbH, Dietzenbach |
| Adenosin triphosphate (ATP) | Fermentas GmbH, St. Leon-Rot |
| Agarose | Carl Roth GmbH & Co. KG, Karlsruhe |
| Albumin Fraction V (BSA) | Carl Roth GmbH & Co. KG, Karlsruhe |
| Ammonium persulfate (APS) | Carl Roth GmbH & Co. KG, Karlsruhe |
| Ammonium sulfate $(NH_4)_2SO_4$ | Carl Roth GmbH & Co. KG, Karlsruhe |
| Aprotinin | Carl Roth GmbH & Co. KG, Karlsruhe |
| Bortezomib | LC Laboratories, Woburn, USA |
| Bromophenol blue | Sigma-Aldrich Co., St. Louis, USA |
| Calcium Chloride (CaCl) | Carl Roth GmbH & Co. KG, Karlsruhe |
| Charcoal/Dextran treated FBS (CSS) | HyClone®, Logan, USA |
| Chelex | Bio-Rad Laboratories GmbH, München |
| Chloramphenicol | Serva Electrophoresis GmbH, Heidelberg |
| Chloroform | Carl Roth GmbH & Co. KG, Karlsruhe |
| Crystal violet | Sigma-Aldrich Co., St. Louis, USA |
| Dexamethasone | Sigma-Aldrich Co., St. Louis, USA |
| Diethylpyrocarbonate (DEPC) | Carl Roth GmbH & Co. KG, Karlsruhe |
| Dimethyl sulfoxide (DMSO) | AppliChem GmbH, Darmstadt |
| Dithiothreitol (DTT) | Carl Roth GmbH & Co. KG, Karlsruhe |
| DMEM | GIBCO®, Invitrogen GmbH, Darmstadt |
| dNTPs | Promega GmbH, Mannheim |
| Doxorubicin | Enzo Life Sciences GmbH, Lörrach |
| Epoxomicin | Biomol GmbH, Hamburg |
| 17ß-Estradiol | Sigma-Aldrich Co., St. Louis, USA |
| Ethanol absolute | Th. Geyer GmbH & Co. KG, Renningen |
| Ethidium bromide | Carl Roth GmbH & Co. KG, Karlsruhe |
| Ethylenediaminetetraacetic acid (EDTA) | Carl Roth GmbH & Co. KG, Karlsruhe |
| Fetal Bovine Serum (FBS) | Thermo Scientific HyClone, Logan, USA |

| | |
|---|---|
| Formaldehyde | Sigma-Aldrich Co., St. Louis, USA |
| Glycerol | Carl Roth GmbH & Co. KG, Karlsruhe |
| ß-Glycerolphosphate (BGP) | Sigma-Aldrich Co., St. Louis, USA |
| Glycine | Carl Roth GmbH & Co. KG, Karlsruhe |
| GlycoBlue | Applied Biosystems/Ambion, Austin, USA |
| Guava Nexin® reagent | Millipore GmbH, Schwalbach |
| Hydrochloric acid (HCl) | Carl Roth GmbH & Co. KG, Karlsruhe |
| *trans*-4-Hydroxytamoxifen | Sigma-Aldrich Co., St. Louis, USA |
| Isopropanol | Carl Roth GmbH & Co. KG, Karlsruhe |
| Kanamycin | AppliChem GmbH, Darmstadt |
| Leupeptin | Carl Roth GmbH & Co. KG, Karlsruhe |
| Magnesium chloride ($MgCl_2$) | Carl Roth GmbH & Co. KG, Karlsruhe |
| Methanol | M. Baker B.V., Deventer, Netherlands |
| MG-132 | Biomol GmbH, Hamburg |
| Monopotassium phosphate ($KH_2PO_4$) | Carl Roth GmbH & Co. KG, Karlsruhe |
| N-ethylmaleimide (NEM) | Sigma-Aldrich Co., St. Louis, USA |
| Nonidet™ P40 (NP-40) | Sigma-Aldrich Co., St. Louis, USA |
| Opti-MEM | GIBCO®, Invitrogen GmbH, Darmstadt |
| PBS tablets | GIBCO®, Invitrogen GmbH, Darmstadt |
| Pefabloc SC Protease Inhibitor | Carl Roth GmbH & Co. KG, Karlsruhe |
| Penicillin-Streptomycin solution | Sigma-Aldrich Co., St. Louis, USA |
| Peptone | Carl Roth GmbH & Co. KG, Karlsruhe |
| Potassium acetate (KOAc) | Carl Roth GmbH & Co. KG, Karlsruhe |
| Potassium chloride (KCl) | AppliChem GmbH, Darmstadt |
| Potassium dihydrogen phosphate ($KH_2PO_4$) | Carl Roth GmbH & Co. KG, Karlsruhe |
| Propidium iodide solution | Sigma-Aldrich Co., St. Louis, USA |
| Protein A Sepharose™ CL-4B | GE Healthcare, Uppsala, Sweden |
| RNase inhibitor | New England Biolabs, Frankfurt am Main |
| RNAiMAX | Invitrogen GmbH, Karlsruhe |
| Roti®-Phenol | Carl Roth GmbH & Co. KG, Karlsruhe |
| Rotiphorese® Gel 30 | Carl Roth GmbH & Co. KG, Karlsruhe |
| Rotipuran® Chloroform | Carl Roth GmbH & Co. KG, Karlsruhe |
| Rotipuran® Isoamylalcohol | Carl Roth GmbH & Co. KG, Karlsruhe |

| | |
|---|---|
| Salmon sperm DNA | Stratagene, La Jolla, USA |
| Sepharose™ CL-4B | GE Healthcare, Uppsala, Sweden |
| Skim milk powder | Carl Roth GmbH & Co. KG, Karlsruhe |
| Sodium acetate | Carl Roth GmbH & Co. KG, Karlsruhe |
| Sodium chloride (NaCl) | Carl Roth GmbH & Co. KG, Karlsruhe |
| Sodium deoxycholate | AppliChem GmbH, Darmstadt |
| Sodium dodecylsulfate (SDS) | Carl Roth GmbH & Co. KG, Karlsruhe |
| di-Sodium hydrogen phosphate dihydrate | Carl Roth GmbH & Co. KG, Karlsruhe |
| Sodium hydroxide (NaOH) | Carl Roth GmbH & Co. KG, Karlsruhe |
| Sodium pyruvate (Na-Pyr) | GIBCO®, Invitrogen GmbH, Darmstadt |
| SYBR Green | Roche Diagnostics GmbH, Mannheim |
| TEMED | Carl Roth GmbH & Co. KG, Karlsruhe |
| α,α-Trehalose Dihydrate | USB Corporation, Cleveland, USA |
| Tris | Carl Roth GmbH & Co. KG, Karlsruhe |
| Triton X-100 | AppliChem GmbH, Darmstadt |
| TRIzol® Reagent | Invitrogen GmbH, Karlsruhe |
| Trypsin-EDTA (0.05%) | GIBCO®, Invitrogen GmbH, Darmstadt |
| Tween-20 | AppliChem GmbH, Darmstadt |
| Yeast Extract | USB Corporation, Cleveland, USA |

## 2.4 Kits and reagents

| | |
|---|---|
| Lipofectamine™ 2000 | Invitrogen GmbH, Karlsruhe |
| Lipofectamine™ RNAiMAX | Invitrogen GmbH, Karlsruhe |
| PureYield™ Plasmid Midiprep | Promega GmbH, Mannheim |
| QIAprep® Spin Miniprep Kit | Qiagen GmbH, Hilden |
| SuperSignal® West Dura | Thermo Fisher Scientific, Waltham, USA |
| SuperSignal® West Femto Maximum | Thermo Fisher Scientific, Waltham, USA |

## 2.5 Nucleic acids

### 2.5.1 Vectors and expression constructs

| | |
|---|---|
| pEGFP-C2 | Clontech Laboratories Inc., Mountain View, USA |
| pGADT7-ERα | |

### 2.5.2 Oligonucleotides

#### 2.5.2.1 siRNA oligonucleotides

| Target Gene | siRNA Target Sequence | Source |
|---|---|---|
| Control 1 Silencer® Select | - | Ambion |
| Control 2 Silencer® Select | - | Ambion |
| PSMB3 Sil.® Sel. (s11348) | GGCUGAACCUGUAUGAGUUTT | Ambion |
| PSMB5 Sil.® Sel. (s11355) | UGAUAGAGAUCAACCCAUATT | Ambion |

#### 2.5.2.2 RT-PCR primers

Reverse transcription primers Metabion AG, Martinsried

#### 2.5.2.3 qPCR primers

Primers utilized in qPCR in 5' to 3' orientation. Primers not obtained from other previous studies were designed using a primer designing tool program (www.ncbi.nlm.nih.gov/tools/primer-blast/).

| Name | Sequence | Source |
|---|---|---|
| CXCL12 F | TGCCAGAGCCAACGTCAAGCATC | this study |
| CXCL12 R | CGGGTCAATGCACACTTGTCTGTTGT | this study |
| ERα F | GCATTCTACAGGCCAAATTCA | this study |
| ERα R | TCCTTGGCAGATTCCATAGC | this study |
| FKBP5 F | TCCCTAAAATTCCCTCGAATG | this study |
| FKBP5 R | AAGGCAGCAAGGAGAAATGAT | this study |
| FRK F | AGGGGCCCTTTGCTCTCCCC | this study |
| FRK R | TCCTCAGCAGTCCGAGCCTGG | this study |
| hnGILZ F | TGAGGGAATGGGTGAAAAAG | this study |
| hnGILZ R | TGGAAATGCCCTAAAAGGTG | this study |
| GREB1 F | GTGGTAGCCGAGTGGACAAT | (Kininis *et al.*, 2009) |
| GREB1 R | ATTTGTTTCCAGCCCTCCTT | (Kininis *et al.*, 2009) |
| h28SrRNA F | CTTTAAATGGGTAAGAAGCC | this study |
| h28SrRNA R | ATCAACCAACACCTTTTCTG | this study |
| hnTFF1 F | TTGGAGAAGGAAGCTGGATGG | (Fan *et al.*, 2004) |
| hnTFF1 R | ACCACAATTCTGTCTTTCACGG | (Fan *et al.*, 2004) |
| KRT13 F | ACGCCAAGATGATTGGTTTC | (Kininis *et al.*, 2009) |
| KRT13 R | CGACCAGAGGCATTAGAGGT | (Kininis *et al.*, 2009) |

| | | |
|---|---|---|
| PGR F | TCCACCCCGGTCGCTGTAGG | this study |
| PGR R | TAGAGCGGGCGGCTGGAAGT | this study |
| PKIB F | ACGTGGAGTCTGGGGTCGCC | this study |
| PKIB R | GAGAGCCTCCAGTTTGAGGGGCA | this study |
| PSMB3 F | AGGTCGGCAGATCAAACCTT | this study |
| PSMB3 R | GGCAATGACTGGCTCAGTGT | this study |
| PSMB5 F | GAACGGCTGTTGGCTCGGCA | this study |
| PSMB5 R | ACTGTCCACGTAGTAGAGGCCAGGG | this study |
| SGK F | AGGATGGGTCTGAACGACTTT | this study |
| SGK R | CCAAGGTTGATTTGCTGAGAA | this study |
| SLC F | TGTTACTGACACCCCAGCTTC | this study |
| SLC R | CACAGACCAGCAGAGAAGAGG | this study |
| WISP2 F | CATGCAGAACACCAATATTAAC | (Fritah *et al.*, 2005) |
| WISP2 R | TAGGCAGTGAGTTAGAGGAAAG | (Fritah *et al.*, 2005) |

#### 2.5.2.4 ChIP primers

Primers utilized in ChIP in 5’ to 3’ orientation.

| **Name** | **Sequence** | **Source** |
|---|---|---|
| CXCL12 1. ERE F | CAGCACCTGCTTCTCGCTTCCC | this study |
| CXCL12 1. ERE R | GGAGTCGGCTCAGGGCCAACAA | this study |
| CXCL12 2. ERE F | GAGTCACCCTGCCCCTCGACA | this study |
| CXCL12 2. ERE R | AGGAGCCCTGTGCTCTCTGGC | this study |
| CXCL12 3. ERE F | GGCCTCCAGCTGCCAGTCAGA | this study |
| CXCL12 3. ERE R | CCTGGACCTACACCACGGGGG | this study |
| FKBP5 GRE F | TAACCACATCAAGCGAGCTG | (So *et al.*, 2007) |
| FKBP5 GRE R | GCATGGTTTAGGGGTTCTTG | (So *et al.*, 2007) |
| GILZ GRE F | TGGGTACTGGCCTTAACTTCA | this study |
| GILZ GRE R | AATTTCCACCAGAAGGAGCA | this study |
| GREB1 1. ERE F | CCTGGGAATGGAGATTTTGATA | this study |
| GREB1 1. ERE R | GAGCTGCGAGTCCCTAACAG | this study |
| GREB1 2. ERE F | GCTGACCTTGTGGTAGGCAC | this study |
| GREB1 2. ERE R | CAGGGGCTGACAACTGAAAT | this study |
| KRT13 ERE F | GCCACAAAGGTCTGGATGAT | this study |

| | | |
|---|---|---|
| KRT13 ERE R | TCGCAAGGCTGTTAGAACACT | this study |
| PGR ERE F | GGCCAGCAGTCCTGCAACAGTC | this study |
| PGR ERE R | CCCAAGCTTGTCCGCAGCCTT | this study |
| PKIB 1. ERE F | ACCTGACCATGTCGTTCCCTTGAGTTT | this study |
| PKIB 1. ERE R | TCCCGCAGTGATCTAATCCATCTGGTAGT | this study |
| PKIB 2. ERE F | GTGGGGGCTCACCCCTACCG | this study |
| PKIB 2. ERE R | GTGGGGATGTTTGGCACCCTGC | this study |
| SGK GRE F | CCACAGAGGAATCGAGGATG | (So *et al.*, 2007) |
| SGK GRE R | GTCCGTTCCGCATGTAATTT | (So *et al.*, 2007) |
| SLC GRE F | GCATTCCCAACAGATGAGC | (Wang *et al.*, 2004) |
| SLC GRE R | GGAGGACATGTGGAACTCC | (Wang *et al.*, 2004) |
| TFF1 ERE F | TTCCGGCCATCTCTCACTAT | Sara Kangaspeska, EMBL |
| TFF ERE R | TCATCTTGGCTGAGGGATCT | Sara Kangaspeska, EMBL |
| WISP2 ERE F | TGGCTTGACCCCATCATCTA | (Johnsen *et al.*, 2009) |
| WISP2 ERE R | GGTGTGACCCAGAGCAAAAC | (Johnsen *et al.*, 2009) |

#### 2.5.2.5 3C primers

Primers utilized in 3C in 5’ to 3’ orientation.

| **Name** | **Sequence** | **Source** |
|---|---|---|
| CXCL12 1 F | GAAGGAAGAAGAAACATGGACTCTGCTCCA | this study |
| CXCL12 1-C R | CTCCCAGTGCAGAGGGAAGCATGT | this study |
| CXCL12 1-2 R | TGCCTGCTTCTCTCCCAGACCATG | this study |
| CXCL12 1-3 R | ACAGAAGCTGGTTTACCGACTTGTCTGT | this study |
| GREB1 Control F | GGGCTGGGTGCCCGTTTTGT | this study |
| GREB1 Control R | CCAGCAGCTGCACGCCACAT | this study |
| GREB1 1-C F | GCCACTACATCCTTGGCTTTGTCCAC | this study |
| GREB1 1-5 F | CTGGGCCTCTCCAGGGGGTTTT | this study |
| GREB1 R | CCGCTGGTCAGCCGTTCAGG | this study |

#### 2.5.2.6 TaqMan probes

| | |
|---|---|
| CXCL12 Template | 5’- FAM-GCCCCAGGGCACAACACACC-BHQ1-3’ |
| GREB1 Control | 5'-FAM-CCTGTGACATCTCTCCCAGCCCC-BHQ1-3' |
| GREB1 Template | 5’-FAM-GTCAGGGCAAAGGACATGGCCAG-BHQ1-3’ |

## 2.6 Proteins

### 2.6.1 Molecular weight standards

| | |
|---|---|
| Gene Ruler™ DNA-Ladder | Fermentas GmbH, St. Leon-Rot |
| PageRuler™ Prestained Protein Ladder | Fermentas GmbH, St. Leon-Rot |

### 2.6.2 Enzymes

| | |
|---|---|
| Proteinase K | Invitrogen GmbH, Karlsruhe |
| Restriction enzymes | New England Biolabs, Frankfurt am Main |
| Reverse Transcriptase (M-MuLV) | New England Biolabs, Frankfurt am Main |
| RNase A | Qiagen GmbH, Hilden |
| *Taq* DNA Polymerase | Prime Tech, Minsk, Belarus |
| T4 DNA Ligase | New England Biolabs, Frankfurt am Main |

### 2.6.3 Antibodies

#### 2.6.3.1 Primary antibodies

Antibodies used for ChIP and Western blot analyses and the respective dilutions:

| **Target Protein** | **Clone** | **Cat. No°** | **ChIP** | **WB** | **Source** |
|---|---|---|---|---|---|
| ERα | HC-20 | sc-543 | 1 µg | 1:1,000 | Santa Cruz |
| GR | E-20 | sc-1003 | 1 µg | 1:500 | Santa Cruz |
| HSC70 | B-6 | sc-7298 | - | 1:25,000 | Santa Cruz |
| IgG (non-specific) | - | ab46540 | 1 µg | - | Abcam |
| PSMB3 | MCP102 | PW8130-0100 | - | 1:1,000 | Enzo/Biomol |
| PSMB5 | - | ab3330 | - | 1:1,000 | Abcam |
| RNAPII | N-20 | sc-899 | - | 1:1000 | Santa Cruz |
| RNAPII P-Ser2 | 3E10 | - | - | 1:10 | (Chapman *et al.*, 2007) |
| RNAPII P-Ser5 | 3E8 | - | - | 1:10 | (Chapman *et al.*, 2007) |
| RNAPII P-Ser7 | 4E12 | - | - | 1:10 | (Chapman *et al.*, 2007) |
| $Ub_n$ | FK1 | PW8805-0500 | - | 1:1,000 | Biomol |
| Ubiquitin | - | Z0458 | - | 1:1,000 | Dako |

#### 2.6.3.2 Secondary antibodies

| | |
|---|---|
| anti-mouse (IgG)-HRP | Santa Cruz Biotechn., Inc., Heidelberg |
| anti-rabbit (IgG)-HRP | Santa Cruz Biotechn., Inc., Heidelberg |
| anti-rat (IgG)-HRP | Jackson ImmunoResearch Ltd., Suffolk, UK |
| goat anti-mouse (IgG + IgM)-HRP | Jackson ImmunoResearch Ltd., Suffolk, UK |

## 2.7 Cells

### 2.7.1 Bacteria cells

| | |
|---|---|
| *Escherichia coli* DH10B$^{TM}$ | Invitrogen GmbH, Karlsruhe |

#### 2.7.1.1 BAC clones

| | |
|---|---|
| CXCL12 | RP-13309I17 (pBACe3.6), Bac Pac Resources, Oakland, USA |
| GREB1 | RPCIB753E0150Q (RPCI-11) (SetNo:753), imaGenes GmbH, Berlin |

### 2.7.2 Eukaryotic cells

| **Name** | **Species** | **Organ** | **Disease** | **Source** |
|---|---|---|---|---|
| A549 | human | lung | carcinoma | DSMZ, Braunschweig |
| H1299 | human | lung | carcinoma | M. Dobbelstein, GZMB, Göttingen |
| MCF-7 | human | mammary gland | adenocarcinoma | K. Pantel, UKE, Hamburg |

## 2.8 Buffers and media

**Blocking solution**: 1× PBS-T, 5% (w/v) milk

**Bortezomib stock solution (1000×)**: 50 µM Bortezomib in 100% EtOH

**Cell culture freezing medium**: DMEM, 50% (v/v) FBS, 8% DMSO

**Chelex (10%)**: 10% (w/v) Chelex in $H_2O$

**ChIP crosslinking buffer**: 40 µl of 37% formaldehyde per 1 ml PBS

**ChIP IP buffer**: 150 mM NaCl, 5 mM EDTA, 50 mM Tris (pH 8), 0.5% (v/v) NP-40, 1% (v/v) Triton X-100

**ChIP IP$^{++++}$ buffer**: ChIP IP buffer supplemented with 1 mM Pefabloc, 1 ng/µl Aprotinin/Leupeptin, 10 mM BGP, 1 mM NEM

**Crystal violet solution**: 10% (v/v) formaldehyde, 0.1% (w/v) crystal violet

**Dexamethasone stock solution (1000×)**: 100 µM Dexamethasone in 100% EtOH

**DMEM cell culture "normal" medium**: phenol red-free, high-glucose DMEM, 10% FBS, 100 U/ml penicillin, 100 µg/ml streptomycin, 1 mM sodium pyruvate

**DMEM cell culture "stripped" medium**: phenol red-free, high-glucose DMEM, 5% CSS, 100 U/ml penicillin, 100 µg/ml streptomycin, 1 mM sodium pyruvate

**Epoxomicin stock solution (1000×)**: 1 mM Epoxomicin in DMSO

**17ß-Estradiol stock solution (100,000×)**: 1 mM 17ß-Estradiol in 100% EtOH

**Kanamycin stock solution**: 25 mg/ml Kanamycin in $H_2O$ (500× for Agar plates and 1000× for 2YT medium)

**6× Lämmli buffer**: 0.35 M Tris (pH 6.8), 30% (v/v) glycerol, 10% (w/v) SDS, 9.3% (w/v) DTT, 0.02% (w/v) bromphenol blue

**LB Agar**: LB medium, 1.5% (w/v) Agar

**LB medium**: 1% (w/v) peptone, 0.5% (w/v) yeast extract, 86 mM NaCl

**Ligation buffer (10×) for 3C**: 500 mM Tris-HCl (pH 7.5), 100 mM $MgCl_2$, 100 mM DTT

**Lysis buffer for 3C**: 10 mM Tris-HCl (pH 8), 10 mM NaCl, 0.2% NP-40

**MG-132 stock solution (1000×)**: 20 mM MG-132 in DMSO

**NEBuffer 3 (10×)**: 100 mM NaCl, 50 mM Tris-HCl, 10 mM $MgCl_2$, 1 mM DTT, adjust pH to 7.9

**P1 solution**: 50 mM Tris (pH 8), 10 mM EDTA, 100 µg/ml RNase A, filter sterilized

**P2 solution**: 0.2 N NaOH, 1% (w/v) SDS, filter sterilized

**P3 solution**: 3 M KOAc, pH 5.5, autoclaved

**PBS (1×)**: 137 mM NaCl, 2.68 mM KCl, 4.29 mM $Na_2HPO_4 \times 2H_2O$, 1.47 mM $KH_2PO_4$, pH 7.4

**PBS$^{++}$**: 1× PBS, 0.9 mM $CaCl_2$, 0.5 mM $MgCl_2$

**PBS for cell culture**: 1 PBS tablet per 500 ml $dH_2O$

**PBS-T**: PBS including 0.1% (w/v) Tween-20

**PCIA**: Phenol : Chloroform : Isoamylalcohol (25 : 24 : 1)

**qPCR buffer**: 75 mM Tris-HCl (pH 8.8), 20 mM $(NH_4)_2SO_4$, 0.01% (v/v) Tween-20, 3 mM $MgCl_2$, 200 µM dNTPs, 0.5 U/reaction *Taq* DNA Polymerase, 0.25% (v/v) Triton X-100, 1:80,000 SYBR Green I, 300 mM α,α-Trehalose, 300 nM Primers

**RIPA buffer**: 1× PBS, 1% (v/v) NP-40, 0.5% (w/v) sodium deoxychelate, 0.1% (w/v) SDS,

**SDS separating gel (12%)**: 12% (v/v) acrylamide, 375 mM Tris-HCl (pH 8.8), 0.1% (w/v) SDS, 0.1% (w/v) APS, 0.04% (v/v) TEMED

**SDS stacking gel (5%)**: 5% (v/v) acrylamide, 125.5 mM Tris-HCl (pH 6.8), 0.1% (w/v) SDS, 0.1% (w/v) APS, 0.1% (v/v) TEMED

**Sodium acetate**: 3 M sodium acetate, pH 5.2

**Stripping buffer**: 200 mM Glycine, 0.1% (w/v) SDS, 1% (v/v) Tween-20, pH 2.2

**TAE buffer (50×)**: 2 M Tris, 1 M Acetic acid, 0.1 M EDTA

**Tamoxifen stock solution (1000×)**: 1 mM Tamoxifen in 100% EtOH

**TE buffer**: 10 mM Tris-HCl, 1 mM EDTA, pH to 8.0

**Transfer buffer**: 10% (v/v) 10× Western salts, 15% (v/v) Methanol

**Tris-glycine electrophoresis buffer**: 25 mM Tris, 200 mM Glycine, 0.1% (w/v) SDS

**10× Western salts**: 1.92 M Glycine, 250 mM Tris-HCl (pH 8.3), 0.02% (w/v) SDS

**2YT medium**: 1.6% (w/v) Peptone, 1% (w/v) Yeast extract, 86 mM NaCl

## 2.9 Software

| | |
|---|---|
| Leica confocal software | Leica Microsystems GmbH, Wetzlar |
| ModFit | Verity Software House, Topsham, USA |
| Primer designing tool | NCBI/Primer-BLAST (www.ncbi.nlm.nih.gov/tools/primer-blast/) |
| SigmaPlot | Systat Software, Inc., San Jose, USA |
| Software R | Free statistical software R, version 2.9.2 (http://www.r-project.org) |

# 3 Methods

## 3.1 Cell culture

### 3.1.1 Cell culture of adherent cells

MCF-7 (human mammary epithelial adenocarcinoma), A549 (human alveolar carcinoma) and H1299 (non-small cell lung carcinoma) cells were routinely cultured in phenol red-free high-glucose Dulbecco's modified Eagle's medium (DMEM) supplemented with 10% fetal bovine serum (FBS), 100 units/ml penicillin, 100 µg/ml streptomycin and 1 mM sodium pyruvate ("normal medium") at 37 °C under 5% $CO_2$ atmosphere. One or two days prior to hormone treatment, growth medium was changed to high-glucose DMEM containing 5% charcoal-dextran treated FBS (CSS), 100 units/ml penicillin, 100 µg/ml streptomycin and 1 mM sodium pyruvate ("stripped medium").

For hormone treatment, MCF-7 cells were treated with 10 nM 17ß-Estradiol and A549 cells either with 100 nM Dexamethasone or solvent (100% EtOH). For blocking proteasome activity, cells were pre-treated for 15 min with one of the three following chemical proteasome inhibitors: 50 nM Bortezomib, 20 µM MG-132 or 1 µM Epoxomicin.

### 3.1.2 Liposome-mediated plasmid transfection

A day before transfection cells were plated in 6-well plates so that they were approximately 70-80% confluent on the day of transfection. The cells were transfected with Lipofectamine™ 2000 as recommended by the manufacturer. Briefly, cell growth medium was removed and after washing twice with PBS, 2 ml of Opti-MEM without any supplements were added. Cells were put back in the incubator. For each transfection 200 µl of Opti-MEM and 2.4 µg of total plasmid DNA were mixed in a reaction tube. In a second tube 200 µl Opti-MEM and 8 µl of Lipofectamine™ 2000 were mixed and incubated for 5 min at RT. After combining the contents of both tubes and mixing gently by inverting, the samples were incubated for another 20 min at RT. The transfection mix was then added to the respective wells containing the cells and 2 ml of Opti-MEM. After incubating the cells for 4 h at 37 °C, transfection medium was removed, the cells washed twice with PBS and hormone-deprived "stripped medium" was added. 24 h following transfection, the cells were treated with proteasome inhibitors or hormones for the indicated time periods.

### 3.1.3 Reverse-transfection with siRNA

Reverse-siRNA transfections were performed using Lipofectamine™ RNAiMAX according to the manufacturer's instructions. Briefly, 30 pmol of the respective siRNA were diluted in 500 µl of Opti-MEM medium in a well of a 6-well plate. 5 µl Lipofectamine™ RNAiMAX were added and incubated for 10-20 min at RT. In the meantime MCF-7 or A549 cells were trypsinized and diluted in "normal medium" without antibiotics (DMEM supplemented with 10% FBS and 1 mM sodium pyruvate) so that 2.5 ml contain 250,000 cells (MCF-7) or 100,000 cells (A549). 2.5 ml of the diluted cells were added to each well already containing the siRNA-Lipofectamine™ RNAiMAX complexes. After 24 h, medium was changed to hormone-deprived "stripped medium" and after another one or two days, hormone treatment was performed.

### 3.1.4 Colony formation assay

20,000 MCF-7 cells per well were seeded in a 6-well plate and cultured overnight in "normal medium". In order to analyze the effects of estrogen on the proliferation of breast cancer cells, growth medium was replaced by hormone-deprived "stripped medium" the next day. Then, cells were treated with 10 nM 17ß-Estradiol and 50 nM Bortezomib for 6 days. Subsequently, colonies were fixed with 70% methanol for 30 min on ice and then stained with 0.1% crystal violet solution overnight. Stained colonies were rinsed thoroughly with water and then scanned with CanoScan 8600F (Canon).

### 3.1.5 Measurement of DNA of single cells by flow cytometry

In order to analyze the effects of various treatments on cell cycle progression, DNA content was measured via flow cytometry. MCF-7 cells were washed twice with PBS, harvested by trypsinization and pelleted by centrifugation. After resuspending the cells in 0.5 ml of $PBS^{++}$, ice-cold ethanol was added dropwise to a final concentration of 75% ethanol. Cells were fixed overnight at 4 °C. Before staining, the cells were centrifuged, rehydrated in $PBS^{++}$ for 10 min, resuspended in $PBS^{++}$ containing 0.5 mg/ml RNAse A and incubated at 37 °C for 30 min. Cells were stained with 15 µl propidium iodide (1 mg/ml) and flow cytometry analysis was performed using the Guava EasyCyte plus FACScan. About 10,000 cells were analyzed for each sample. Distribution of cells in distinct cell cycle phases was determined and graphically displayed using ModFIT cell cycle analysis software.

### 3.1.6 Apoptosis assay

The Guava Nexin® assay (Millipore) is based on two distinct cellular alterations of the apoptotic process. Shortly after induction of apoptosis, phosphatidylserine is translocated from the inner side of the cell membrane to the outer cell surface when the cell membrane still remains intact. Annexin V-PE, an annexin group protein labeled with phycoerythrin, binds in a calcium-dependent manner to phosphatidylserine. Alteration in plasma membrane integrity can be evaluated by staining with 7-AAD which is excluded from intact cells.

Cell growth medium was collected in a 15 ml falcon tube. Cells were washed twice with PBS, trypsinized and detached. Free as well as trypsinized cells were added to the Falcon tube containing the growth medium. After centrifuging at 500×*g* for 7 min, the supernatant was discarded and cell pellets were resuspended in 500 µl of medium. Cells were counted and diluted to a concentration of $2\times 10^5$ - $1\times 10^6$ cells/ml. 100 µl of each diluted cell suspension and 100 µl of Guava Nexin solution were mixed in a well of a 96-well plate. After incubation in the dark for 20 min, the samples were analyzed using the Guava FACScan.

### 3.1.7 Fluorescence recovery after photobleaching (FRAP)

MCF-7 cells were seeded onto 18 mm glass coverslips so that they reached a confluence of 70-80% the next day when transfection with an EGFP-hERα fusion construct using Lipofectamine™ 2000 reagent was performed. 4 h after transfection, the medium was changed to hormone-deprived "stripped" medium. The actual FRAP analysis was carried out together with Dr. Chieh Hsu in the laboratory of Prof. Dr. Simons at the MPI for Experimental Medicine, Göttingen. One day before FRAP analysis, the transfected cells were transferred to the MPI and put in an incubator at 37 °C under 7% $CO_2$ atmosphere. Cells were pre-treated with 50 nM Bortezomib or vehicle for 15 min followed by a 6 h treatment with 10 nM 17ß-Estradiol and then analyzed via FRAP assay. The 8-bit time-lapse images of the cells were acquired at a frame rate of 3 frames/s at 37 °C in 500 µl of medium with a confocal microscope set-up and its software (TCS SP2 AOBS; Leica) with a 40× oil immersion objective (Type HCX PL Apo CS, NA 1.25; Leica). The pinhole was set at 81.40 µm and the zoom-factor was adjusted to obtain 62.5 × 62.5 µm images with voxel size of 244.26 × 244.26 nm. After recording 10 images, the GFP signal in a 13.2 × 2.9 µm region within a nucleus was bleached with 488 nm laser beam and 120 post-bleaching images were taken. To correct the intensity from imaging bleaching and background signal in the bleached region of the post-bleaching series, the formula

$$I_{corr}(t) = \left(I_{ori}(t) - I_{bg}\right) \times \frac{I_{ref}(t) - I_{bg}}{I_{ref}(0) - I_{bg}}$$

was used where $I_{corr}\,(t)$ represents the corrected intensity at a certain time point, $I_{ori}$ represents the original intensity, $I_{bg}$ is the average of background signal in the series and $I_{ref}$ is the GFP signal from another nucleus in the image field. Using the software, SigmaPlot (Sytstat Software), the fluorescence recovery of the bleached region was then fitted with a simple exponential function with three variables, $I_{theor}(t) = y_0 - a \times e^{\frac{-t}{b}}$, where $y_0$ is the theoretical maximum intensity and $b$ is the time constant. The significance of the data was evaluated with R (software environment for statistical computing and graphics).

## 3.2 Molecular biology

### 3.2.1 Restriction enzyme digestion

Restricition enzyme digestion was performed to cut pEGFP vector and hERα insert DNA for a cloning strategy. The restriction digestion mixture was setup as follows: 2-4 µg DNA, 3 µl 10× restriction buffer, 3 µl 10× BSA, 15 U of each restriction enzyme, filled with $H_2O$ to a total volume of 30 µl. The reaction was incubated at 37 °C for 2 h.

### 3.2.2 DNA ligation

In order to ligate the hERα insert into the pEGFP plasmid the ligation mixture was setup as follows: 50 ng restriction enzyme cut vector DNA, 58 ng restriction enzyme cut insert DNA (ratio vector : insert, approximately 1:5), 1.86 µl 10× ligase buffer, 400 U T4 DNA ligase and 1 µl 10 mM ATP. The ligation reaction was performed at 16 °C for 3 h.

### 3.2.3 Heat shock transformation and plasmid preparation

The bacteria strain *Escherichia coli* DH10B™ was used to amplify the EGFP-hERα fusion construct. The chemically competent DH10B™ cells were thawed, incubated with ligation product for 10 min on ice and then heat shocked for 2 min at 42 °C before placing them back on ice for 2 min. Cells were transferred into 1.5 ml 2YT medium and incubated for 30 min at 37 °C on the thermal shaker. After centrifuging for 30 s at 1,000×*g*, the cells were resuspended, plated on LB agar plates containing Kanamycin which selects for the resistance gene of the introduced EGFP-hERα fusion plasmid, and incubated at 37 °C overnight. The next day, 4 ml 2YT medium aliquots containing Kanamycin were inoculated and cultured for 5 h at 37 °C. After purifying the DNA using the QIAprep® Miniprep Kit, performing a check

restriction digestion and analyzing the digestion products on an agarose gel, 1 ml of one positive bacteria culture was used to inoculate 100 ml of 2YT medium supplemented with Kanamycin. The culture was incubated with shaking at 37 °C overnight. On the next day, DNA was purified using the Pure Yield™ Plasmid Midiprep System according to the manufacturer's instructions.

### 3.2.4 Reverse-transcription-PCR

RNA was isolated from cells with the TRIzol® reagent according to the manufacturer's instructions. Briefly, cells were scraped in TRIzol® reagent and RNA was extracted by a double chloroform extraction and isopropanol precipitation. Afterwards, the pellet was washed twice with 70% EtOH and resuspended in DEPC-treated water. For reverse-transcription, 1 µg of total RNA was mixed with 2 µl 15 µM random nonamer primers, 4 µl 2.5 mM dNTPs and brought to a volume of 16 µl in RNAse-free water. Samples were incubated at 70 °C for 5 min and then placed on ice. A total volume of 4 µl containing 2 µl 10× reaction buffer, 0.25 µl (10 U) RNAse inhibitor and 0.125 µl (25 U) M-MuLV reverse transcriptase was added to each sample. Reverse transcription was performed at 42 °C for 1 h and samples were heated at 95 °C for 5 min to inactivate the enzyme. Finally, samples were diluted with water to a final volume of 50 µl.

### 3.2.5 Chromatin immunoprecipitation

ChIP analyses were performed as described in (Nelson *et al.*, 2006). Shortly, after removing the medium, DNA and its binding complexes were crosslinked with 1.42% formaldehyde in PBS and incubated for 15 min at room temperature. The fixation was quenched with glycine (final concentration of 156 mM) for 5 min. Fixed cells were washed twice with ice-cold PBS and then scraped in IP buffer, supplemented with protease inhibitors. After washing the nuclear pellet once with IP buffer, it was resuspended in 300 µl of IP buffer. The samples were sonicated using a Bioruptor with high power setting for 3× 10 min each with alternating pulses and pauses for 10 s each. After centrifuging the sheared chromatin at full speed, the supernatant was pre-cleared with 100 µl Sepharose 4B 50% slurry in IP buffer (plus supplements), rotating for 1 h at 4 °C. After a second centrifugation step, the pre-cleared chromatin was diluted with IP buffer (plus supplements), aliquoted in appropriate volumes, shock frozen in liquid nitrogen and stored at -80 °C.

For ChIP analysis, 50 µl of chromatin (corresponding to approximately 75,000 cells) was diluted to a final volume of 500 µl in IP buffer supplemented with protease inhibitors.

Indicated amounts of antibody (see antibody table) were added and incubated rotating overnight at 4 °C. Chromatin complexes were captured by adding 30 µl of a Protein-A Sepharose slurry and incubated for additional 2 h rotating at 4 °C. Samples were centrifuged at 2,000×*g* for 2 min at 4 °C and washed six times with IP buffer. The immunoprecipitated chromatin complexes were reverse crosslinked by adding 100 µl of 10% (w/v) Chelex slurry and heating at 95 °C for 10 min. In order to eliminate all DNA-bound proteins, 2 µl Proteinase K (20 µg/µl) was added to each sample and incubated at 55 °C with shaking at 1,000 rpm for 30 min. The enzyme was inactivated by heating to 95 °C for 10 min. Finally, samples were centrifuged at 12,000×*g* for 1 min at 4 °C and supernatants transferred to a new tube.

Experimental background was determined by performing a ChIP assay with non-specific IgG antibody. In order to normalize the ChIP samples, inputs were prepared. To 50 µl of chromatin, 1 µl of GlycoBlue (15 µg/µl) was added, precipitated by adding 100 µl of 100% EtOH and incubated overnight at -20 °C. The input samples were centrifuged at 12,000×*g* at 4 °C and washed twice with 70% EtOH. Afterwards the DNA was prepared by the Chelex method as described above.

### 3.2.6 Quantitative real-time PCR

One µl of each ChIP or cDNA sample was used for subsequent quantitative real-time PCR analysis with a final reaction volume of 25 µl. A PCR reaction was setup as follows: 75 mM Tris-HCl (pH 8.8), 20 mM $(NH_4)_2SO_4$, 0.01% Tween-20, 3 mM $MgCl_2$, 200 µM dNTPs, 0.5 U/reaction Taq DNA Polymerase, 0.25% Triton X-100, 1:80,000 SYBR Green I, 300 mM Trehalose and 30 nM primers.

A two-step PCR protocol was used for each primer pair:

| | | |
|---|---|---|
| 95 °C | 2 min | |
| 95 °C | 15 s | 40 cycles |
| 60 °C | 1 min | |

The PCR reaction was followed by a melting curve analysis from 60 °C to 95 °C with read every 0.5 °C.

ChIP and ChIP input samples were quantified using a standard curve made from ChIP input DNA. ChIP samples were normalized to their corresponding input samples and expressed as "percent input".

Also cDNA samples were quantified using a standard curve made from all cDNA samples. Prior to statistical analysis all qRT-PCR samples were normalized to 28S ribosomal RNA as an internal reference gene. The expression levels were determined relative to the vehicle treated control sample and expressed as "relative mRNA expression".

### 3.2.7 Microarray analyses

The Affymetrix DNA microarray analysis was performed at the Transcriptome Analysis Laboratory (TAL), University of Göttingen. The GeneChip® whole transcript labeling was carried out together with Susanne Luthin and Dr. Gabriela Salinas-Riester and Lennart Opitz performed the initial analyses of the microarray data. The bioinformatic analysis data was performed by Prof. Dr. Tim Beißarth and Frank Kramer in the Department of Medical Statistics, at the University of Göttingen.

The GeneChip® whole transcript sense targeting labeling assay (Affymetrix) generates amplified and biotinylated sense-strand DNA targets from the entire expressed genome.
The GeneChIP® Whole Transcript Labeling Assay is based on the "GeneChIP® Whole Transcript (WT) Sense Target Labeling Assay Manual" (Affymetrix, Santa Clara, USA). This method is well established at the TAL and available as Standard Operating Procedure, SOP Nr. TAL027.1 "GeneChIP® Whole Transcript (WT) Labeling" and therefore, only a short summary of the method is followed.

Target Preparation

RNA for the Microarray analysis was isolated from cells as described above. In order to ensure GeneChip® whole transcript labeling of high-quality samples, RNA quality was first checked using the Bioanalyzer 2100 (Agilent). This on-chip gel electrophoresis provides information about size, quantification and quality of RNA. Additionally, the RNA integrity number (RIN) can be utilized for estimating the integrity of RNA samples.
300 ng of each total RNA sample were first reverse transcribed into single-stranded cDNA using T7-(N)6 primers. Performing a second strand cDNA synthesis generated double-stranded cDNA which in turn was used as a template for *in vitro* transcription (IVT). The IVT reaction was performed in the presence of T7 RNA polymerase at 37 °C for 16 h. The generated antisense cRNA samples were purified and then used for the second cycle of cDNA synthesis. During the first strand cDNA synthesis reaction, dUTP was incorporated in

the DNA in order to reproducibly fragment single-stranded DNA. After purifying the single-stranded cDNA samples, they were fragmented using a mix of uracil DNA glycosylase (UDG) and apurinic/apyrimidinic endonuclease 1 (APE 1) which together specifically break the DNA at the unnatural dUTP residues. Subsequently, the single-stranded DNA samples were labeled by using terminal deoxynucleotidyl transferase (TdT) and biotin-linked Affymetrix® DNA labeling reagent.

Target Hybridization

The target cocktail including fragmented and labeled target DNA as well as hybridization controls was prepared according to the manufacturer for a 169 format array. Upon injecting the specific samples into the respective probe arrays, hybridization was performed in the GeneChip® hybridization oven at 45 °C, at 60 rpm for 17 h.

Washing, staining and scanning of array

The washing and staining of the probe arrays was carried out in the GeneChIP® Fluidics Station 450 (Affymetrix, Santa Clara, USA) according to the manufacturer's instructions. Afterwards, probe arrays were scanned with the GeneChIP® Scanner 3000 7G (Affymetrix, Santa Clara, USA).

Data analysis

Gene expression data was analyzed using log2 transformation and quantile normalization of expression levels (Bolstad *et al.*, 2003). Background correction was applied according to manufacturer's advice. T-tests were applied on a gene-by-gene basis to assess significant differences between expression levels of different groups. To avoid a high number of false positives and to stay below a false discovery rate of 5%, p-values were adjusted for multiple testing using Benjamini-Hochbergs method (Benjamini and Hochberg, 1995). All analyses were performed using the free statistical software R (version 2.9.2). Tests were computed using the 'limma' package (Smyth, 2004).

### 3.2.8 Chromosome conformation capture (3C)

#### 3.2.8.1 Preparation of 3C template

Chromosome conformation capture analysis was performed as described in (Miele and Dekker, 2009) with slight modifications.

Medium was removed from cells growing in 145×20 mm cell culture dishes. Covalent crosslinking of interacting chromatin segments was achieved by adding 16 ml of 1.1% formaldehyde in PBS and incubating on a shaker for 15 min at RT. In order to quench the crosslinking reaction, 863 µl of 2.5 M glycine were added to the formaldehyde-PBS solution and incubated on the shaker for additional 5 min. After washing twice with ice-cold PBS, cells were scraped in ice-cold lysis buffer supplemented with 1 mM Pefabloc, 1 ng/µl Aprotinin/Leupeptin, 10 mM BGP and 1 mM NEM and incubated on ice for 15 min. The fixed cells were then dounce homogenized with a pestle L using 2× 15 strokes. After transferring into microcentrifuge tubes, cells were pelleted at 2,500×*g* for 5 min, washed once with 1× NEBuffer 3 and subsequently resuspended in 500 µl of 1× NEBuffer 3. Cells were distributed evenly between 5 micocentrifuge tubes, centrifuged for 5 min at 2,500×*g* and after discarding the supernatant, pellets were shock frozen in liquid nitrogen and stored at -80 °C till further processing. Upon thawing, two pellets from the same sample were pooled and resuspended in 362 µl of 1× NEBuffer 3. For the digestion of the crosslinked chromatin, first 38 µl 1% SDS and 0.4 µl 10% Triton X-100 were added and incubated at 65 °C for 10 min. Afterwards, 44 µl 10% Triton X-100 and 400 U of BtgI restriction enzyme as well as 100 µg/ml BSA were added, mixed and incubated at 37 °C overnight.

The next day, for enzyme inactivation, 86 µl 10% SDS were added and incubated at 65 °C for 30 min. Samples were transferred into 15 ml disposable tubes and 745 µl of 10% Triton X-100, 745 µl of 10× ligation buffer, 80 µl of 10 mg/ml BSA, 5,960 µl of $ddH_2O$ and 4,000 cohesive-end units of T4 DNA ligase were added to each sample and incubated for 2 h at 16 °C. In order to reverse crosslinking, 50 µl of 10 mg/ml Proteinase K in TE buffer (pH 8.0) were added and incubated at 65 °C overnight. After adding additional 50 µl of 10 mg/ml Proteinase K, samples were incubated at 42 °C for 2 h. Afterwards, the solutions were transferred into 50 ml disposable tubes. To extract the DNA, an equal volume of phenol was added, vortex-mixed for 30 s and centrifuged at 2,500×*g* for 5 min. The upper, aqueous phase was collected and the phenol extraction repeated. The upper layer was collected, again and the same volume of PCIA (phenol : chloroform : isoamylacohol, 25 : 24 : 1) was added,

vortex-mixed for 30 s and centrifuged at 2,500×*g* for 5 min. After transferring the upper phase into a new tube, 2 µl of GlycoBlue and 1/10 volume of 3 M sodium acetate (pH 5.2) were added and briefly mixed. Then 2.5 volumes of ice-cold 100% ethanol were added before incubating at -20 °C overnight. After centrifuging at 12,000×*g* for 20 min at 4 °C, the supernatants were discarded and each pellet was redissolved in 1 ml TE buffer and transferred into a microcentrifuge tube. A second DNA extraction was performed, by adding an equal volume of the following solvents in the described order: phenol, PCIA, PCIA and chloroform. After adding each solvent, the phases were separated by centrifugation at 2,500×*g* for 5 min and the upper, aqueous layer was transferred into a new tube. Afterwards, 2 µl of GlycoBlue as well as 1/10 volume of 3 M sodium acetate (pH 5.2) were added to the upper phase. After mixing shortly, DNA was precipitated by adding 1.5 volumes of ice-cold 100% ethanol and incubating at -20 °C overnight. The next day, samples were pelleted by centrifugation at 4 °C, 18,000×*g* for 20 min and washed five times with 1 ml of 70% EtOH. The DNA pellets were completely dried before resuspending in 50 µl of TE buffer. 1 µl of 10 mg/ml RNase A was added and 3C template samples were incubated at 37 °C for 15 min.

#### 3.2.8.2 Preparation of control template

A prerequisite for comparing PCR signal intensities of 3C template samples in a quantitative manner is the use of a control template containing all ligation products in equal amounts. Therefore, bacterial artificial chromosome clones (BACs, purchased from imaGenes or Bac Pac Resources) covering the *GREB1* or *CXCL12* loci were used.

DNA isolation from BAC clones

The *E.coli* carrying the BAC clone were streaked out on a chloramphenicol plate and grown at 37 °C overnight. The next day, using a sterile pipette tip, 100 ml of LB media supplemented with 20 µg/ml chloramphenicol were inoculated and grown overnight at 37 °C. Upon centrifuging the bacterial suspensions at 3000×*g* for 10 min, each pellet was resuspended in 5 ml of P1 solution. 5 ml of solution P2 were added, gently mixed and incubated 5 min at RT. 5 ml of P3 solution were slowly added and mixed carefully during addition. After incubating on ice for 5 min, the samples were pelleted at 10,000×*g*, 10 min at 4 °C. Each supernatant was then transferred into a fresh 50 ml tube which contained 10 ml of ice-cold isopropanol. The samples were mixed by inverting the tubes several times and then incubated on ice for 5 min. After centrifuging at 10,000×*g* at 4 °C for 15 min, each pellet was washed with 10 ml of 70% EtOH and centrifuged again at 10,000×*g* at 4 °C for 10 min.

Finally, the pellets were air-dried, resuspended in 1 ml of $ddH_2O$ and the concentration was measured by spectrophotometry at 260 nm using the NanoDrop.

After the successful BAC clone DNA isolation, this control DNA was digested with the BtgI enzyme, was ligated with T4 DNA ligase and purified by phenol-chloroform extraction and ethanol precipitation as explained for the 3C template DNA. Subsequently, control DNA was serial diluted and applied as standard curve in the PCR analysis of 3C templates.

#### 3.2.8.3 Quantitative PCR with TaqMan probes

One µl of each 3C control and template sample was used for quantitative real-time PCR analysis. The PCR setup for 3C DNA analysis was slightly different than the one already described for ChIP and cDNA sample analysis. A 25 µl PCR reaction was setup as follows: 75 mM Tris-HCl (pH 8.8), 20 mM $(NH_4)_2SO_4$, 0.01% Tween-20, 3 mM $MgCl_2$, 200 µM dNTPs, 1 U/reaction Taq DNA Polymerase, 0.25% Triton X-100, 30 nM primers, 300 mM Trehalose and 250 nM TaqMan probe (5'-FAM and 3'-BHQ1-labeled).

The qPCR protocol was also adjusted:

| | | |
|---|---|---|
| 95 °C | 2 min | |
| 95 °C | 15 s | ⎫ 45 cycles |
| 60 °C | 30 s | ⎭ |

The serial dilution of the BAC clone DNA (control DNA) served as standard curve in the qPCR analysis. 3C template values were normalized with values from an internal control site. The normalized levels were graphed relative to the non-treated control sample (set to one) and represented as "normalized relative interaction".

## 3.3 Protein biochemistry

### 3.3.1 SDS-PAGE

Target proteins were separated via sodium dodecylsulfate polyacrylamide gel electrophoresis (SDS-PAGE) (Laemmli, 1970). Cells were lysed in RIPA buffer containing 1 mM Pefabloc, 1 ng/µl Aprotinin/Leupeptin, 10 mM BGP and 1 mM NEM. In order to shear genomic DNA, samples were sonicated for 10 s at 10% power using a Bandelin Sonoplus sonicator. Protein samples were boiled in Laemmli Buffer for 5 min and then subjected to SDS-PAGE. The composition of stacking and resolving gel are described in section 2.8 (Buffers and media). Polyacrylamide gels were run in SDS running buffer at 25 mA.

### 3.3.2 Western blot analysis

Subsequently, upon electrophoresis proteins were detected by Western blot analysis (Towbin *et al.*, 1979) using target protein specific antibodies. Separated proteins were transferred at 25 V to PVDF membranes using transfer buffer for 2-4 h, depending on the size of the protein. The membranes were incubated for 1 h in PBS-T and 5% (w/v) dry milk to block non-specific antibody binding. Afterwards the membranes were incubated for 1 h at room temperature or overnight at 4 °C in the same blocking buffer containing the respective primary antibodies, diluted as described in the antibody table (2.6.3.1). After washing three times with PBS-T, the membranes were incubated for 1 h with the corresponding horseradish peroxidase-conjugated anti-mouse IgG, anti-rabbit IgG, anti-rat IgG or anti-mouse IgG+IgM secondary antibodies at a dilution of 1:10,000. After washing three times with PBS-T, HRP signals were detected using enhanced chemoluminescence and exposed to X-ray films.

# 4 Results

In this study, the role of the ubiquitin-proteasome system (UPS) in the regulation of gene transcription was analyzed for two nuclear hormone receptors, namely estrogen receptor-alpha (ERα) and glucocorticoid receptor (GR). However, the main focus was put on the investigation of the molecular mechanisms by which the UPS controls ERα-mediated transcription in MCF-7 breast cancer cells.

The ERα is the primary target of endocrine treatment for breast cancer. Because of the ineffectiveness of endocrine therapies over time, it is necessary to discover additional combination treatments which directly target specific aspects of ERα-mediated transcription. One such candidate target is the proteasome which plays a decisive role in nuclear hormone receptor-regulated transcription and is the target of anti-cancer therapy with Bortezomib (Velcade®) in multiple myeloma and mantle cell lymphoma. It was therefore the goal to elucidate the mechanisms by which the UPS regulates estrogen-responsive gene transcription and thereby reveal insights into the characterization and efficacy of proteasome inhibitors in ERα-positive breast cancer therapy.

## 4.1 Effects of proteasome inhibition or knockdown on estrogen-induced cellular responses

### 4.1.1 Proteasome inhibition or knockdown increases the amount of polyubiquitinated proteins and Bortezomib blocks hormone-induced ERα-downregulation

The prerequisite for analyzing the effect of the ubiquitin-proteasome system on the regulation of nuclear hormone receptor-dependent transcription is an effective blockage of the proteasomal enzyme function. In order to accomplish this blockage of proteolytic function, two different experimental setups were performed in this study. On the one hand, proteasomal activity was inhibited with chemical proteasome inhibitors and on the other hand, transient siRNA-mediated knockdown of 20S proteasomal subunit components was performed.

For the pharmacological inhibition of proteasomal enzymatic function, three different proteasome inhibitors were used: MG-132, a widely-used, reversible proteasome inhibitor; Bortezomib (Velcade®), a reversible proteasome inhibitor which is in clinical use for the treatment of multiple myeloma and mantle cell lymphoma; and Epoxomicin which irreversibly inhibits proteasome activity. MCF-7 cells were treated either with MG-132,

Bortezomib or Epoxomicin and whole protein extracts were analyzed by Western blot analysis using a specific antibody against polyubiquitinated proteins. Each of the three pharmacological inhibitors increased the amount of higher molecular weight ubiquitinated proteins ($Ub_n$) compared to control cells (Figure 5A). These results indicate that treating the cells either with MG-132, Bortezomib or Epoxomicin led to an at least partial inhibition of the proteasomal enzymatic function.

Due to their limitations, such as non-specific protease inhibition, poor stability and bioavailability, peptide aldehydes such as MG-132 and the irreversible proteasome inhibitor Epoxomicin are not suitable for clinical use. Bortezomib, the first proteasome inhibitor approved for cancer therapy, is highly selective, potent and has manageable toxicities. These differences were the rationale for choosing Bortezomib as the proteasome inhibitor in these studies.

Several studies showed that ERα activity is dependent on its degradation by the ubiquitin-proteasome pathway and that the estrogen-dependent degradation of ERα can be blocked by the proteasome inhibitors MG-132 and lactacystin (Nawaz *et al.*, 1999a; Reid *et al.*, 2003; Tateishi *et al.*, 2004). Therefore, we sought to determine if the proteasome inhibitor Bortezomib has a similar effect on the estrogen-induced ERα protein degradation. Pre-treating MCF-7 cells with Bortezomib followed by estrogen treatment resulted in an increase in the polyubiquitination of proteins as depicted as $Ub_n$ in Figure 5B. Importantly, Bortezomib treatment blocked the ligand-induced ERα proteolysis.

To determine whether the knockdown of proteasomal components similarly increases the amount of polyubiquitinated proteins, siRNAs against the 20S proteasomal subunit components PSMB3 and PSMB5 were used. PSMB3 and PSMB5 are both subunits of the ß-ring of the 20S proteolytic core particle. Figure 5C shows that siRNAs targeted to PSMB3 and PSMB5 efficiently reduced the amounts of PSMB3 and PSMB5 proteins compared to control siRNA. Like proteasome inhibition, knockdown of PSMB3 and PSMB5 increased the amount of polyubiquitinated proteins in MCF-7 cells which in turn confirmed the inhibition of proteasome-mediated proteolysis.

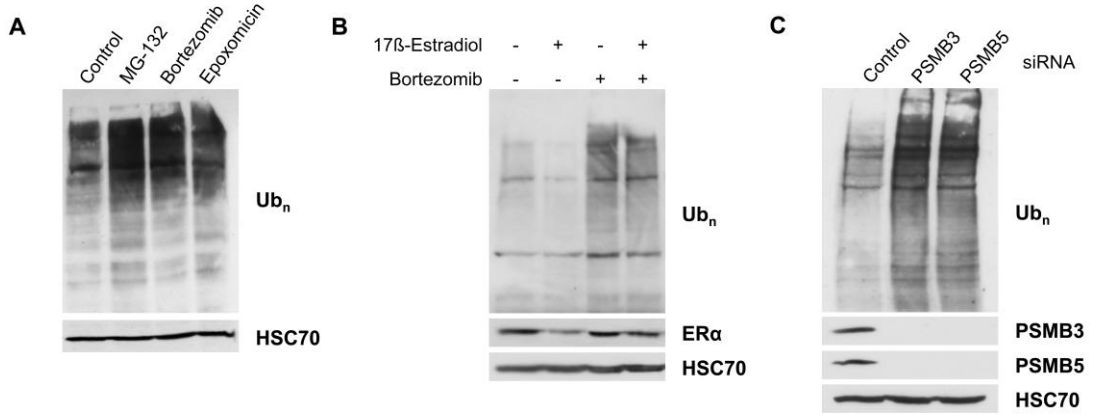


**Figure 5: Pharmacological proteasome inhibition and proteasome subunit depletion increase the amount of polyubiquitinated proteins in MCF-7 cells and Bortezomib blocks estrogen-induced ERα downregulation.** (**A**) MCF-7 cells were treated with 20 µM MG-132, 50 nM Bortezomib or 1 µM Epoxomicin for 4 h. Protein extracts were analyzed by Western blot analysis using a specific antibody against polyubiquitinated proteins. $Ub_n$ indicates higher molecular weight ubiquitinated proteins. (**B**) After 15 min pre-treatment with 50 nM Bortezomib, MCF-7 cells were treated with 10 nM 17ß-Estradiol for 6 h. Protein extracts were analyzed by Western blot for polyubiquitinated proteins and ERα protein levels. (**C**) MCF-7 cells were transfected with 30 pmol control, PSMB3 or PSMB5 siRNA for 72 h and polyubiquitinated proteins as well as PSMB3 and PSMB5 protein levels were detected by Western blot analysis using the indicated antibodies. HSC70 serves as a loading control in all blots.

### 4.1.2 Upon proteasome inhibition RNA polymerase II protein levels remain unchanged in MCF-7 cells

A previous report indicated that the effects of proteasome inhibition on target gene expression may be due to its effect on RNA polymerase II (RNAPII) phosphorylation (Kinyamu and Archer, 2007). During the transcription cycle, RNAPII gets phosphorylated at its carboxy-terminal domain (CTD) that comprises 52 repeats of a heptapeptide with the consensus sequence Tyr-Ser-Pro-Thr-Ser-Pro-Ser ($Y_1S_2P_3T_4S_5P_6S_7$). RNAPII phosphorylation on Ser5 is a hallmark for transcription initiation and is followed by Ser2 phosphorylation which leads to productive elongation. Recently, also the phosphorylation of Ser7 within in the CTD was described to play a role in non-coding small nuclear (sn) RNA gene expression (Chapman *et al.*, 2007; Egloff *et al.*, 2007).

In order to check the effect of proteasome inhibition on RNAPII protein levels and phosphorylation status, MCF-7 cells were treated with Bortezomib or MG-132. Then, protein extracts were analyzed via Western blot using antibodies against total RNAPII, or the Ser2-phosphorylated (RNAPII P-Ser2), Ser5-phosphorylated (RNAPII P-Ser5) and Ser7-phosphorylated (RNAPII P-Ser7) forms. In Figure 6 it is shown that neither protein levels of RNAPII nor RNAPII P-Ser2, RNAPII P-Ser5 and RNAPII P-Ser7 were markedly

affected upon proteasome inhibition with Bortezomib. There was a hint of an increase in total RNAPII protein level upon Bortezomib treatment compared to control. MG-132 treatment also did not result in an increase in RNAPII protein levels but rather in a slight decrease in RNAPII P-Ser2, RNAPII P-Ser5 and RNAPII P-Ser7 levels. These results have to be verified. But all in all, there was no increase in global protein levels of total and phosphorylated forms of RNAPII after proteasome inhibition using Bortezomib or MG-132.

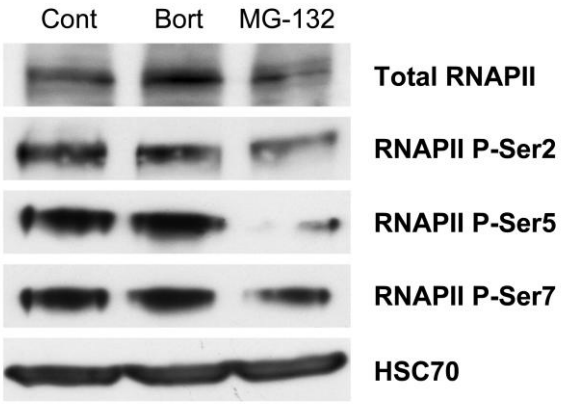


**Figure 6: Proteasome inhibition has no significant effect on global RNAPII protein levels or Ser2-, Ser5- or Ser7-phosphorylation.** MCF-7 cells were treated with either vehicle (100% EtOH + DMSO), 50 nM Bortezomib or 1 µM MG-132 for 20 h and protein extracts analyzed via Western blot with the indicated antibodies. HSC70 is shown as loading control. Bort, Bortezomib; Cont, Control; RNAPII, RNA polymerase II; RNAPII P-Ser2, RNA polymerase II phosphorylated at Ser2; RNAPII P-Ser5, RNA polymerase II phosphorylated at Ser5; RNAPII P-Ser7, RNA polymerase II phosphorylated at Ser7 of the CTD.

### 4.1.3 Bortezomib dose definition in MCF-7 studies

Monitoring the increase of polyubiquitinated proteins was performed initially to establish the dose of Bortezomib that is necessary to inhibit the proteolytic activity in MCF-7 breast cancer cells. Thus, cells were treated with increasing concentrations of Bortezomib and inhibition of the proteasome enzymatic function was determined via Western blot analysis using an antibody against polyubiquitinated proteins. Figure 7 shows that Bortezomib concentrations ranging from 10 to 100 nM strongly increased the accumulation of multiple, higher-molecularweight bands which indicate polyubiquitinated proteins. At higher Bortezomib doses (500 nM to 1 µM) the amount of polyubiquitinated proteins decreased, again. Based on this data, all following experiments were performed using 50 nM Bortezomib in order to assure efficient chemical proteasome inhibition.

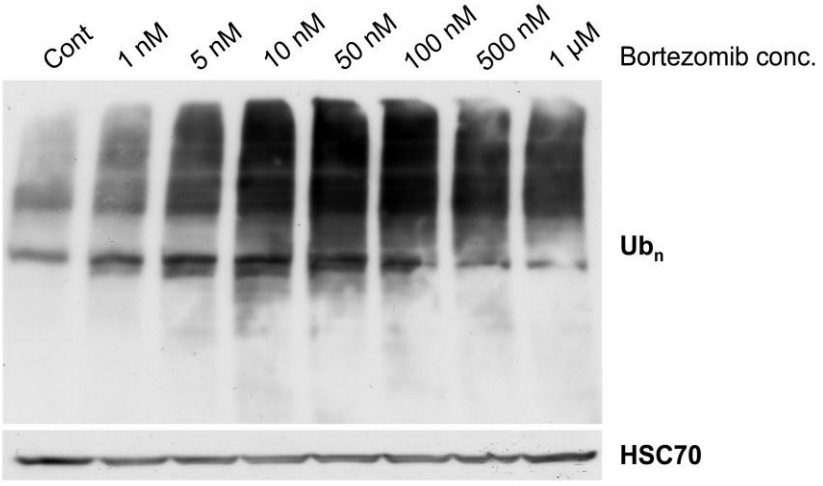


**Figure 7: Titration of Bortezomib reveals an effective dose of 50 nM for proteasome inhibition in MCF-7 breast cancer cells.** MCF-7 cells were treated either with 100% EtOH (Cont) or with increasing amounts of Bortezomib (1 nM to 1 µM). Whole protein extracts were analyzed via Western blot using antibodies against polyubiquitinated proteins ($Ub_n$) and HSC70 as loading control.

### 4.1.4 Effect of blockage of proteasome function on MCF-7 cell viability

The induction of apoptosis by proteasome inhibitors could complicate the interpretation of the role of the UPS in nuclear hormone receptor-regulated gene transcription. Therefore, before starting gene expression studies, the induction of apoptosis upon Bortezomib treatment or knockdown of proteasome subunits had to be ruled out within a certain, experimental time frame. Apoptosis was quantitatively determined via flow cytometry using fluorescently-conjugated Annexin V (Annexin V-PE) and 7-AAD.

#### 4.1.4.1 Prolonged Bortezomib administration induces apoptosis in MCF-7 cells

First, the induction of apoptosis in MCF-7 cells was examined upon exposure to the proteasome inhibitor Bortezomib for either 24 or 48 h. Figure 8 shows that in a population of untreated MCF-7 cells, 8.9% were undergoing apoptosis. 2.4% of these cells were in a pro-apoptotic (Annexin V-PE positive) and 6.5% in a late apoptotic phase (Annexin V-PE and 7-AAD positive). 24 h after treatment with either estrogen, Bortezomib, the selective estrogen receptor modulator (SERM) Tamoxifen or the positive control Doxorubicin, only Doxorubicin-treated cells were almost completely (99.3%) undergoing apoptosis. Bortezomib did not significantly induce apoptosis in that period of time. However, treating the cells with Bortezomib for 48 h resulted in a significant increase in apoptosis. 32.4% of the Bortezomib-treated cells were indicated as apoptotic (12.2% pro-apoptotic and 20.2% late-apoptotic), compared to control cells with only 9.5% undergoing apoptosis (4.6% pro-apoptotic and 4.9% late-apoptotic). Interestingly, the apoptosis-inducing effect of Bortezomib dominated over the effect of estrogen or Tamoxifen. Estrogen and Tamoxifen each alone showed no significant difference compared to control cells. But the combined treatment of each of these two compounds with Bortezomib resulted in very similar distribution of cells undergoing apoptosis compared to Bortezomib alone. These results imply that treatment with 50 nM Bortezomib for up to 24 h does not significantly increase the percentage of MCF-7 cells undergoing apoptosis. Therefore, all following experiments were performed in a time frame up to 24 h to simply rule out that the detected effects were due to apoptosis.

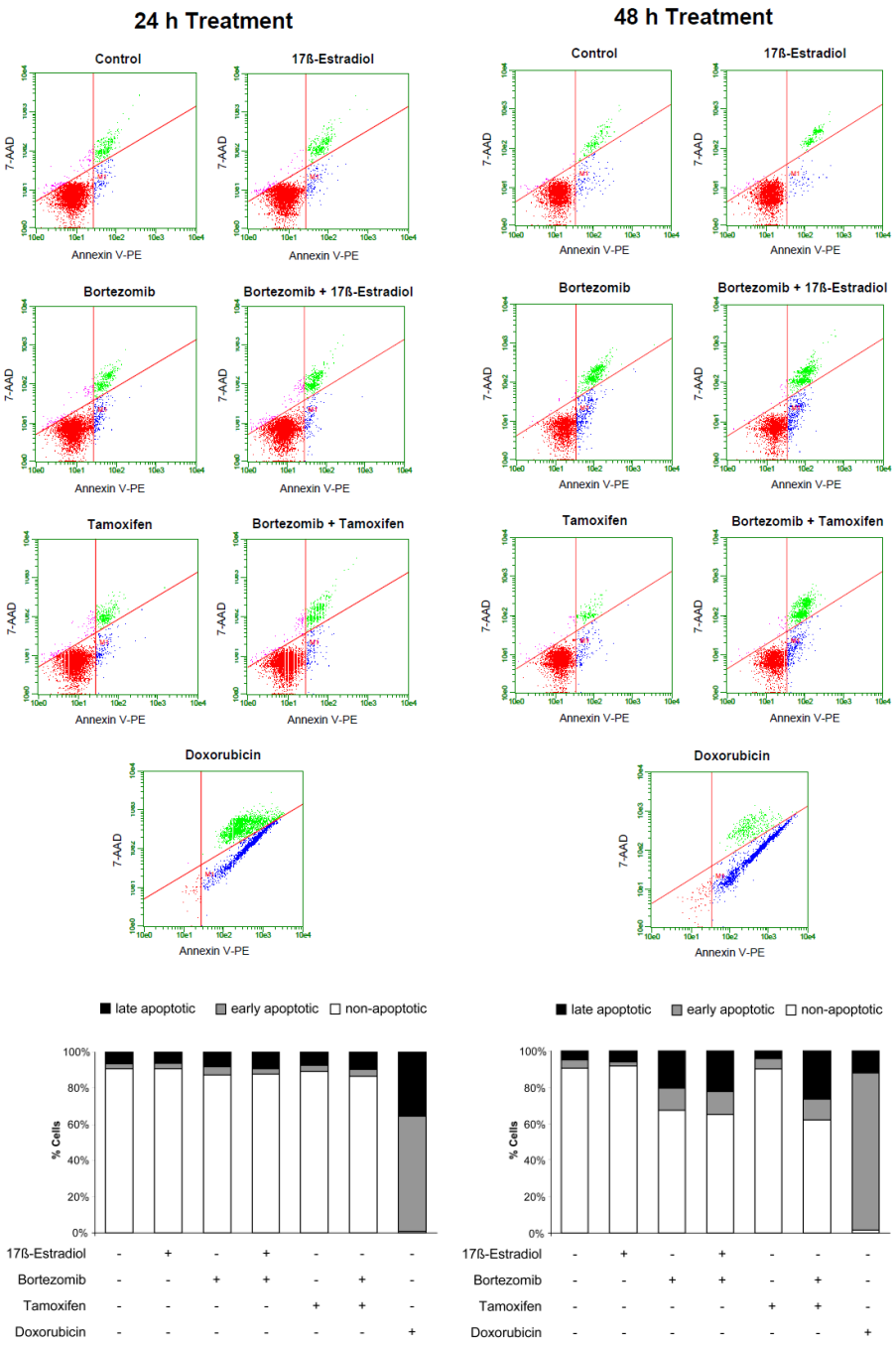


**Figure 8: Prolonged exposure to Bortezomib induces apoptosis in breast cancer cells**. Annexin staining was conducted with the use of Guava Nexin® Assay (Guava Technologies) which utilizes Annexin V-PE and 7-AAD. MCF-7 cells were cultured in hormone-deprived 5% CSS growth medium and treated with either vehicle (negative control), 10 nM 17ß-Estradiol, 50 nM Bortezomib, 1 µM Tamoxifen or 5 µM Doxorubicin (positive control) for 24 h or 48 h. Cells were stained with Annexin V-PE and propidium iodide (PI) according to the manufacturer's protocol before analysis by flow cytometry. Cells in the lower left gated quadrant (Annexin V-PE negative/7-AAD negative) reflect non-apoptotic cells, cells in the lower right quadrant (Annexin V-PE positive/7-AAD negative) reflect early apoptotic cells, and cells in the upper right quadrant (Annexin V-PE positive/7-AAD positive) reflect late apoptotic cells. Representative samples from an experiment with $n = 2$ are shown. The fractions of gated cells were quantified and are shown as "% cells" in bar graphs; mean values, $n = 2$.

### 4.1.4.2 Proteasome subunit depletion has no impact on apoptosis of MCF-7 cells

Concomitant with analyzing the effect of Bortezomib on the induction of apoptosis, the same assay was performed with cells transfected with siRNAs against the proteasome subunits PSMB3 or PSMB5. Figure 9 shows the percentage of each cell population in either non-, pro- or late-apoptotic phase. In the control siRNA transfected and vehicle-treated cell population, 88.2% of the cells were viable, 4.7% in a pro-apoptotic phase and 6.1% of the cells were in a late apoptotic state. Depletion of PSMB3 or PSMB5 did not lead to an increase in early or late apoptosis, neither with estrogen nor with Tamoxifen treatment.

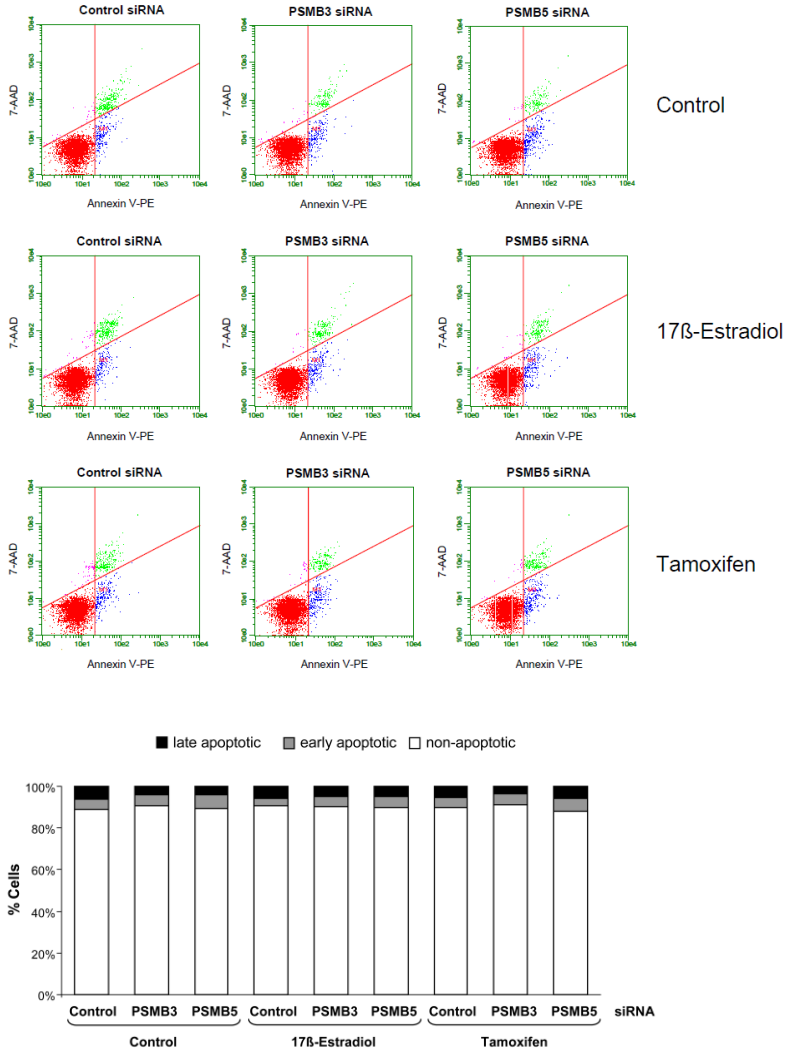


**Figure 9: Proteasome knockdown does not induce apoptosis in MCF-7 breast cancer cells.** MCF-7 cells were control, PSMB3 or PSMB5 siRNA transfected and the next day subjected to hormone-deprived 5% CSS growth medium. After 24 h, cells were treated with either vehicle (100% EtOH), 10 nM 17ß-Estradiol or 1 µM Tamoxifen for another 24 h. Cells undergoing apoptosis were defined via Annexin V-PE and 7-AAD staining (Guava Technologies) and subsequent flow cytometry analysis according to the manufacturer's protocol. For gating definitions in Annexin V-PE and 7-AAD histograms refer to Figure 8. Representative samples from an experiment with $n$ = 2 are shown. The fractions of gated cells were quantified and are shown as "% cells" in a bar graph; mean values, $n$ = 2.

### 4.1.5 Bortezomib induces a downregulation of ERα mRNA but not protein levels

Prior to analyzing the effects of proteasome inhibition on ERα-regulated target gene transcription, the transcriptional and post-transcriptional control of the estrogen receptor itself was investigated. ERα expression upon blocking proteasomal activity was determined both on the mRNA and protein level. Therefore, MCF-7 cells were either treated with estrogen, Bortezomib or with the combination of estrogen and Bortezomib for 2, 6 and 24 h. Evaluation of ERα mRNA levels using qRT-PCR (Figure 10A) revealed that estrogen stimulation resulted in a decreased ERα mRNA expression compared to control with lowest ERα mRNA expression after 6 h of estrogen treatment. After 2 and 6 h, ERα mRNA levels were only mildly affected by proteasome inhibition compared to control samples. However, there was a highly significant reduction in ERα mRNA expression to nearly undetectable levels after 24 h of Bortezomib treatment in the presence or absence of estrogen. However, monitoring ERα protein levels upon proteasome inhibition revealed that even after 24 h exposure to Bortezomib, ERα protein level remained unchanged (Figure 10B). These results indicate that even though ERα mRNA levels are negatively influenced by 24 h proteasome inhibition there are still significant levels of ERα protein in the cell thus validating this time point for analyses of ERα target gene regulation.

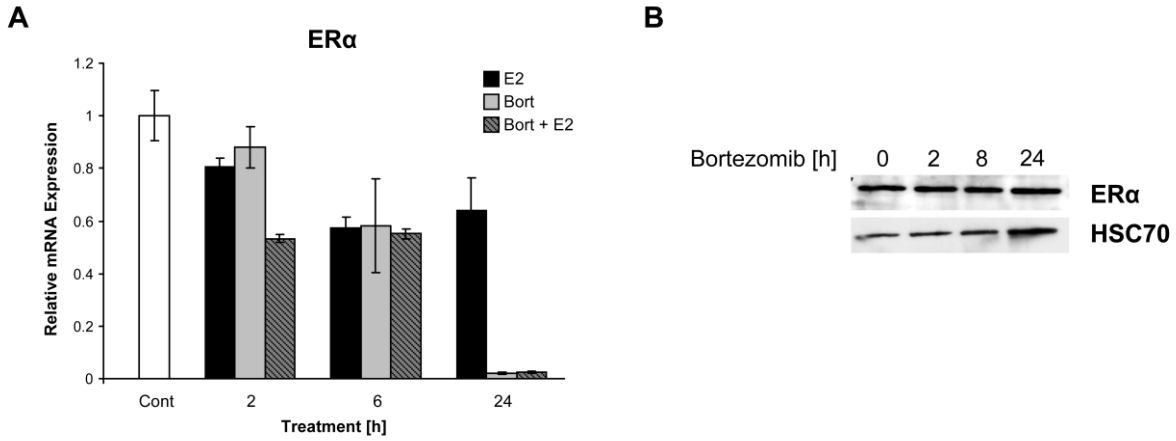


**Figure 10: Treatment with Bortezomib for 24 h induces the downregulation of ERα on mRNA but not protein levels.** (**A**) MCF-7 cells were grown in phenol red-free DMEM supplemented with 5% CSS for 24 h before treatment. Cells were pre-treated either with vehicle (100% EtOH, Cont) or 50 nM Bortezomib (Bort) for 15 min and then incubated with 10 nM 17ß-Estradiol (E2) for 2, 6 or 24 h; Bort + E2, combined treatment with 10 nM 17ß-Estradiol and 50 nM Bortezomib. RNA was isolated, reverse transcribed with random primers and then analyzed via qPCR. The ERα expression levels were normalized to a control gene, 28 S ribosomal RNA. The normalized values were graphed relative to the control sample and were expressed as "relative mRNA expression"; mean values + s.d., *n* = 2. (**B**) MCF-7 cells were treated with either 100% EtOH as control or with 50 nM Bortezomib for 2, 8 or 24 h. ERα protein levels were analyzed by Western blot using a specific antibody against the estrogen receptor-alpha. HSC70 serves as loading control.

### 4.1.6 Effects of proteasome blockage on cell proliferation

The colony formation assay is an *in vitro* cell survival assay which is based on the fact that a single cell can grow into a colony. The assay detects all cells which are still able to produce progeny under certain treatments. Therefore, it is the method of choice in this study to determine the effects of proteasome inhibition using Bortezomib and proteasome depletion via siRNA-mediated knockdown of 20S subunit components on the proliferative capacity of MCF-7 breast cancer cells.

#### 4.1.6.1 Bortezomib dose-dependently decreases proliferation of breast cancer cells

Figure 11 shows the outcome of the clonogenic assay upon proteasome inhibition. Since estrogen regulates the proliferation and development of tissues expressing estrogen receptors, it was not surprising that estrogen showed a pro-proliferative effect on MCF-7 cells in this study, as depicted by a higher amount of crystal violet-stained colonies compared to control cells. Strikingly, there was a strong difference between low and high doses of Bortezomib on the proliferation of MCF-7 cells after a 6-day treatment. While cells treated with 5 nM Bortezomib showed a very similar proliferative capacity compared to the control cells, in the presence of 50 nM Bortezomib colony formation was completely abrogated. Actually, the same picture of the dose-dependency of Bortezomib occurred when cells were simultaneously treated with estrogen. Again, cells treated with the lower concentration of Bortezomib showed almost identical colony formation capacity to the estrogen treated cells while the high dose of Bortezomib abolished colony formation. The presence of Tamoxifen, a selective estrogen receptor modulator (SERM) with potent anti-estrogen properties in MCF-7 cells, resulted in a slight decrease in colony formation compared to control cells. The cell's proliferation rate was even stronger decreased by the combined treatment of Tamoxifen and low dosage of Bortezomib (5 nM) and totally abolished by adding 50 nM Bortezomib.

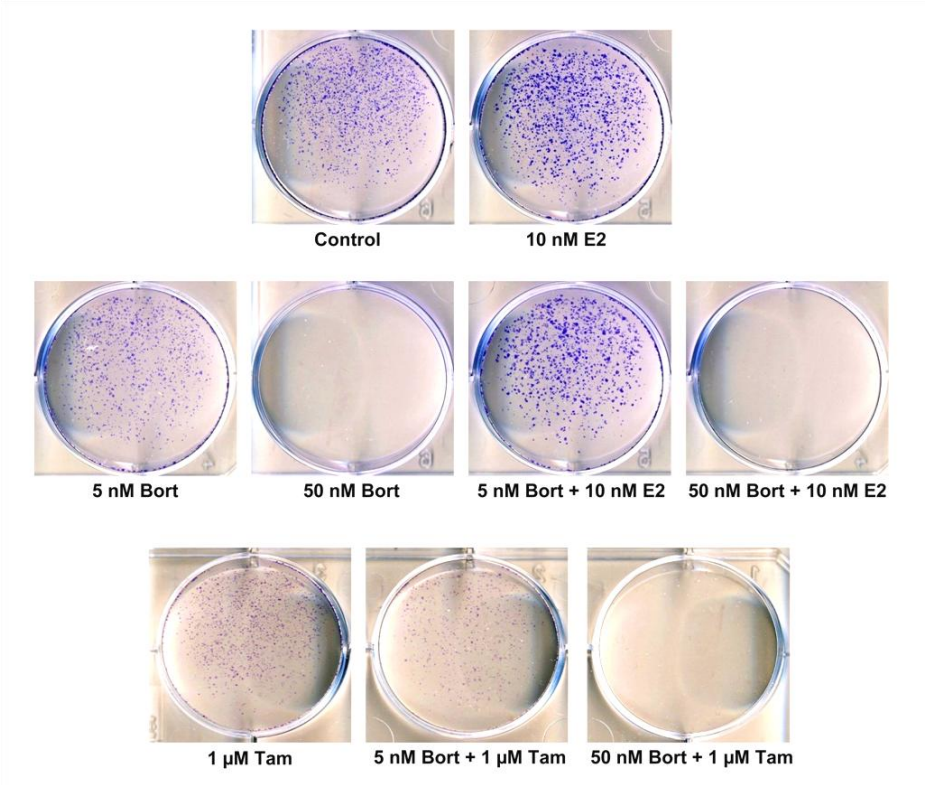


**Figure 11: Bortezomib decreases colony formation in MCF-7 cells dose-dependently and at higher concentrations also inhibits the pro-proliferative effect of estrogen**. Clonogenic assay with clones produced by MCF-7 cells. 20,000 MCF-7 cells were seeded in a 6-well plate. After 24 h medium was changed to estrogen-free medium and cells were treated with 100% EtOH (Control), 10 nM 17ß-Estradiol (E2), 1 µM Tamoxifen (Tam) and 5 nM or 50 nM Bortezomib (Bort) for 6 days. Colonies were fixed with 70% methanol and stained with 0.1% crystal violet. Representative samples from an experiment with $n = 2$ are shown.

#### 4.1.6.2 Knockdown of proteasome subunit components has no major effect on breast cancer cell proliferation

After showing that blockage of proteasomal activity via proteasome inhibition had negative effects on the proliferative capacity of MCF-7 cells, these findings were compared to the effects induced by siRNA-mediated knockdown of 20S components. First of all, as in Figure 11, estrogen increased colony formation irrespective of PSMB3 or PSMB5 knockdown and confirmed the pro-proliferative effect of estrogen on breast cancer cells (Figure 12A). Second, it showed that the effect of 20S proteasomal subunit knockdown on colony formation was not as pronounced as the effect of proteasome inhibition. The knockdown of PSMB5 did not alter colony formation in untreated cells at all, while in the presence of estrogen it resulted in a slightly decreased number of colonies compared to control-transfected cells (Figure 12A; lane 3). After knockdown of PSMB3, there were less stained cells under control as well as estrogen conditions compared to control-transfected cells (Figure 12A; lane 2). But this

negative effect on colony formation however, was only minor compared to the one detected upon proteasome inhibition with the high dose of Bortezomib.

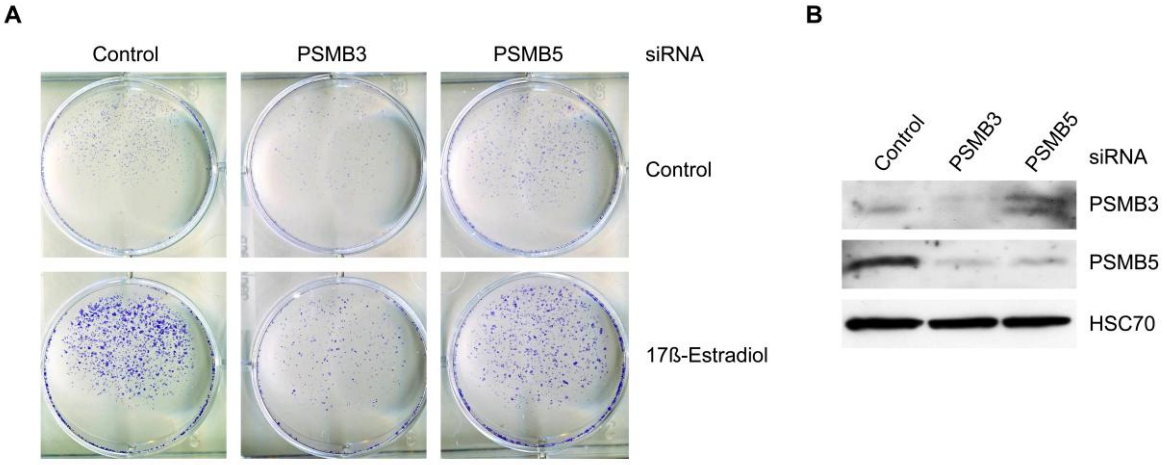


**Figure 12: Proteasome knockdown slightly decreases colony formation in MCF-7 cells.** (**A**) Clonogenic assay after 20S proteasomal subunit depletion. One day after reverse-transfection with 30 pmol control, PSMB3 or PSMB5 siRNA, transfected MCF-7 cells were re-plated into 6-well plates with a density of 20,000 cells per well. After attachment of cells to the dishes, growth medium was changed to hormone-deprived, 5% CSS growth medium. Every second day, cells were treated with 10 nM 17ß-Estradiol for 7 days. After fixation with 70% methanol, colony formation was visualized by staining with 0.1% crystal violet. Representative samples from an experiment with $n = 2$ are shown. (**B**) In parallel, efficient knockdown of PSMB3 and PSMB5 was confirmed by Western blot analysis using the indicated antibodies. Again, HSC70 serves as loading control.

### 4.1.7 Effects of proteasome blockage on cell cycle distribution

#### 4.1.7.1 Bortezomib blocks estrogen-induced cell cycle changes and induces a G2/M arrest in MCF-7 cells

In order to determine whether the anti-proliferative effect of Bortezomib in MCF-7 cells involved alterations in cell cycle progression, flow cytometry analysis was performed in the presence of either estrogen, Bortezomib, Tamoxifen or combined treatments. Under normal conditions (control), MCF-7 cells showed the following cell cycle distribution (Figure 13): 63.24% of the cells were in G1, 25.54% in S and 11.23% in G2/M phase. Consistent with the estrogen-induced cell proliferation observed in Figures 11 and 12, treatment with estrogen increased the fraction of MCF-7 cells in S phase (38.8% *vs.* 25.54% in control cells). Treatment with Bortezomib for 48 h substantially increased the G2/M cell fraction (35.74% *vs.* 11.23% in control cells). Interestingly, proteasome inhibition dominated the effects of estrogen as the elevated fraction of cells in G2/M phase remained constant in the combined treatment with Bortezomib and 17ß-Estradiol (34.57% in G2/M phase). Importantly, Bortezomib blocked the ability of estrogen to increase the fraction of cells in S phase.

Tamoxifen decreased the percentage of cells in S phase (17.12% *vs.* 25.54% in control cells). Again, the combined treatment with Bortezomib increased the fraction of cells in G2/M cell cycle phase (40.25% *vs.* 11.23% in control cells) and decreased the S phase fraction.

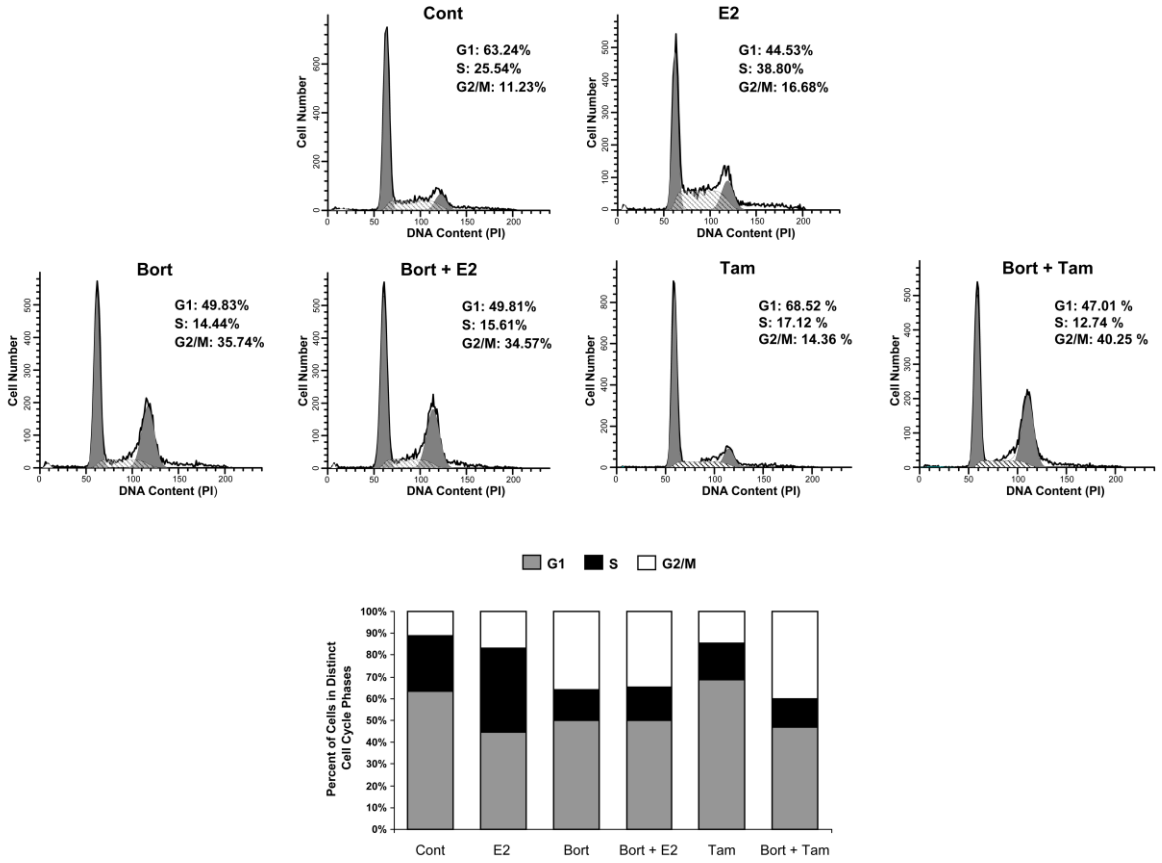


**Figure 13: Proteasome inhibition increases the percentage of MCF-7 cells in G2/M phase of the cell cycle and dominates the effects of estrogen and Tamoxifen.** MCF-7 cells were treated with control (Cont), 50 nM Bortezomib (Bort), 10 nM 17ß-Estradiol (E2) and 1 µM Tamoxifen (Tam) for 48 h. For analysis of cell cycle distribution, MCF-7 cells were stained with propidium iodide (PI) and analyzed by flow cytometry using a FACScan. Distribution of cells in distinct cell cycle phases was determined and graphically displayed using ModFIT cell cycle analysis software. The percentage of cells in distinct cell cycle phases is shown as a bar graph underneath; representative samples from an experiment with $n = 2$ are shown.

These data indicate that the detected negative effect of 50 nM Bortezomib on the colony formation capacity of MCF-7 cells breast cancer cells (Figure 11) was due to an increase in apoptotic cells after 48 h of treatment (Figure 8) as well as a Bortezomib-induced G2/M cell cycle arrest (Figure 13).

#### 4.1.7.2 Proteasome subunit depletion reduces estrogen-induced increase in DNA synthesis phase

After showing that proteasome inhibition with Bortezomib dominated the effects of estrogen and induced an accumulation of cells in G2/M arrest, next the effects on cell cycle progression upon knockdown of proteasomal subunit components PSMB3 and PSMB5 were analyzed. As shown in Figure 14, control-transfected and untreated MCF-7 cells showed a similar cell cycle distribution pattern to the control cells in the previous flow cytometry analysis (Figure 13). Consistent with the previous analysis, estrogen increased the fraction of control-transfected MCF-7 cells in S phase (37.43% *vs.* 30.57% in control-treated cells) (Figure 14). In contrast, Tamoxifen treatment again decreased the percentage of control-transfected cells in S phase (16.41%). While Bortezomib markedly increased the fraction of cells in G2/M phase, siRNA-mediated knockdown of neither PSMB3 nor PSMB5 resulted in a strong accumulation of cells in this fraction (17.26% in PSMB3 and 16.40% in PSMB5 *vs.* 12.65% in control-transfected cells). Depletion of these two 20S proteasome subunits rather led to an increased fraction of cells in G1 phase (64.56% in PSMB3 and 70.39% in PSMB5 *vs.* 56.78% in control-transfected cells). This higher percentage of cells in G1 phase also persisted in the presence of estrogen. Thus, like proteasome inhibition, the knockdown-induced effect dominated the effects induced by estrogen. In the presence of Tamoxifen, PSMB3 and PSMB5-transfected cells were distributed in similar cell cycle fractions as the control-transfected cells.

All in all, these results showed that also the effects on MCF-7 cell cycle progression upon siRNA-mediated knockdown were less pronounced as upon proteasome inhibition.

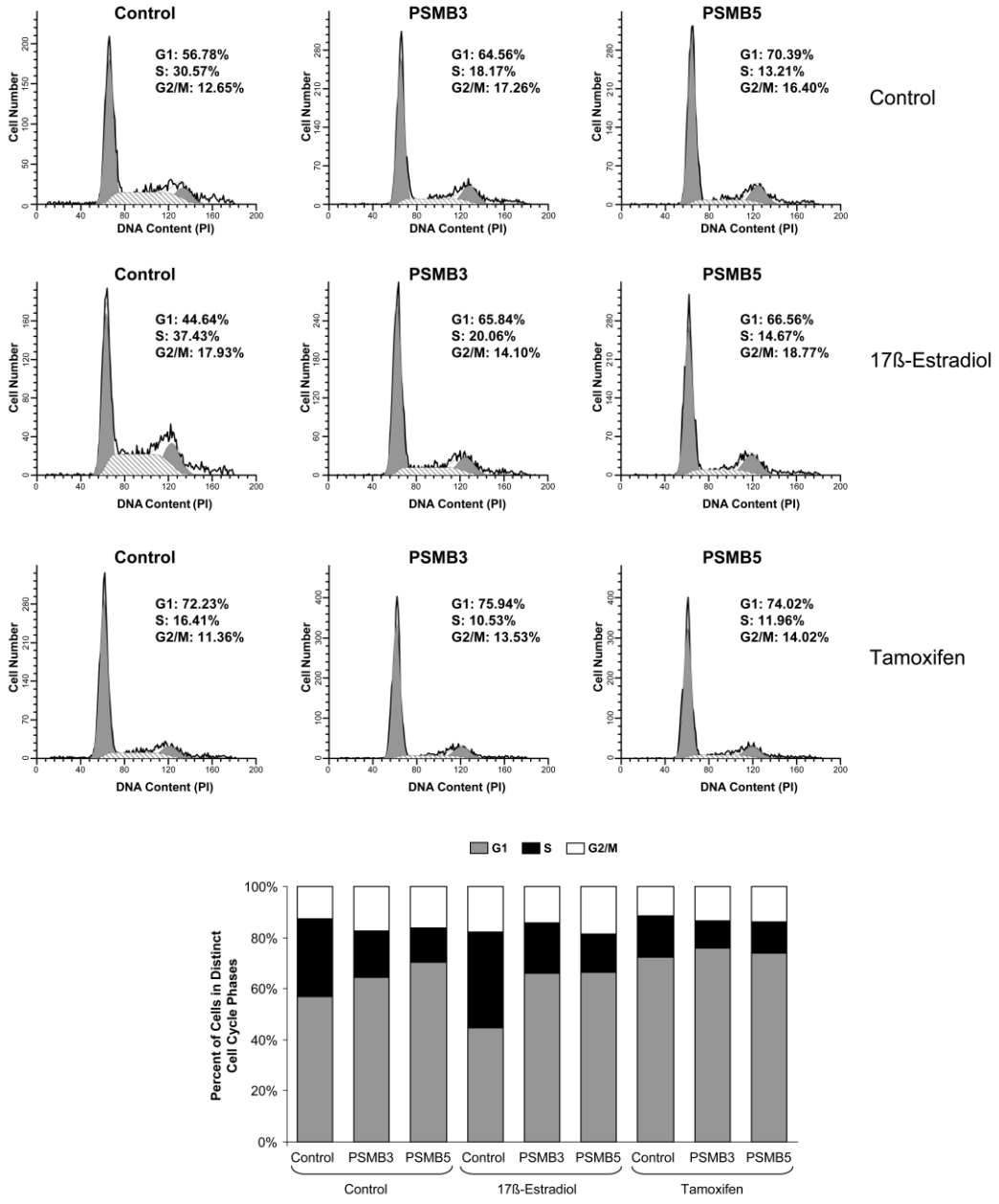


**Figure 14: Knockdown of proteasome subunit components increases the percentage of MCF-7 cells in G1 phase and blocks the proliferative effects of estrogen.** PSMB3, PSMB5 or control siRNA-transfected MCF-7 cells were treated with either vehicle (control), 10 nM 17ß-Estradiol or 1 µM Tamoxifen for 48 h. Cell cycle distribution was determined by staining MCF-7 cells with propidium iodide (PI) and analysis by flow cytometry. Distribution of cells in distinct cell cycle phases was determined and graphically displayed using ModFIT cell cycle analysis software. The respective siRNAs are indicated above the ModFIT graphs. The bar graph underneath displays the percentage of cells in distinct cell cycle phases for each treatment; representative samples from an experiment with $n = 2$ are shown.

## 4.2 Messenger RNA expression profiling

The main goal of this thesis work was to elucidate the role of the ubiquitin-proteasome system in the regulation of estrogen receptor-mediated gene transcription. Therefore, a global overview of the transcriptional response of ERα-positive MCF-7 breast cancer cells to blocked proteasomal enzyme function was an essential component. The mRNA expression profiling was accomplished by DNA microarray analysis for a total of 13,323 genes.

Two main questions were addressed with this DNA microarray experiment. On the one hand, the influence of proteasome inhibition on estrogen-responsive genes was investigated. Thereby, most emphasis was placed on estrogen-activated genes. On the other hand, possible differences in the regulation of transcription upon chemical proteasome inhibition compared to knockdown of proteasomal subunits were scrutinized. Therefore, gene expression profiling was tested both after proteasome inhibition with Bortezomib as well as siRNA-mediated knockdown of the 20S proteasomal subunit components PSMB3 and PSMB5. siRNAs against these two independent proteasome subunits were utilized in order to minimize the effects of "off targets" of either of the siRNAs.

The heatmap (Figure 15) shows the fold-changes (FCs) in the expression of 807 genes which are significantly ($q < 0.05$) regulated by estrogen ($FC < -\log2\ (1.5)$ or $FC > \log2\ (1.5)$). 302 genes are upregulated while the expression of 505 genes is decreased upon treatment with estrogen for 24 h.

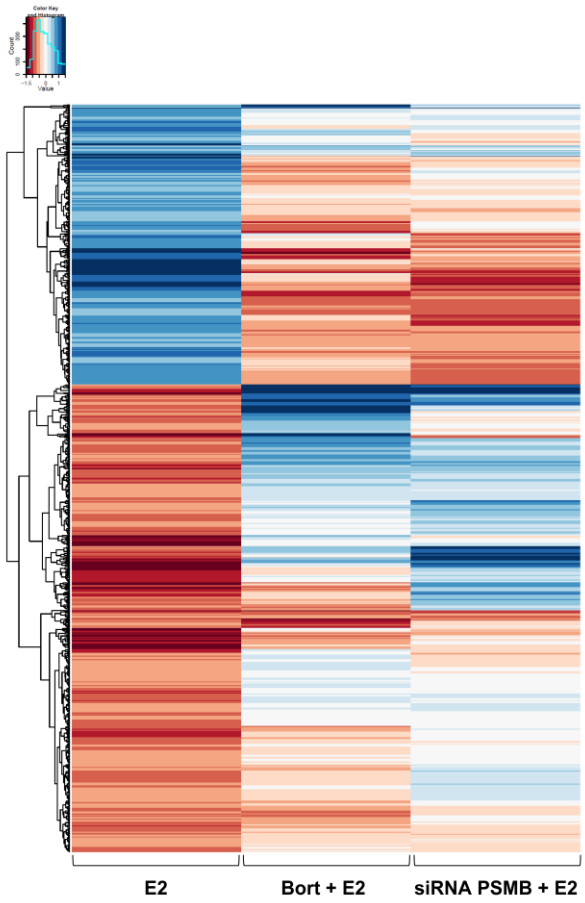


**Figure 15: mRNA expression profiling of estrogen-regulated genes.** The heatmap shows fold-changes in experiments 17ß-Estradiol *vs.* control (E2), Bortezomib + 17ß-Estradiol *vs.* 17ß-Estradiol (Bort + E2) and PSMB siRNA + 17ß-Estradiol *vs.* control siRNA + 17ß-Estradiol (siRNA PSMB + E2) (columns) for genes which are significantly ($q < 0.05$; q = p-values adjusted to FDR) regulated by 17ß-Estradiol (FC < -log2 (1.5) or FC > log2 (1.5)) (rows). For proteasome inhibition, MCF-7 cells were incubated in hormone-deprived growth medium for 24 h before pre-treatment with 50 nM Bortezomib or solvent (100% EtOH) for 15 min followed by stimulation with 10 nM 17ß-Estradiol for 24 h. For the siRNA samples, MCF-7 cells were reverse-transfected with 30 pmol PSMB3, PSMB5, control 1 or control 2 siRNA. After 24 h, growth medium was replaced by hormone-deprived 5% CSS medium and the next day cells were treated with 10 nM 17ß Estradiol for 24 h. Total mRNA was harvested and single-stranded cDNA fragments were generated, biotinylated and hybridized to Affymetrix DNA probe arrays. The arrays were scanned and analyzed as described. The color key is depicted on the top left side ranging from red marking downregulated to blue marking upregulated genes; mean values, $n = 3$. The PSMB knockdown samples depict all genes which were either up- or downregulated in all four following comparisons: PSMB3 *vs.* control 1, PSMB3 *vs.* control 2, PSMB5 *vs.* control 1 and PSMB5 *vs.* control 2 siRNAs.

The bulk of estrogen-upregulated genes were negatively influenced by concomitant proteasome inhibition using Bortezomib. The expression of 209 out of 302 estrogen-upregulated genes was decreased while only 19 genes were hyper-activated by Bortezomib treatment. A very similar distribution was demonstrated upon siRNA-mediated knockdown of 20S ß subunits PSMB3 and PSMB5. In that case, 171 out of these 302 estrogen-upregulated genes were decreased in their expression and merely 11 genes were super-induced (Figure 16).

The analysis of the effects of proteasome blockage on the 505 estrogen-repressed genes revealed that in case of proteasome inhibition a similar number of genes was up- or

downregulated (147 genes showed an increase in gene expression while 139 genes were even further downregulated by Bortezomib). Upon knockdown of PSMB subunits, 142 out of the 505 estrogen-repressed genes showed recovered gene expression and 26 genes were even stronger repressed in their expression.

| | | Bort + E2 | | |
|---|---|---|---|---|
| | | **- 1** | **0** | **+ 1** |
| E2 | **- 1** | 139 | 219 | 147 |
| | **0** | 2252 | 7977 | 2287 |
| | **+ 1** | **209** | 74 | **19** |

| | | PSMB + E2 | | |
|---|---|---|---|---|
| | | **- 1** | **0** | **+ 1** |
| E2 | **- 1** | 26 | 337 | 142 |
| | **0** | 1013 | 10071 | 1432 |
| | **+ 1** | **171** | 120 | **11** |

**Figure 16: Effect of proteasome inhibition and knockdown on genes which are significantly influenced by estrogen.** Numbers of genes depicted in the heatmap which are affected by estrogen, Bortezomib or the knockdown of 20S ß subunits. E2 genes: -1 = q < 0.05, FC < -log2 (1.5); +1 = q < 0.05, FC > log2 (1.5); Bort + E2/PSMB + E2 genes: -1 = q < 0.1, negative FC; +1 = q < 0.1, positive FC; E2, 17ß-Estradiol; Bort, Bortezomib; PSMB, combined genes of PSMB3 and PSMB5 siRNA-mediated knockdown.

As already stated, the emphasis was put on genes whose expression is activated by estrogen since these are more likely to be direct ERα target genes. Strikingly, there was a large overlap in estrogen-induced genes which were negatively affected by either proteasome inhibition or knockdown as shown in the Venn-diagram in Figure 17. Out of 234 genes which were upregulated by estrogen and decreased upon proteasome blockage, either by Bortezomib or by siRNA-mediated knockdown, 146 genes were common in both gene lists (which represent 69.9% in the Bortezomib and 85.4% in proteasome subunit knockdown gene list).

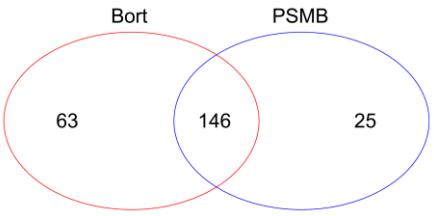


**Figure 17: Bortezomib induced proteasome inhibition and siRNA-mediated knockdown of 20S subunits show very similar effect on the bulk of estrogen-induced genes.** Venn-Diagram showing the overlap of genes that are significantly upregulated by 17ß-Estradiol (q < 0.05, FC > log2 (1.5)) and that are downregulated by Bortezomib and/or knockdown of PSMB3 and PSMB5 (negative FC); Bort, Bortezomib; PSMB depicts all genes which were either up- or downregulated in all four following comparisons: PSMB3 *vs.* control 1, PSMB3 *vs.* control 2, PSMB5 *vs.* control 1 and PSMB5 *vs.* control 2 siRNAs.

The results obtained by the mRNA expression profiling clearly demonstrate that a large proportion of genes which are significantly upregulated by estrogen are negatively influenced in their expression by concomitant proteasome blockage by either inhibition using Bortezomib or knockdown of 20S subunits.

## 4.3 ERα target gene expression and chromatin immunoprecipitation analysis

The results of the microarray experiment on target gene expression upon proteasome activity inhibition or depletion of proteasomal subunit components were verified in quantitative RT-PCR studies with primers for well-characterized estrogen-responsive genes and for genes which were highly regulated in previously described microarray analyses.

### 4.3.1 Proteasome knockdown affects ERα target gene expression similar to proteasome inhibition

The microarray experiment revealed that gene expression of most estrogen-activated ERα target genes was decreased upon proteasome inhibition as well as upon depletion of 20S proteasome subunits. The finding of mostly decreased target gene expression in proteasome siRNA-depleted cells was confirmed in qRT-PCR experiments.

First, the efficient knockdown of PSMB3 and PSMB5 was confirmed on mRNA levels (Figure 18B). Interestingly, PSMB3 knockdown resulted in increased PSMB5 mRNA levels and vice versa.

Figure 18A shows gene expression levels of a subset of estrogen-induced ERα target genes upon siRNA-mediated knockdown of the proteasome subunits PSMB3 or PSMB5 and a subsequent estrogen time course for 2, 6 or 24 h. In five out of six genes the expression was decreased upon proteasome knockdown. Especially after 24 h of estrogen treatment, *CXCL12*, *PGR* and *PKIB* genes showed a strong decrease in gene expression compared to the respective control transfected samples. *GREB1* and *WISP2* genes were only mildly affected by the knockdown of the two 20S proteasome subunits. The expression level after 24 h of estrogen treatment was still high compared to control-treated cells, but there was a general tendency of decreased expression compared to the control transfected samples, especially after knockdown of PSMB3. Only *TFF1* gene showed increased expression after PSMB5 and even stronger after PSMB3 knockdown. These results were again most pronounced after long exposure (24 h) to estrogen and consistent with the microarray analysis.

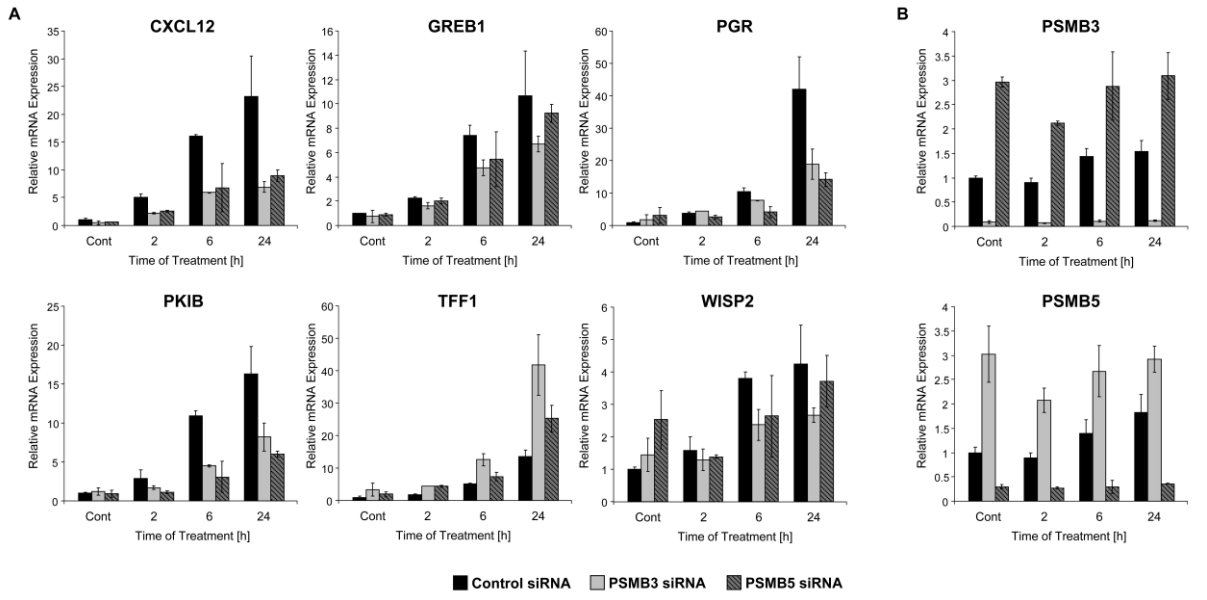


**Figure 18: Target gene expression analysis upon knockdown of proteasome subunit components PSMB3 and PSMB5.** MCF-7 cells were reverse-transfected with 30 pmol control, PSMB3 or PSMB5 siRNA for 72 h and treated with vehicle (Cont) or 10 nM 17ß-Estradiol for 2, 6 or 24 h. Isolated RNA was reverse-transcribed with random primers and analyzed by qPCR. Target gene expression levels were normalized to 28S ribosomal RNA, graphed relative to the control-transfected and vehicle-treated sample and expressed as "relative mRNA expression"; mean values + s.d., *n* = 2. (**A**) Relative mRNA gene expression levels of a subset of estrogen-upregulated ERα target genes. (**B**) Efficient knockdown of PSMB3 and PSMB5 was confirmed on mRNA level.

### 4.3.2 Various chemical proteasome inhibitors induce similar effects on the expression of estrogen-activated target genes

In the microarray experiment proteasome inhibition was accomplished by using the anticancer compound Bortezomib. To reveal potential differences between proteasome inhibitors in the regulation of estrogen-activated gene transcription, gene expression analysis via qRT-PCR upon treatment with three different chemical proteasome inhibitors was performed. In separate experiments, cells were pre-treated with Bortezomib, MG-132 or Epoxomicin and then cultured with estrogen for 2, 6 or 24 h. Gene expression was analyzed for a set of classical ERα target genes. With the intent to delineate if the effects of blocking proteasome activity on target gene transcription by either up- or downregulation were consistent between proteasome inhibitors, genes out of both categories were chosen: I) downregulated and II) upregulated upon proteasome inhibition. Three representative genes are depicted in Figure 19. *TFF1* gene represented the category of estrogen-responsive genes which were hyper-upregulated upon proteasome inhibition. Expression of *WISP2* and *GREB1* genes on the other hand was dramatically decreased after blocking proteolytic activity. Incubation of MCF-7 cells with each of the three mentioned proteasome inhibitors resulted in a similar

target gene expression pattern for each gene. The similar effects of the proteasome inhibitors on target gene expression was most pronounced after 24 h of treatment. These results (as well as data of more tested genes not shown) show that regardless of the mode of action of the proteasome inhibitors used (e.g. reversible *vs*. irreversible inhibition) or the specificity of inhibition (e.g. chymotrypsin-like *vs*. trypsin-like activity), the impact on ERα target gene expression was similar for all three inhibitors.

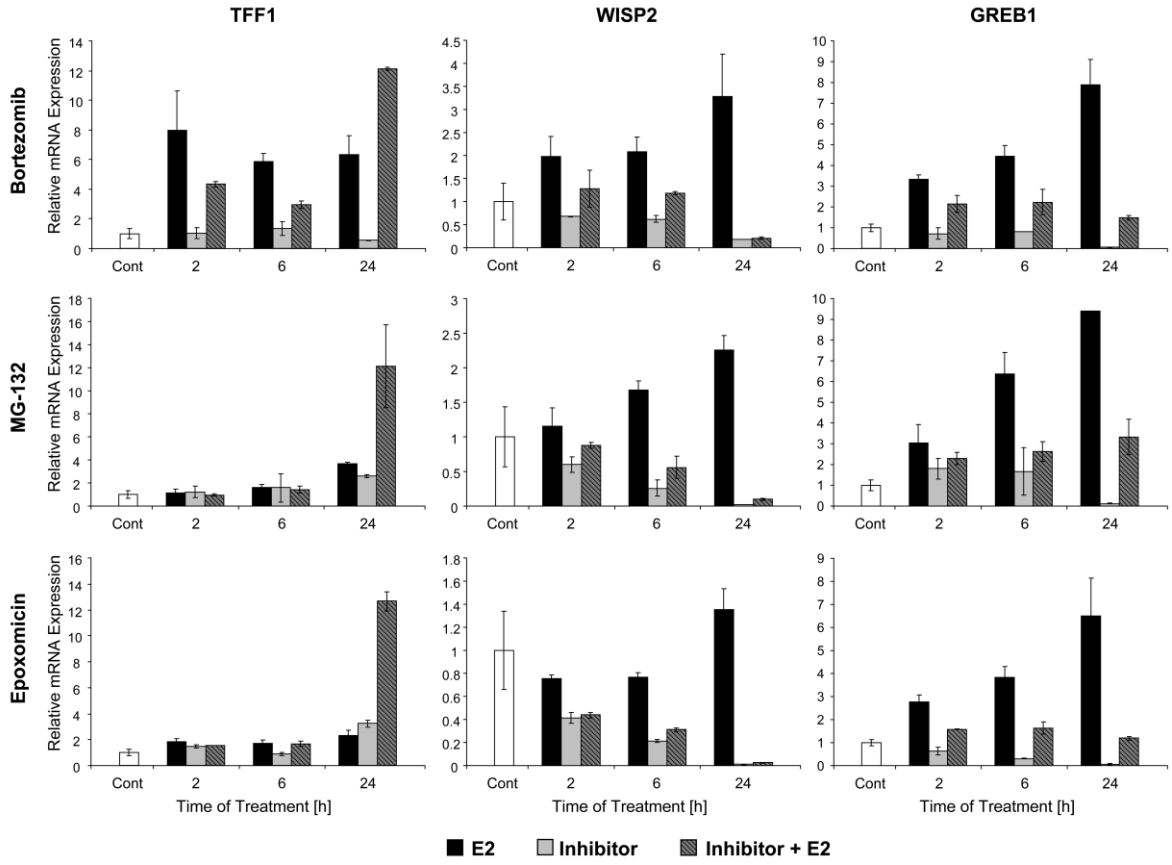


**Figure 19: Similar effects of three chemical proteasome inhibitors on ERα target gene expression.** MCF-7 cells were either pre-treated with 50 nM Bortezomib, 20 µM MG-132 or 1 µM Epoxomicin for 15 min (Inhibitor) followed by 10 nM 17ß-Estradiol (E2) for the indicated times. Total mRNA was harvested, reverse-transcribed with random primers and analyzed with qPCR. The expression levels of *TFF1* (hnRNA), *WISP2* and *GREB1* gene were normalized to 28 S ribosomal RNA (control). The normalized expression levels are graphed relative to control sample which is set to one. The expression levels are represented as "relative mRNA expression"; mean values + s.d., $n = 2$.

### 4.3.3 Proteasome inhibition with Bortezomib affects the expression of estrogen target genes as wells as ERα recruitment in a gene- and time-dependent manner

Further qRT-PCR experiments on more well-known estrogen-responsive genes were performed to confirm the mostly negative effects of Bortezomib on ERα-mediated gene transcription. ERα transcriptional activity was determined by analysis of endogenous *KRT13*, *PGR*, *TFF1*, *WISP2*, *CXCL12*, *GREB1* and *PKIB* gene expression (Figures 20A, 21A, 22A and 23A). In parallel, the association of ERα with estrogen responsive elements (EREs) in the presence of estrogen and/or Bortezomib was analyzed. The occupancy of EREs by ERα was assessed via chromatin immunoprecipitation (ChIP) assays on the tested estrogen-responsive genes (Figures 20B, 21B, 22B and 23B). The ChIP-ERE sites were based on published ChIP-Chip (Carroll *et al.*, 2006), ChIP-Seq (Welboren *et al.*, 2009) and ChIA-PET (Fullwood *et al.*, 2009) data and are depicted in the appendix section 6.1 (Figure 35).

Figure 20A shows gene expression analysis on four well-characterized estrogen-responsive genes. As already outlined in Figure 19, *TFF1* gene was one of the few estrogen-responsive genes which were hyper-activated upon 24 h proteasome inhibition. But interestingly, *TFF1* induction is decreased by proteasome inhibition after 2 h and 6 h compared to estrogen samples. The other three genes *KRT13*, *PGR* and *WISP2* were significantly downregulated upon Bortezomib treatment. As described before, these effects are most profound after 24 h of estrogen treatment. The most striking estrogen- and Bortezomib effects were detected for the progesterone receptor (*PGR*) gene. Exposure to estradiol for 24 h increased *PGR* gene expression 150-fold compared to control while concomitant inhibition of the proteasome decreased it again almost down to control level (3.2-fold).

ChIP analysis (Figure 20B) was performed to examine whether the observed effects on target gene expression correlated with ERα occupancy levels on the EREs. In case of these four representative genes, there was a clear correlation between ERα binding to the EREs and expression level of the particular genes at the 24 h time point. Proteasome inhibition resulted in a decreased ERα recruitment to the tested ERE of *KRT13*, *PGR* and *WISP2* gene after long-term treatment (24 h) and also reduced the respective gene expression level. In contrast, ERα binding to the ERE of *TFF1* gene was highly increased after inhibition of proteasomal activity which in turn correlated with increased *TFF1* gene expression after 24 h. However, after 6 h of treatment, Bortezomib exhibited a clear negative effect on ERα-induced gene transcription with no obvious effects on ERα occupancy.

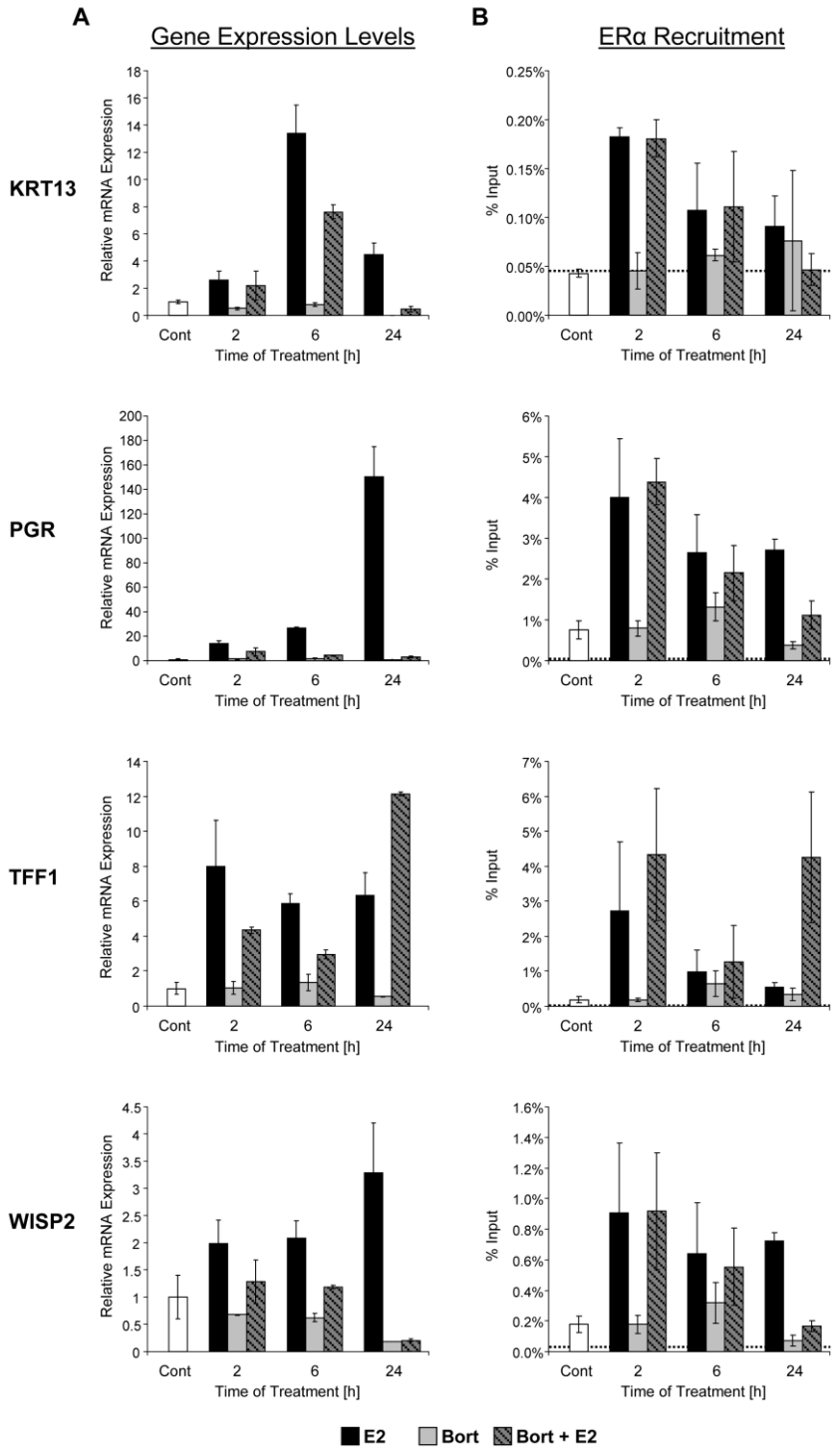


**Figure 20: Proteasome inhibition affects ERα target gene expression as well as ERα recruitment.** MCF-7 cells were pre-treated for 15 min with 50 nM Bortezomib (Bort) or 100% EtOH (vehicle, Cont) and then incubated with 10 nM 17ß-Estradiol (E2) for 2, 6 or 24 h. (**A**) ERα target gene expression analysis. Total mRNA was extracted and analyzed by random-primed qRT-PCR. The expression levels of estrogen target genes *KRT13*, *PGR*, *TFF1* (hnRNA) and *WISP2* were normalized to 28 S ribosomal mRNA, graphed relative to the control sample and expressed as "relative mRNA expression"; mean values + s.d., *n* = 2. (**B**) Chromatin immunoprecipitation (ChIP) analysis revealed a gene- and time-dependent effect of proteasome inhibition on ERα recruitment to target genes. ERα recruitment to *KRT13*, *PGR*, *TFF1* and *WISP2* genes was analyzed by ChIP analysis using a specific ERα antibody. Non-specific IgG was used to distinguish between specific and background binding (depicted as dotted line). ChIP samples were normalized to input samples and expressed as "percent input"; mean values + s.d., *n* = 3.

For three other ERα target genes (*CXCL12*, *GREB1* and *PKIB*), the ERα recruitment to more than one ERE was analyzed. Gene expression and ChIP results for these genes are displayed in Figures 21, 22 and 23.

*CXCL12* gene expression was also increased upon estrogen exposure but strongly decreased upon Bortezomib treatment (Figure 21A). The correlation between gene expression and ERα binding to three different EREs was not consistent for this particular gene (Figure 21B). While there was a decreased ERα occupancy of the second ERE after 24 h of treatment, ERα binding to the first and third ERE was not markedly changed upon proteasome inhibition.

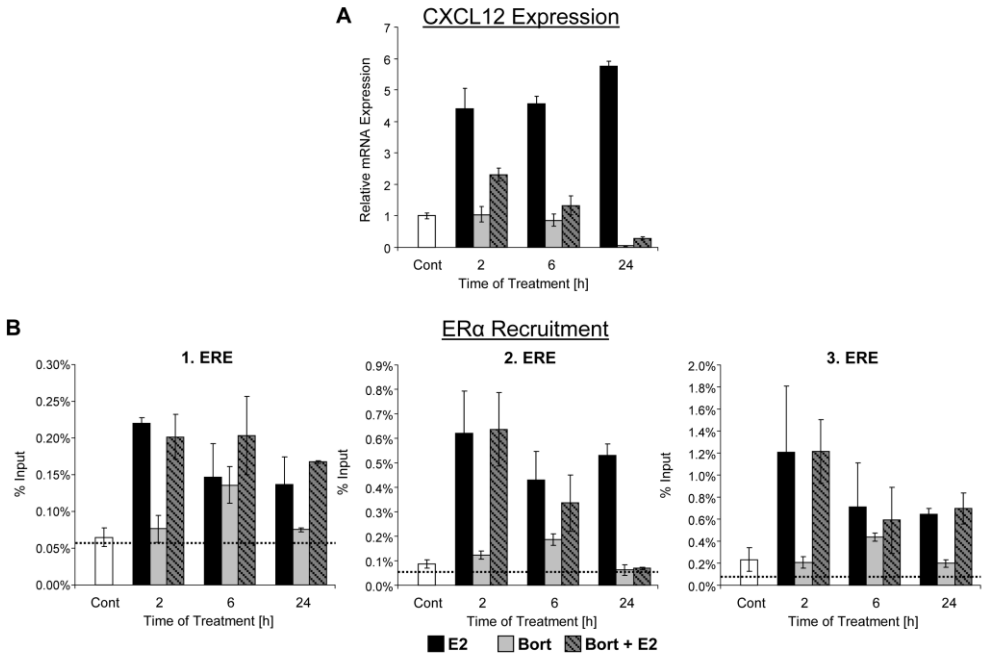


**Figure 21: Bortezomib decreases *CXCL12* gene expression and has an ERE-dependent impact on ERα occupancy.** (**A**) Gene expression analysis showed a strong decrease in *CXCL12* expression upon proteasome inhibition. (**B**) ChIP analysis on three different ERE binding sites revealed an ERE site-dependent ERα occupancy on that gene. For gene expression as well as ChIP analysis please refer to Figure 20 (**A**) and (**B**), respectively; mean values + s.d., $n = 2$ for gene expression and $n = 3$ for ChIP.

Like most of the estrogen-induced ERα target genes, *GREB1* expression was decreased upon concomitant proteasome inhibition with Bortezomib, especially after 24 h of treatment (Figure 22A). But ChIP analysis revealed that the ERα was still present on both tested EREs (Figure 22B). In fact, after 24 h ERα occupancy at the first ERE was slightly decreased upon proteasome inhibition while it was increased at the second ERE. But on both sites ERα binding was well above IgG background binding, meaning also for this gene there was no apparent correlation between ERα recruitment and respective target gene expression.

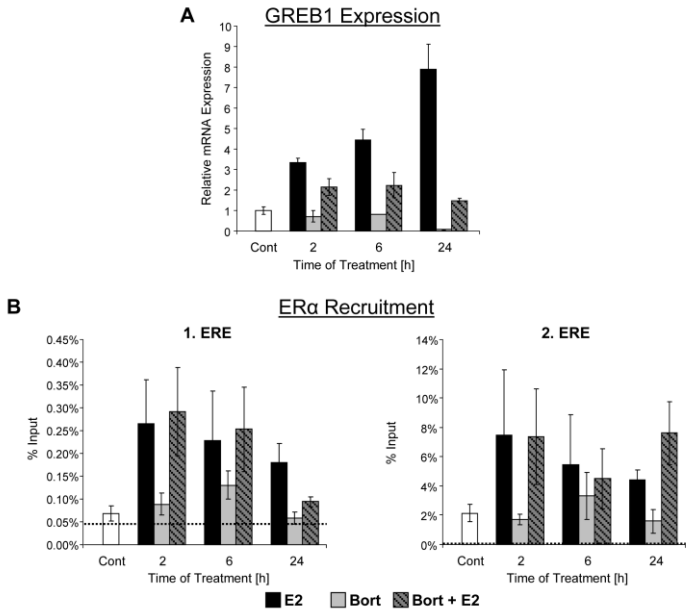


**Figure 22: Despite retained ERα occupancy, *GREB1* gene expression is decreased upon proteasome inhibition.** (**A**) Gene expression analysis revealed a decrease in *GREB1* expression levels upon Bortezomib treatment. (**B**) ChIP analysis on two different EREs revealed again an ERE site-dependent ERα occupancy. For gene expression as well as ChIP analysis please refer to Figure 20 (**A**) and (**B**), respectively; mean values + s.d., $n = 2$ for gene expression and $n = 3$ for ChIP.

For the last of the depicted ERα target genes, there was again a correlation between ERα binding to two tested EREs and *PKIB* expression (Figure 23A and B). Both, receptor binding and gene expression were decreased upon proteasome inhibition using Bortezomib. However, as with all four genes shown in Figure 20 (*KRT13*, *PGR*, *TFF1* and *WISP2*) as well as several of the EREs for *CXCL12* (Figure 21), *GREB1* (Figure 22) and *PKIB* (Figure 23), there were clear effects of proteasome inhibition on target gene induction at 6 h without any significant effects on ERα occupancy.

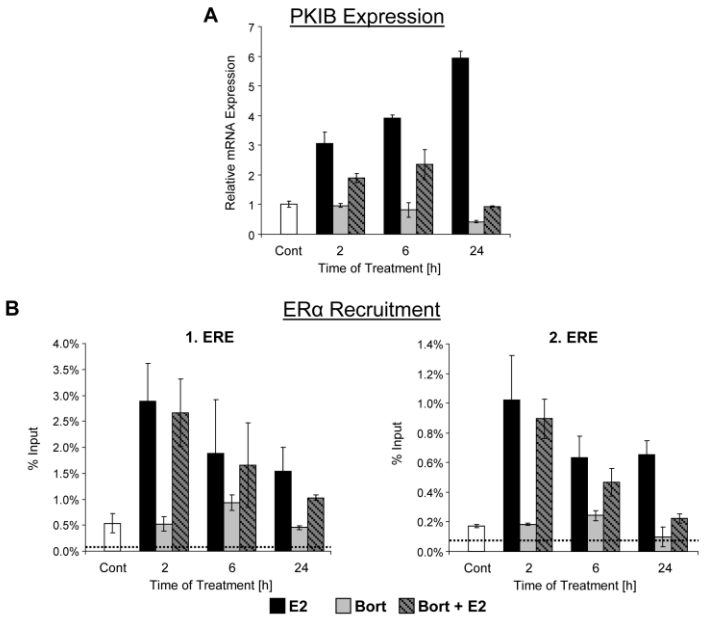


**Figure 23: Decrease in *PKIB* gene expression correlates with a decrease in ERα recruitment to both tested EREs.** For gene expression (**A**) as well as ChIP analysis (**B**) please refer to Figure 20 (**A**) and (**B**), respectively; mean values + s.d., *n* = 2 for gene expression and *n* = 3 for ChIP.

Further gene expression and ChIP studies for more ERα target were performed (data not shown). These analyses confirmed that for the bulk of estrogen-activated genes, expression is decreased upon Bortezomib treatment. Additional tested genes belonging to that class are *NPY1R*, *Cyclin D1* and *CYP1B1*. Other genes which were upregulated by estrogen were not significantly affected by Bortezomib treatment, e.g. *RAB31*. But also additional genes were tested which, like *TFF1*, are estrogen-induced and even super-induced upon Bortezomib exposure, e.g. *AREG* and *FRK*. However, unlike *TFF1*, the expression of these two genes was also induced by proteasome inhibition alone and therefore, probably indicate a mechanism of regulation independent of ERα. Also estrogen-repressed genes were tested and it could be shown that proteasome inhibition with Bortezomib recovered the estrogen-induced repressive effect for the genes tested (*EPAS*, *LIPH* and *GDF15*). But also for these genes, the Bortezomib-induced effect seemed to be ERα-independent since gene expression was increased by Bortezomib in the absence of estrogen. Since the scope of this study was the analysis of proteasome inhibition on estrogen-activated gene expression, the gene expression data of estrogen-repressed genes are not shown and further mechanistic analyses were not performed.

### 4.3.4 Proteasome subunit knockdown affects expression of estrogen target genes and ERα recruitment in a gene- and time-dependent manner similar to proteasome inhibition

In accordance with proteasome inhibition using Bortezomib (Figures 20-23), the correlation between gene expression and estrogen receptor binding to EREs was also analyzed after knockdown of PSMB3 (Figure 24). The expression patterns of the three represented genes (*GREB1*, *TFF1* and *WISP2*) were similar to the ones obtained in the proteasome inhibition studies. Again, *TFF1* gene was further upregulated and *GREB1* and *WISP2* showed a decrease in gene expression upon knockdown of PSMB3 (Figure 24A). For the latter two genes the effect of proteasome subunit knockdown was not as pronounced as the effect upon proteasome inhibition with Bortezomib.

Furthermore, ChIP analysis (Figure 24B) revealed that ERα recruitment to these three genes was comparable to the proteasome inhibition data. ERα binding to the tested *GREB1*-ERE (corresponds to the 2. *GREB1*-ERE in Figure 22) and *TFF1*-ERE was similar although weaker than after proteasome inhibition (Figure 20 and 22). The ERα binding to *WISP2*-ERE was slightly different in both experimental setups. While there was highest ERα recruitment after 2 h of estrogen treatment in the proteasome inhibition experiment (Figure 20), ERα binding increased up to 6 h in the knockdown experiment. Further, ERα binding was markedly decreased after 24 h Bortezomib treatment, whereas it rather remained unchanged at that time point after PSMB3 knockdown (Figure 24B).

These data implicate that the effects of proteasome inhibition and knockdown of proteasomal subunit components on ERα target gene expression as well as ERα binding to EREs are similar but the effects upon proteasome knockdown are weaker and in some cases slightly different than after proteasome inhibition.

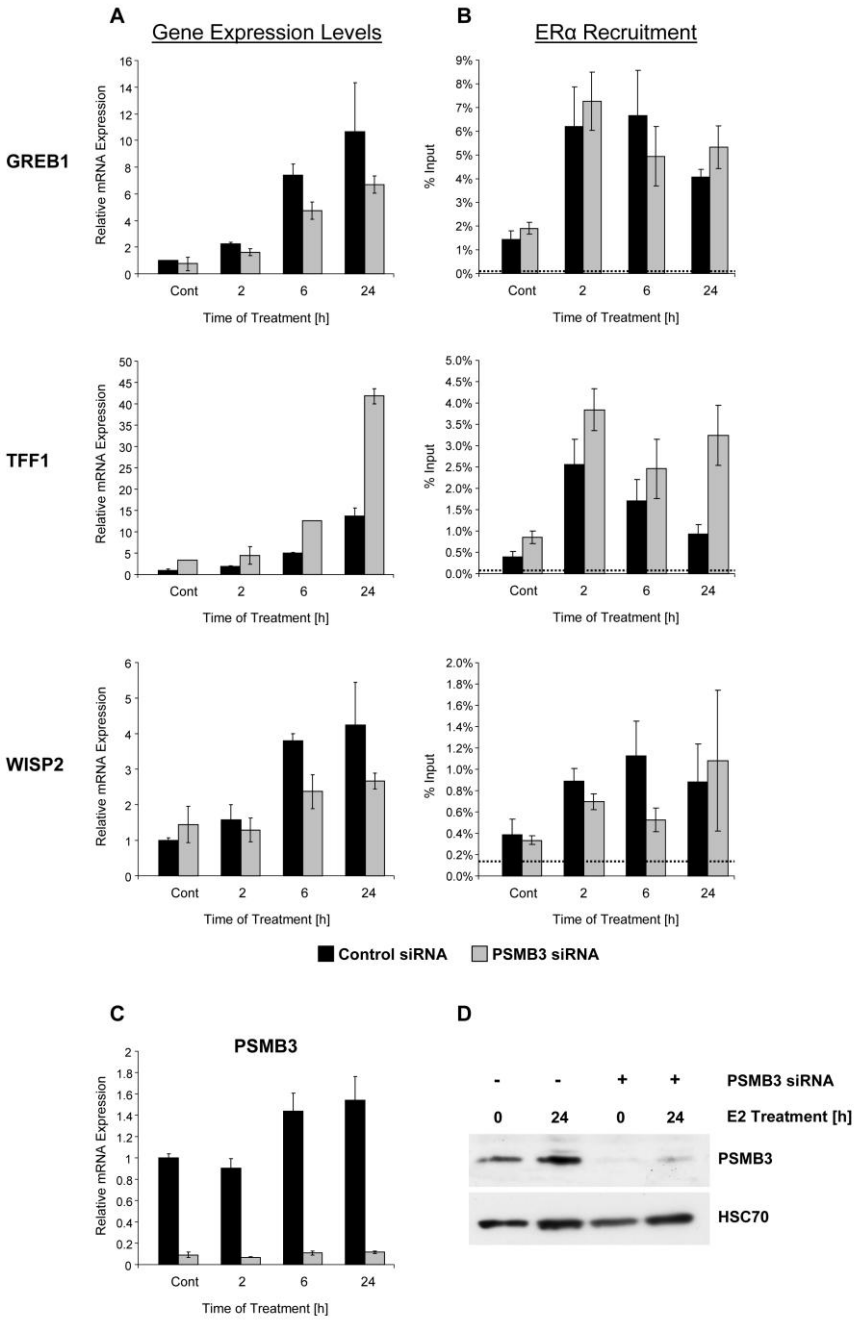


**Figure 24: 20S proteasome subunit depletion affects estrogen-responsive gene expression and ERα recruitment to these target genes.** MCF-7 cells were transfected with 30 pmol control or PSMB3 siRNA for 72 h and treated with 10 nM 17ß-Estradiol for 2, 6 or 24 h. (**A**) Target gene expression analysis was performed as described in Figure 20A. (**B**) ERα binding to EREs on target genes was examined via ChIP analysis as described in Figure 20B. Mean values + s.d., $n = 2$ for gene expression and $n = 3$ for ChIP. (**C**), (**D**) Efficient knockdown of PSMB3 was confirmed on the mRNA level (**C**) as well as on the protein level (**D**). The Western blot analysis was performed on whole MCF-7 ChIP lysates. Blots were probed with antibodies for PSMB3 and HSC70 as loading control.

## 4.4 Effect of Bortezomib on ERα mobility

Proteasome inhibition with MG-132 leads to an immobilization of ERα in the nucleus (Reid *et al.*, 2003; Stenoien *et al.*, 2001). Therefore, we sought to determine the effect which Bortezomib has on the mobility of unliganded as well as estrogen-bound ERα. To investigate this effect, a fluorescence recovery after photobleaching (FRAP) analysis was performed with the help of Dr. Chieh Hsu in the laboratory of Prof. Dr. Mikael Simons at the MPI for Experimental Medicine.

Before the actual FRAP experiment, the expression of the correct EGFP-hERα fusion protein was investigated by transient transfection. The ERα-positive MCF-7 and ERα-negative H1299 cells were either transfected with the pEGFP-hERα construct or the empty pEGFP vector as a control. Whole protein extracts were then analyzed for ERα protein level via Western blot analysis using an ERα-specific antibody. As shown in Figure 25, in H1299 cells indeed ERα protein was only detectable upon transfection with the pEGFP-hERα construct but not upon transfecting the control vector (pEGFP) alone. The protein band was detected at about 93 kDa which reflected the ERα fused to GFP protein (ERα = 66 kDa, GFP = 27 kDa). In pEGFP-transfected MCF-7 cells, the endogenous ERα protein was clearly detectable. Upon transfection with the pEGFP-hERα construct, both endogenous ERα (66 kDa) as well as the EGFP-hERα protein (93 kDa) were detected with the used ERα antibody.

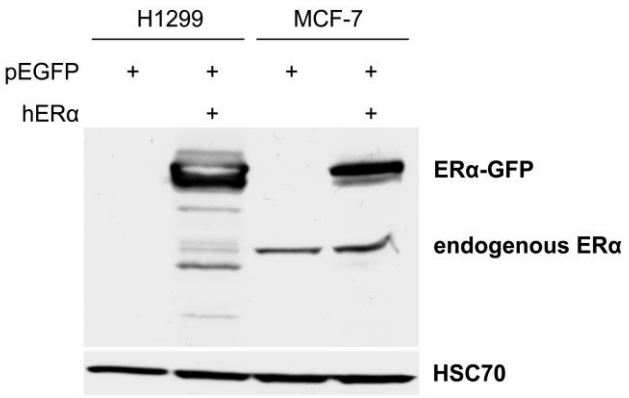


**Figure 25: Efficient overexpression of EGFP-hERα protein in H1299 and MCF-7 cells.** The hERα construct was cloned into a pEGFP vector. Transfection efficiency was investigated by transfecting H1299 (ERα-negative) and MCF-7 (ERα-positive) cells with either pEGFP-ERα plasmid or the empty pEGFP vector as a control. 24 h after transfection, whole protein extracts were analyzed by Western blot analysis using a specific antibody against ERα. The antibody recognizes both endogenous (66 kDa) and EGFP-tagged ERα (~ 93 kDa). HSC70 serves as loading control.

After confirmation of overexpression of the correct EGFP-hERα fusion protein, MCF-7 cells were again transiently transfected with the EGFP-hERα construct for FRAP analyses. The EGFP-hERα fusion protein exhibited nuclear localization.

In order to reproduce already published data on ERα immobilization after proteasome inhibition using MG-132 (Reid *et al.*, 2003; Stenoien *et al.*, 2001), pEGFP-hERα-transfected MCF-7 cells were treated with either control or MG-132 for 12 h. As depicted in Figure 26, the recovery after photobleaching of the untreated EGFP-hERα was very fast and already right after photobleaching (0 s in Figure 26) the bleached area was only visible as a faint shade. In contrast, MG-132 treatment resulted in the already described immobilization of the EGFP-hERα in the nucleus. The bleached area was still clearly visible after 30 s which indicated to a highly immobile receptor.

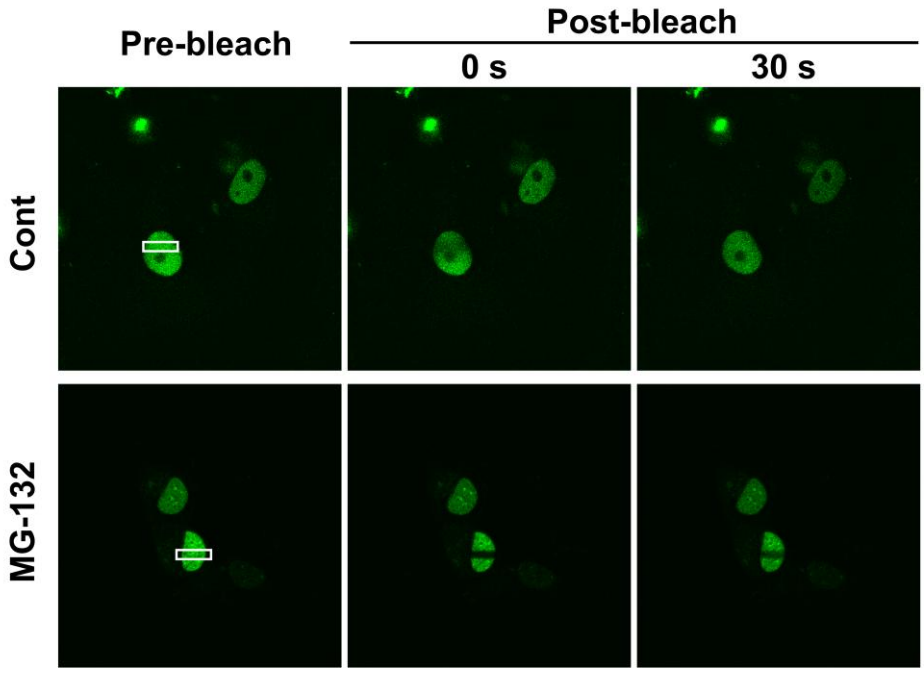


**Figure 26: MG-132 immobilizes the ERα in the nucleus.** MCF-7 cells, transiently expressing the pEGFP-hERα fusion protein, were treated with either DMSO (vehicle, Cont) or 20 µM MG-132 for 12 h before the fluorescence recovery after photobleaching (FRAP) analysis. The images show single representative nuclei before bleaching (pre-bleach), 0 s and 30 s after bleaching (post-bleach). The bleached area is indicated as a white rectangle in the first picture.

After establishing the conditions for the FRAP experiment and reproducing the MG-132 results, we sought to determine the effects of Bortezomib on the mobility of EGFP-hERα. Therefore, pEGFP-hERα-transfected MCF-7 cells were treated with control, estrogen, Bortezomib or the combination of estrogen and Bortezomib and for each condition 36-41 nuclei from three independent experiments were analyzed via FRAP. As depicted in Figure 27, upon photobleaching the unliganded EGFP-hERα protein showed again a fast recovery with a time constant of 6.29 s (Figure 27B). After treatment with 17ß-Estradiol for 6 h, the bleached zone persisted longer than in control nuclei with a time constant of 10.15 s. This ligand-mediated reduction in ERα mobility was in accordance with the already published data (Reid *et al.*, 2003; Stenoien *et al.*, 2001). Similar to the estrogen-induced reduction of ERα mobility, Bortezomib treatment also slowed down ERα recovery rate and increased the time constant to 9.01 s. The negative effect on ERα mobility caused by estrogen or Bortezomib alone was amplified by the combined treatment. Time constant was increased more than two-fold (14.81 s) compared to control, meaning that ERα mobility was affected both by ligand-binding and appropriate functioning of the proteasome.

Interestingly, these FRAP results revealed that the magnitude of the negative effect on ERα mobility depends on the proteasome inhibitor used. While MG-132 immobilized unliganded as well as estrogen-bound ERα in the nucleus completely (Figure 26) and (Reid *et al.*, 2003; Stenoien *et al.*, 2001), ERα still retained some mobility even in the presence of Bortezomib (Figure 27).

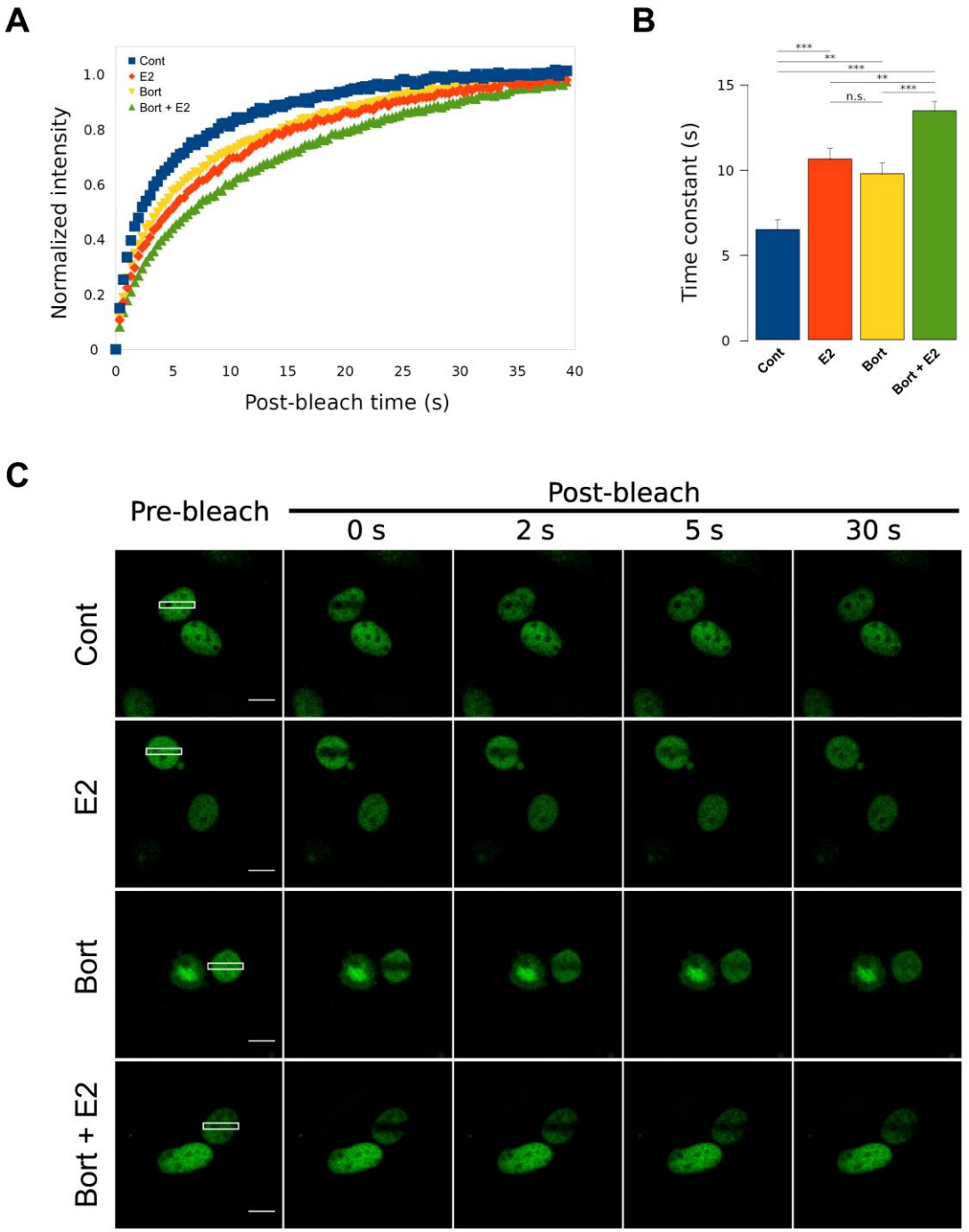


**Figure 27: Proteasome inhibition with Bortezomib decreases ERα mobility in the nucleus.** MCF-7 cells, transiently expressing the pEGFP-hERα fusion protein, were pre-treated either with vehicle (100% EtOH, Cont) or 50 nM Bortezomib (Bort) for 15 min and then subjected to a 6 h treatment with 10 nM 17ß-Estradiol (E2). Fluorescence recovery after photobleaching (FRAP) analysis was performed. (**A**) The FRAP signal in each treatment was normalized with the initial intensity after bleaching (t = 0) set to zero and the theoretical maximum value set to one. The averaged values in each treatment are shown. (**B**) Time constant of each treatment. The error bars represent SEM; *n* = 36-41 cells from three independent experiments; n.s., non-significant; **0.001 < p < 0.01; ***p < 0.001; Welch's two sample *t* test. (**C**) Images showing single representative nuclei were obtained before bleaching (pre-bleach) and after the indicated time points (post-bleach). The bleached area is indicated as a white rectangle in the first picture; bar = 10 µm.

## 4.5 Chromatin conformation capture analysis

Estrogen stimulation induces the interaction of promoter and distal ERα binding sites via long distance chromatin interactions (Bretschneider *et al.*, 2008; Carroll *et al.*, 2005). Furthermore, this long range interaction is not restricted to single genes but could also be shown between different ERα target genes on different chromosomes (Hu *et al.*, 2008). Importantly, the spatial proximity of various ERα binding sites as well as chromosomal reorganization seems to be required for maximal gene transcription.

After showing that proteasome inhibition with Bortezomib decreased gene expression for the vast majority of estrogen-induced target genes and reduced ERα mobility without a direct correlation to ERα binding, we hypothesized that the blockage of proteasome activity may specifically affect the chromosomal organization in the 3-dimensional space of the nucleus.

To answer this question, the method of choice for analyzing genomic organization, chromosome conformation capture (3C), was performed. Based on already published 3C data, long-range interaction analysis was tested on the *GREB1* locus on chromosome 2 (Pan *et al.*, 2008) and the *CXCL12* locus on chromosome 10 (Fullwood *et al.*, 2009). MCF-7 cells were pre-treated with vehicle or 50 nM Bortezomib and stimulated with 10 nM 17ß-Estradiol for 24 h. The 3C assay was performed as described in the methods section (3.2.8), and interacting DNA was analyzed via qPCR using TaqMan-based real-time PCR.

Figure 28A shows the long-range interactions on *GREB1* gene between an anchor site (1) and either a negative control site (C) or an experimental site (5). In Figure 28B, the results of the 3C experiment for *GREB1* interactions are depicted as bar graphs. The interaction of site (1) and control site (C) (1/C) was only slightly increased upon estrogen treatment (3.5-fold compared to control). Proteasome inhibition with or without concomitant estrogen stimulation did not markedly change this increased interaction although there was a hint of a decrease. More remarkable were the results obtained from the interaction analysis between sites (1) and (5) (1/5). Estrogen stimulation induced a 9.7-fold increase in interaction compared to control. This enhanced long-range interaction upon estrogen stimulation was consistent with previous reports (Fullwood *et al.*, 2009; Pan *et al.*, 2008). Interestingly, proteasome inhibition using Bortezomib resulted in a distinct decline of the estrogen-induced long-range interactions between the anchor site (1) and site (5) (from 9.7-fold down to 3.5-fold).

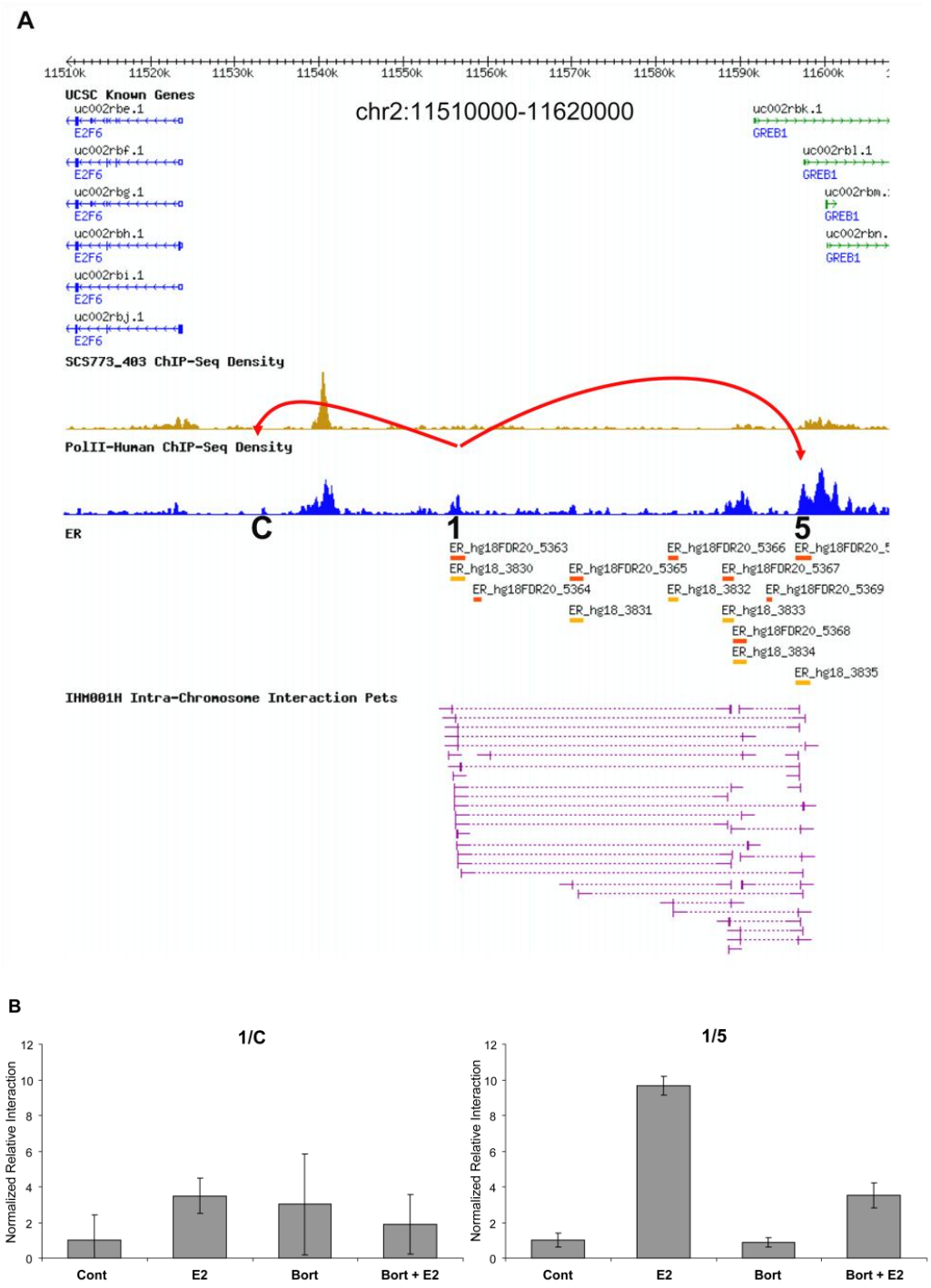


**Figure 28: Proteasome inhibition limits estrogen-induced long-range interaction on *GREB1* locus.** Chromatin conformation capture (3C) analysis at the *GREB1* locus. (**A**) Screenshot of ChIA-PET genome browser with the three chosen 3C testing sites. These sites were chosen based on their 3C interactions in (Pan *et al.*, 2008). Location (1) is an anchor site for the interaction with either the negative control site (C) or the experimental site (5). (**B**) 3C experiment results. MCF-7 cells were pre-treated with 50 nM Bortezomib or vehicle (100% EtOH) for 15 min, followed by 10 nM 17ß-Estradiol treatment for 24 h. Formaldehyde-crosslinked chromatin was harvested, digested with BtgI enzyme and intramolecular ligation was performed with T4 DNA ligase. After de-crosslinking via Proteinase K treatment at a higher temperature to remove chemical crosslinks, DNA was purified and the samples were subsequently quantified by qPCR using a TaqMan probe and primers specific for the ligated restriction fragments. In order to compare signal intensities in a quantitative manner, a *GREB1* BAC clone was digested with BtgI and ligated in accordance with the 3C template. The serial dilution of the BAC clone DNA served as standard curve in the PCR analysis (displayed in the appendix section 6.2). 3C template values were normalized with values from an internal control site that lies between BtgI sites. The normalized levels were graphed relative to the control sample (set to 1) and represented as "normalized relative interaction"; mean values + s.d., $n = 3$.

In order to test if the effects observed on the *GREB1* gene reflect a general inhibition of ERα-dependent long-range interactions a second gene *CXCL12* was selected and interactions were analyzed between an anchor site (1), a negative control site (C) and two experimental sites (2) and (3) (Figure 29A).
As depicted in Figure 29B, 3C analysis on *CXCL12* revealed similar results as obtained for *GREB1* locus. While estrogen did not have an effect on the interaction between the anchor (1) and control sites (C), it resulted in an increase in the interaction of site (1) and (2) (5.1-fold compared to control) and a significantly stronger positive effect on the interaction between sites (1) and (3) (17.5-fold compared to control). And also in case of *CXCL12* gene, simultaneous proteasome inhibition using Bortezomib resulted in a decrease of the estrogen-induced long-range interactions (from 5.1-fold down to 2.6-fold for the (1/2) interaction and from 17.5-fold down to 6-fold for the (1/3) interaction).

These results imply that proteasome activity is necessary for proper estrogen-induced intrachromosomal long-range interactions of the *GREB1* and *CXCL12* genes.

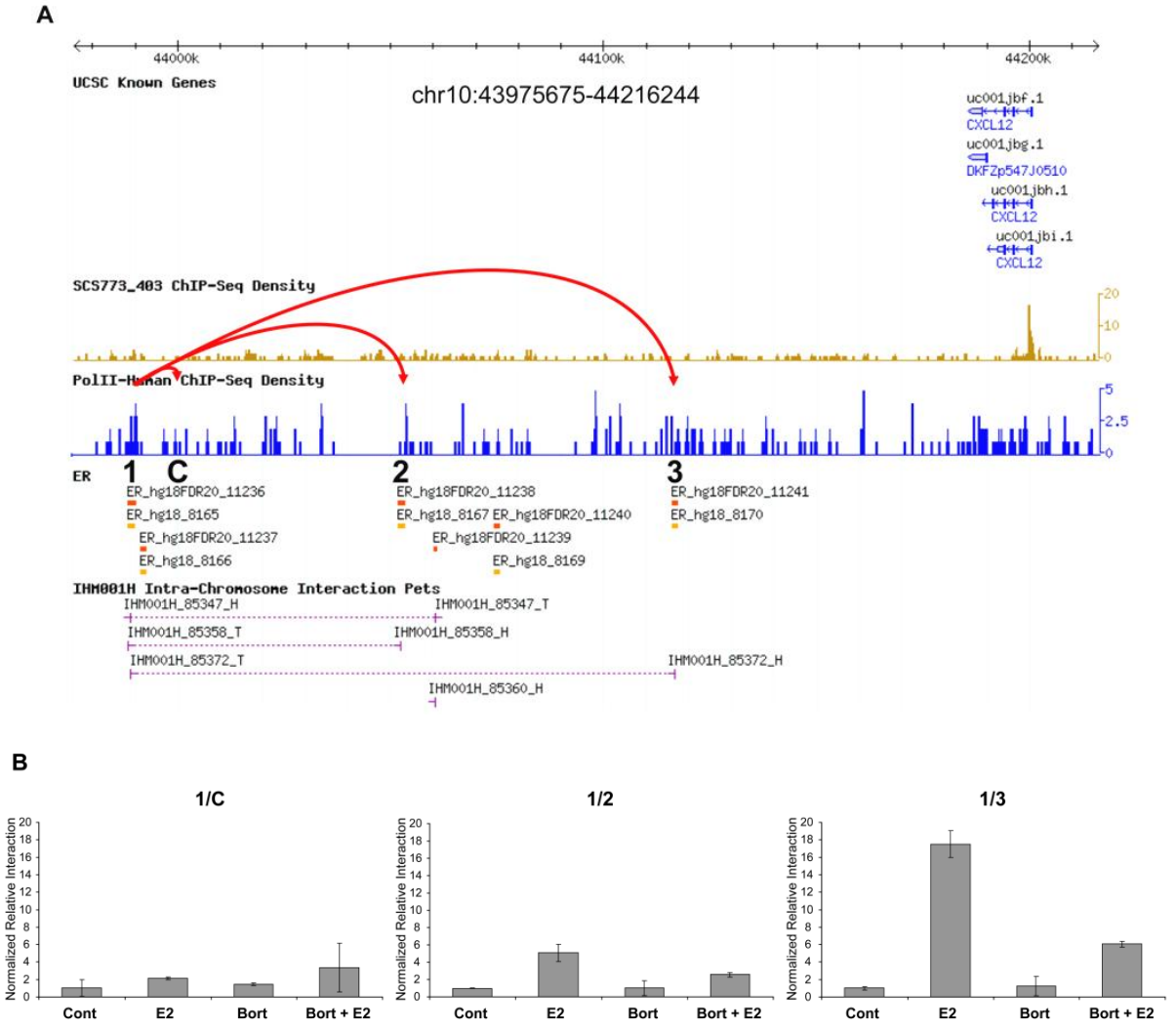


**Figure 29: Bortezomib treatment also inhibits estrogen-induced long-range interaction on *CXCL12* locus.** Chromatin conformation capture (3C) analysis at the *CXCL12* locus. (**A**) Screenshot of ChIA-PET genome browser with the four selected 3C testing sites. These sites were chosen based on their ChIA-PET interactions in (Fullwood *et al.*, 2009). Location (1) is an anchor site for the interaction with either the negative control site (C) or the experimental sites (2) and (3). (**B**) 3C experiment results. 3C analysis was performed as described in Figure 28 using a *CXCL12* BAC clone and specific primers and a TaqMan probe for quantitative analyses. 3C template values were normalized to an internal control site on the *GREB1* locus that lies between BtgI sites. The normalized levels were graphed relative to the control sample and represented as "normalized relative interaction"; mean values + s.d., $n = 3$.

## 4.6 Effect of proteasome inhibition and knockdown on glucocorticoid receptor-mediated gene induction

All previously described results were obtained from experiments with MCF-7 breast cancer cells. The complex role of the ubiquitin-proteasome system in the regulation of estrogen-responsive genes was demonstrated. The described results are an important basis for further studies on the effect of Bortezomib on ERα-mediated transcription especially in regard to anti-tumor therapy of ERα-positive breast cancer.

But nevertheless, it is desirable to know if the described results in ERα-mediated transcription also apply to other nuclear hormone receptors. Thus, the effects of proteasome inhibition and knockdown of 20S proteasome subunit components were also analyzed in glucocorticoid receptor (GR)-induced transcription. Proteasome inhibition and knockdown effects in GR-positive A549 cells were first tested on protein level followed by target gene expression studies and completed by investigating GR recruitment to various known GR target genes via chromatin immunoprecipitation (ChIP) analysis.

### 4.6.1 Proteasome inhibition or knockdown of proteasomal subunit components increases the amount of polyubiquitinated proteins

Consistent with the studies in MCF-7 cells, the pharmacological inhibition of the proteasome was tested using three different proteasome inhibitors in A549 cells. Treating A549 cells with either MG-132, Bortezomib or Epoxomicin for 4 h and subsequent analysis of whole protein extracts via Western blot analysis revealed an increase of polyubiquitinated proteins ($Ub_n$) upon treatment with each of the three inhibitors (Figure 30A). Furthermore, in parallel to MG-132 studies (Wallace and Cidlowski, 2001) treatment with Dexamethasone and concomitant inhibition of the proteasome with Bortezomib showed a partial blockage of ligand-induced GR degradation (Figure 30B). In accordance with the ERα studies, the effects of 20S proteasomal subunit depletion were examined and compared to the effects obtained with proteasome inhibition. As depicted in Figure 30C, PSMB3 and PSMB5 siRNAs efficiently reduced the amounts of the corresponding proteins in A549 cells. Again, also proteasome subunit depletion by siRNA-mediated knockdown increased the amount of polyubiquitinated proteins ($Ub_n$).

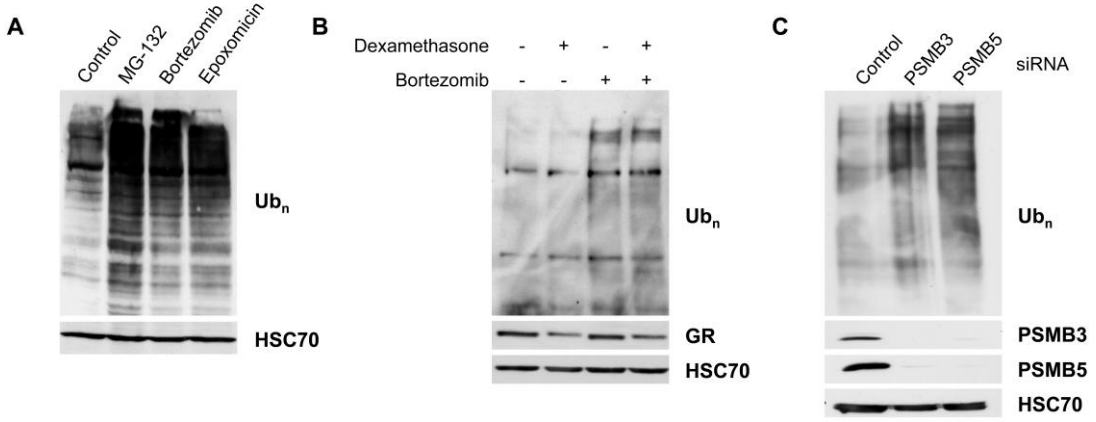


**Figure 30: Equivalent to MCF-7, also in A549 cells proteasome inhibition and knockdown of proteasome subunit components increase the amount of polyubiquitinated proteins and Bortezomib blocks the hormone-induced receptor downregulation. (A)** A549 cells were treated with 20 µM MG-132, 50 nM Bortezomib or 1 µM Epoxomicin for 4 h. Whole protein extracts were analyzed by Western blot analysis using a specific antibody against polyubiquitinated proteins. $Ub_n$ indicates higher molecular weight ubiquitinated proteins. (**B**) Upon 15 min pre-treatment with 50 nM Bortezomib, A549 cells were subjected to 100 nM Dexamethasone for 6 h. Western blot analysis was performed against polyubiquitinated protein and GR protein levels. (**C**) A549 cells were transfected with 30 pmol control, PSMB3 or PSMB5 siRNA for 72 h and protein levels of the indicated proteins were analyzed via Western blot. HSC70 serves as a loading control in (A), (B) and (C).

### 4.6.2 Bortezomib has no effect on RNA polymerase II protein levels or phosphorylation status

The mechanisms by which the UPS promotes or inhibits transcription are still poorly understood. One suggested mechanism for an enhanced GR target gene expression after proteasome inhibition is a correlated increase in the global levels of phosphorylated RNA polymerase II (RNAPII) (Kinyamu and Archer, 2007). Before monitoring the effect of proteasome inhibition on the regulation of GR target gene expression it was therefore of interest to reproduce these published results and also check RNAPII, RNAPII P-Ser2, RNAPII P-Ser5 and RNAPII P-Ser7 protein levels in A549 cells upon proteasome inhibition using either MG-132 or Bortezomib.

Indeed, treatment with MG-132 as a positive control seemed to slightly increase RNAPII P-Ser2 protein levels (Figure 31) which is generally associated with the elongation competent form of RNAPII and thus likely indicates enhanced target gene expression. But this finding of increased RNAPII P-Ser2 protein levels is less pronounced as in the published data. Total RNAPII, RNAPII P-Ser5 and RNAPII P-Ser7 protein levels on the other hand did not increase after proteasome inhibition using MG-132. RNAPII P-Ser7 levels rather seemed to decrease slightly. Similar to the studies in MCF-7 cells (Figure 6), also in A549 cells

proteasome inhibition using Bortezomib did not alter total RNAPII, RNAPII P-Ser2, RNAPII P-Ser5 and RNAPII P-Ser7 protein levels (Figure 31). These results indicate that the proposed transcriptional regulatory mechanism via changes in RNAPII phosphorylation upon proteasome inhibition cannot be applied to Bortezomib.

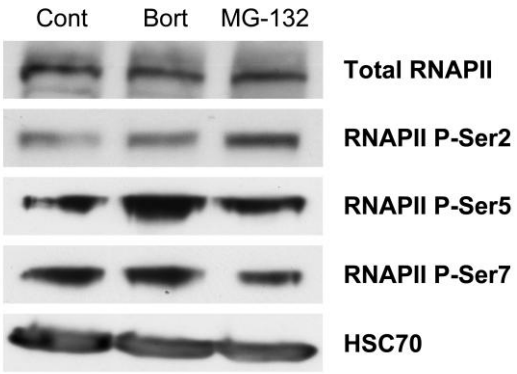


**Figure 31: Bortezomib has no effect on the levels of total and Ser2-, Ser5- and Ser7-phosphorylated RNAPII.** A549 cells were treated either with solvent (100% EtOH + DMSO), 50 nM Bortezomib or 1 µM MG-132 for 20 h. Whole protein extracts were harvested and analyzed via Western blot analysis with the indicated antibodies. HSC70 is shown as loading control. Bort, Bortezomib; Cont, Control; RNAPII, RNA polymerase II; RNAPII P-Ser2, RNA polymerase II phosphorylated at Ser2; RNAPII P-Ser5, RNA polymerase II phosphorylated at Ser5; RNAPII P-Ser7, RNA polymerase II phosphorylated at Ser7 of the CTD.

### 4.6.3 Effects of Bortezomib-induced proteasome inhibition and proteasomal knockdown on GR target gene expression and GR recruitment

#### 4.6.3.1 Proteasome inhibition induces altered gene expression and GR binding

Next, the question was addressed if proteasome inhibition with Bortezomib has an impact on GR target gene expression. As with the ERα studies, GR target gene expression and GR recruitment to several glucocorticoid-inducible genes were tested. The GRE-ChIP primers were obtained from or based on previous studies (So *et al.*, 2007; Wang *et al.*, 2004). In Figure 32, both "relative mRNA expression" levels (Figure 32A) as well as the binding of the GR to the glucocorticoid responsive elements (GREs) (Figure 32B) of four target genes were combined. The represented genes *FKBP5*, *GILZ*, *SGK* and *SLC* are well-characterized GR target genes.

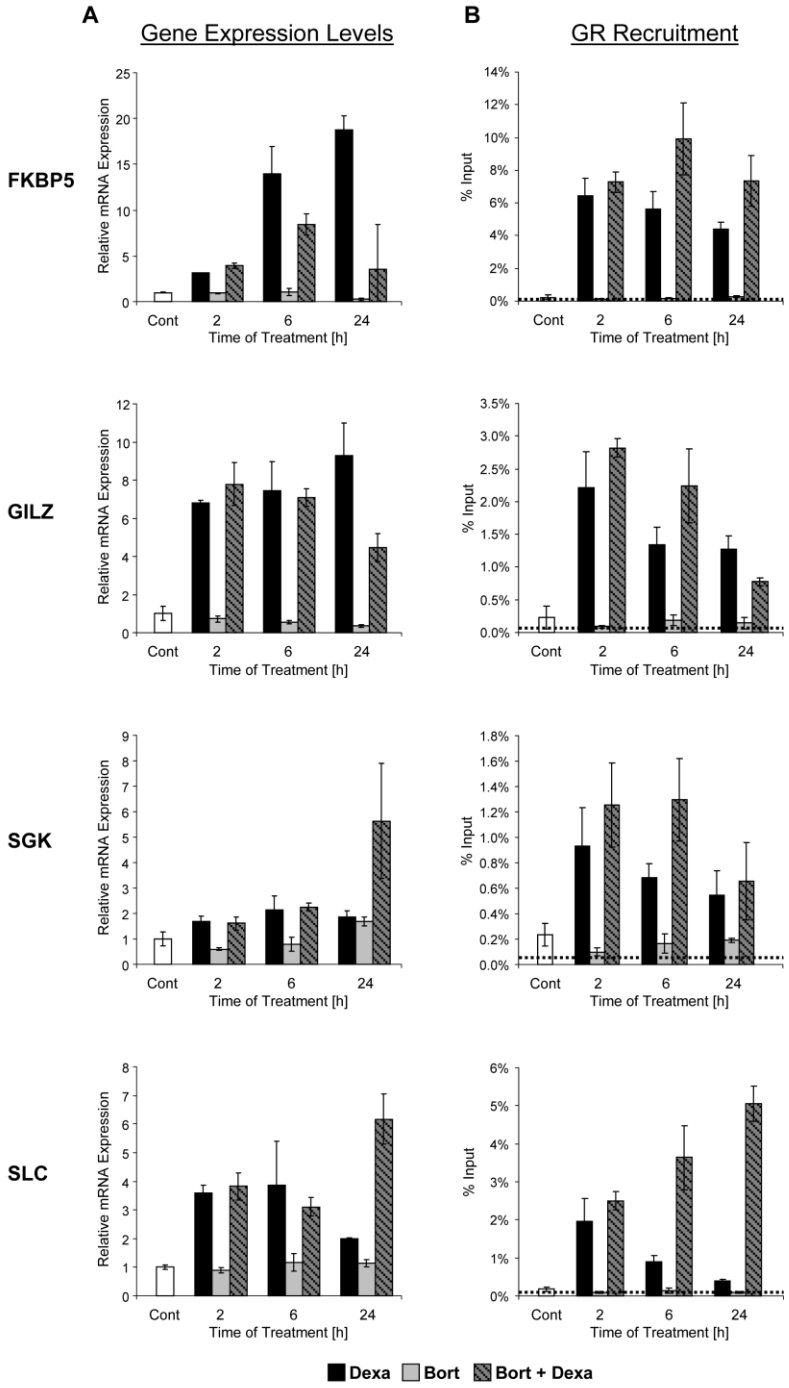


**Figure 32: Proteasome inhibition affects both GR target gene expression and GR recruitment in a gene-dependent manner.** A549 cells were grown in DMEM supplemented with 5% CSS for 48 h before treatment. Following a 15 min pre-treatment with either 100% EtOH (Cont) or 50 nM Bortezomib (Bort), A549 cells were treated with 100 nM Dexamethasone (Dexa) for the indicated time points. (**A**) Gene expression analysis showed that, similar to ERα studies, proteasome inhibition with Bortezomib also affects GR-regulated transcription in a time- and gene-dependent manner. Total mRNA was harvested, reverse-transcription with random primers was performed and cDNA subsequently analyzed via qPCR. The expression levels of *FKBP5*, *GILZ*, *SGK* and *SLC* genes were normalized to 28 S ribosomal RNA (control) and graphed relative to control sample (set to one). The normalized expression levels were represented as "relative mRNA expression"; mean values + s.d., $n = 2$. (**B**) Chromatin immunoprecipitation (ChIP) analysis revealed also a time- and gene-dependent effect of Bortezomib on GR recruitment to these target genes. ChIP assay was performed using a specific GR antibody or non-specific IgG. The experimental background binding is depicted as a dotted line. ChIP samples were normalized to input samples and expressed as "percent input"; mean values + s.d., $n = 3$.

As shown in Figure 32A, the expression of all four genes is induced by the synthetic glucocorticoid Dexamethasone. Interestingly, treatment with Dexamethasone and concomitant inhibition of the proteasome with Bortezomib caused downregulated glucocorticoid-induced gene expression for two genes (*FKBP5* and *GILZ*) compared to the ligand-induced samples while the other two genes (*SGK* and *SLC*) showed an increase in gene induction. These effects were most prominent after 24 h treatment.

A correlation of gene expression levels and GR recruitment to these genes was analyzed. As depicted in Figure 32B, for two genes (*GILZ* and *SLC*) a clear correlation could be seen via ChIP analysis. For example, *GILZ* gene expression as well as GR binding were both decreased after 24 h of proteasome inhibition, while *SLC* gene expression and also GR binding showed a strong upregulation. However, for one of the four genes (*FKBP5*) an inverse correlation between receptor binding and gene expression level was observed. While GR binding to the GRE of *FKBP5* gene was increased upon proteasome inhibition compared to the only Dexamethasone-induced sample after 24 h, gene expression level of that gene was strongly decreased at that time point. In the case of *SGK*, no clear correlation could be seen.

### 4.6.3.2 Proteasome subunit knockdown mildly affects glucocorticoid-induced gene expression

After showing that proteasome inhibition using Bortezomib affected GR target gene expression in a gene- and time-dependent manner, the effects of siRNA-mediated knockdown of the 20S subunit component PSMB3 on the transcription of these genes (*FKBP5*, *GILZ*, *SGK* and *SLC*) were also analyzed.

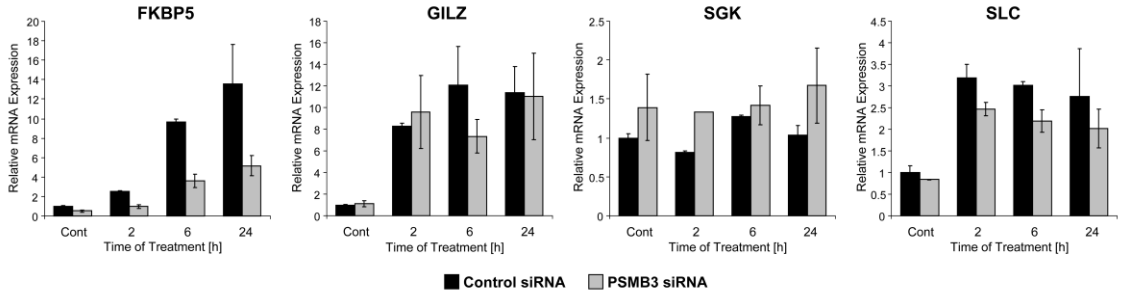


**Figure 33: The effect of proteasome knockdown on GR target gene expression is weaker than upon proteasome inhibition.** A549 cells were reverse-transfected with 30 pmol control or PSMB3 siRNA. Upon changing growth medium to 5% CSS medium, cells were treated with 100 nM Dexamethasone for the indicated time points. mRNA samples were analyzed via qRT-PCR and expression levels were represented as described in Figure 32A; mean values + s.d., $n = 2$.

As shown in Figure 33, actually after PSMB3 knockdown only the expression levels of *FKBP5* gene were similar to the results obtained from proteasome inhibition studies (Figure 32). The ligand-induced gene expression was decreased upon either PSMB3 knockdown or inhibition of the proteasome. PSMB3 knockdown did not appreciably affect gene expression of the other three genes *GILZ*, *SGK* and *SLC* compared to the control-transfected, Dexamethasone-treated samples. There was only a slight tendency of up- (*SGK*) or down- (*SLC*) regulated gene expression upon PSMB3 knockdown.

All in all, this experiment showed that the effects on the expression levels of target genes were much more pronounced upon pharmacological proteasome inhibition compared to the knockdown of a 20S proteasome subunit component.

# 5 Discussion

Gene expression has to be tightly controlled in order to ensure adequate cell responses to physiological signals or external stimuli. Transcription can be divided into different steps: formation of the pre-initiation complex (PIC), transcriptional initiation, elongation, and termination with cotranscriptional processes such as mRNA processing and export into the cytoplasm coupled to each of them. In a concerted manner various proteins such as transcription factors, coregulatory proteins, chromatin modifying enzymes and the RNA polymerase II machinery facilitate proper gene expression (Naar *et al.*, 2001; Orphanides and Reinberg, 2002).

As DNA-binding and ligand-regulated transcription factors, nuclear hormone receptors mediate endocrine signaling through highly dynamic mechanisms which require the interaction between multiple different coactivator complexes including ubiquitin-proteasome components. The ubiquitin-proteasome pathway is involved in NHR-mediated transcription either through proteolytic or non-proteolytic mechanisms. The receptors themselves and their coactivators are polyubiquitinated and degraded by the proteasome which may enable dynamic exchange and thereby facilitate multiple rounds of transcription. The non-proteolytic effects of the proteasome in NHR-regulated transcription involve the association of proteasomal subunits with target gene promoters.

Although it is proven that the UPS plays important roles at various stages during NHR-regulated gene transcription, the molecular mechanisms still remain unknown.

## 5.1 Proteasome activity and NHR-mediated gene expression

There are controversial results about the impact of proteasome inhibition on the transcriptional activity of different nuclear hormone receptors. While proteasomal activity was shown to be required for ERα- (Lonard *et al.*, 2000; Reid *et al.*, 2003), AR- (Kang *et al.*, 2002) and PR- (Dennis *et al.*, 2005) regulated target gene expression, inhibiting the proteasome enhanced GR-mediated transcription (Deroo *et al.*, 2002; Wallace and Cidlowski, 2001). This discrepancy was the rationale for our gene expression analyses in ERα-positive MCF-7 breast cancer as well as GR-positive A549 lung carcinoma cells after proteasome inhibition. In case of the GR, representative target genes were examined in their expression status after blocking proteasome activity with Bortezomib. It could be shown that the effect of proteasome inhibition on GR-mediated target gene transcription is gene-specific since half of

the tested genes were upregulated in their expression, while the other half was downregulated after inhibiting the proteasome (Figure 32).

A more global overview of the transcriptional response to blocked proteasomal enzyme function via Bortezomib was obtained for the ERα through mRNA expression profiling in MCF-7 cells for a total of 13,323 genes. The microarray analysis revealed that the expression of the majority (69.2%) of estrogen-activated genes was decreased while only 6.3% of these genes were hyper-activated after Bortezomib treatment (Figures 15 and 16).

These results obtained with Bortezomib are similar to a recent genome-wide study using MCF-7 cells stably expressing GR and endogenous ERα and in which the proteasome was inhibited with MG-132 (Kinyamu *et al.*, 2008). This study pointed out that the requirement for proteasome activity is gene- rather than receptor-specific. Our DNA microarray results rather support most of the former studies which demonstrated that proteolytic activity is required for efficient ERα transactivation (Lonard *et al.*, 2000; Reid *et al.*, 2003).

Gene expression analysis for a subset of ERα target genes showed that three different proteasome inhibitors, the boronic acid inhibitor Bortezomib; the peptide aldehyde MG-132 and the irreversible proteasome inhibitor Epoxomicin, all showed similar effects on ERα target gene expression (Figure 19) which suggests a similar mode of action. In general, chemical inhibitors have the disadvantage of not only inhibiting the target itself but also having non-specific effects (for example on other non-proteasomal proteases). Therefore, in parallel to our Bortezomib studies, we also performed knockdown experiments using siRNAs directed against two different 20S proteasomal subunits. By analyzing and comparing the effects on target gene expression in both experimental setups, we showed for the first time that inhibiting the proteasome with Bortezomib also seems to be specific in MCF-7 cells since similar, although weaker gene expression effects were observed following knockdown of the 20S subunits PSMB3 and PSMB5 (Figures 15 and 18).

In order to answer the question of how proteasome inhibition impairs ERα-mediated transcriptional activation, chromatin immunoprecipitation (ChIP) analysis on the promoter of the estrogen-responsive gene *TFF1* was performed in one study. The results indicated that proteasome inhibition using MG-132 reduces the association of liganded ERα with the *TFF1* promoter (Reid *et al.*, 2003). In contrast, our ChIP analyses following proteasome inhibition using Bortezomib (Figure 20) and MG-132 (data not shown) revealed that ERα binding to the ERE of *TFF1* is not reduced but rather increased compared to estrogen-treated samples. ERα recruitment to the EREs of other selected genes such as *KRT13* (Figure 20),

*CXCL12* (Figure 21) and *GREB1* (Figure 22) was also not markedly diminished up to 6 h after treatment. This discrepancy between our and the former study may be explained by the pre-treatment with the RNAPII inhibitor α-amanitin applied by Reid *et al*. used to deplete both RNAPII and ERα from gene promoters. It is likely that α-amanitin not only clears RNAPII and ERα from the promoters before the experimental start but also influences the recruitment of transcription factors and RNAPII machinery at later stages in the transcriptional process. It is also unclear from this study if the recruited RNAPII actually elongates and produces a mature mRNA following α-amanitin removal.

Results of a more recent study (Powers *et al.*, 2010) stated that Bortezomib regulates ERα directly by reducing RNAPII binding at the ERα gene promoter and thus leading to a remarkable decrease in ERα mRNA levels after 24 h. In our studies, 24 h Bortezomib treatment also resulted in a significant decrease of the ERα mRNA level (Figure 10A) but importantly not of the ERα protein level (Figure 10B). This finding of unchanged ERα protein levels up to 24 h after Bortezomib treatment demonstrates that there has to be a different mechanism than decreased ERα levels, which leads to the pronounced effects on target gene expression already detectable after 2 h and 6 h of treatment.

Further, Powers *et al.* claimed that the expression of two ERα target genes (*PGR* and *TFF1*) correlates with ERα and RNAPII occupancy on the respective gene promoters. In the beginning of our studies, we expected to see similar results in respect to ERα binding to EREs and the transcriptional output. Indeed, we also observed the correlation between receptor binding and magnitude of expression for the two tested genes after 24 h (Figure 20). However, after testing several ERα target genes both in their expression profile and ERα occupancy of EREs in time course analyses (Figures 20, 21, 22 and 23) we cannot confirm the ERα binding/gene expression correlation proposed by Powers *et al.*. The gene expression studies in this work clearly showed that proteasome inhibition using Bortezomib strongly influences ERα- and GR-target gene expression at different time points, most pronounced after 24 h treatment. However, parallel ChIP experiments revealed that for the majority of target genes there is no direct correlation of nuclear hormone receptor binding to their respective HREs and the observed effects on target gene expression, particular at early time points. For example there were already clear effects of proteasome inhibition on the induction of most ERα target genes at 6 h (e.g. *GREB1*, *KRT13*, *PGR* and *WISP2*) without any significant effects on ERα occupancy (Figures 20 and 22). And in case of GR-regulated gene transcription, one gene (*FKBP5*) even showed an inverse correlation between receptor

binding and gene expression level (Figure 32). These results together with the notion of gene- rather than receptor-specific effects (own work and (Kinyamu *et al.*, 2008)) imply that other mechanisms (than simply enhancing/inhibiting receptor binding and thereby inducing/preventing gene expression) determine the effects of proteasome inhibition on NHR-mediated gene transcription.

One other previously suggested mechanism proposed that enhanced GR target gene expression upon proteasome inhibition was due to an increase in global pools of the phosphorylated foms of RNAPII (Kinyamu and Archer, 2007). This finding could neither be reproduced in our MCF-7 (Figure 6) nor in our A549 cells (Figure 31). The conflicting results could be reasoned in the different systems used. While Kinyamu *et al.* performed their studies in MCF-7 cells which stably express the GR and the mammary tumor virus promoter long terminal repeat (LTR) promoter fused to the luciferase gene reporter (MMTV-LUC), in this study ERα-positive MCF-7 and GR-positive A549 cells were used for analyzing ERα- and GR-regulated gene transcription, respectively. In our system, changes in global RNAPII levels and its phosphorylation status can be excluded as a possible mechanism.

In order to mediate endocrine signaling, nuclear hormone receptors have to translocate into and move within the nucleus to bind to their respective HREs and thereby activate target gene expression. FRAP analysis showed that the unliganded estrogen receptor is extremely mobile. After estrogen binding the receptor interacts with the nuclear matrix resulting in a decreased ERα mobility (Stenoien *et al.*, 2001). In addition, the decreased mobility is probably due to increased ERα and coactivator binding to the EREs. It seems that there are two ERα subtypes in the nucleus: highly mobile, unliganded and transcriptionally inactive ERα molecules and slower, estrogen-bound and transcriptionally engaged ERα molecules. Increased ERα binding in turn results in enhanced transcriptional activity as known for many estrogen responsive genes. Further, two independent studies (Reid *et al.*, 2003; Stenoien *et al.*, 2001) as well as our own data (Figure 26) showed that proteasome inhibition using MG-132 immobilizes the ERα within the nucleus which was shown to be due to the association with the nuclear matrix in a ligand-independent manner (Reid *et al.*, 2003; Stenoien *et al.*, 2001). These results suggest that proteasomal inhibition may induce a third subtype of ERα which is (mostly) transcriptionally inactive but displays a reduced mobility.

The FRAP analysis performed in this study demonstrated that also Bortezomib reduced ERα mobility. In addition, the combined treatment with estrogen and Bortezomib even amplified the negative effect on ERα mobility caused by both agents alone (Figure 27). Our

FRAP experiment further revealed that depending on the proteasome inhibitor used this negative effect on ERα mobility is differently pronounced, as compared to the MG-132-induced immobilization, the receptor still retained some mobility after Bortezomib treatment. These different effects of proteasome inhibitors on ERα mobility still remain to be elucidated.

The three main results obtained in MCF-7 cells treated with Bortezomib: I) the decreased nuclear ERα mobility; II) the unaffected ERα binding to the EREs of target genes up to 6 h and III) the mostly negative effects on the expression of estrogen-activated target genes, necessitate deciphering the underlying molecular mechanisms. We hypothesized an effect on the three-dimensional interactions between intrachromosomal sites which will be discussed in the last section.

## 5.2 The UPS as potential target in breast cancer therapy

In women, breast cancer is the most common type of cancer and it is expected to account for 28% of all new cancer cases among American women in 2010 (Jemal *et al.*, 2010). The expression of the estrogen receptor is one of the major molecular markers for the prediction of the outcome and therapeutic responsiveness, where ER-positive breast tumors (which account for approximately 70% of all breast tumors) show a higher differentiation and a better prognosis than ER-negative tumors. The ERα was also shown to be increased in premalignant lesions compared to normal mammary tissue and prophylactic anti-estrogen therapy such as Tamoxifen treatment may prevent breast cancer development (Shaaban *et al.*, 2002).

Tamoxifen was the first selective estrogen receptor modulator (SERM) which was used in the treatment of advanced ER-positive breast cancer patients and which was later also introduced into adjuvant therapy for women with high risk of developing breast cancer (Cuzick *et al.*, 2003). Due to its partial agonist activity and severe side effects like increasing the incidence of endometrial cancer, thromboembolic events (Fisher *et al.*, 2005) and the development of resistance particularly after long-term use (Massarweh *et al.*, 2008), pure anti-estrogens such as Fulvestrant and aromatase inhibitors (AIs) are coming to the forefront and could replace Tamoxifen as first-choice breast cancer therapy. In recent years strong emphasis was also put on the search for new targets and the development of new agents in breast cancer therapy such as the antibody Trastuzumab (Herceptin) against the human epidermal growth factor receptor 2 (HER2) (Slamon *et al.*, 2001; Vogel *et al.*, 2002); Lapatinib which targets the

human epidermal growth factor receptor (EGFR, HER1) and HER2; and Bevacizumab directed against vascular endothelial growth factor (VEGF) (Alvarez *et al.*, 2010).

The ubiquitin-proteasome system accomplishes an indispensable function in all cells by controlling intracellular protein levels which is important for cell viability. But numerous UPS-controlled cellular processes may also promote cancer cell growth. Indeed, several studies revealed high proteasome expression and/or activity in various cancer types: in breast cancer tissues high proteasome activity as well as higher expression levels of proteasome subunits, ubiquitin-conjugating enzymes and translation elongation factor eEF1A have been shown (Chen and Madura, 2005); abnormally high expression of proteasomes was shown in leukemic cells (Kumatori *et al.*, 1990); in gastric cancer hyper-expression of muscle ubiquitin mRNA goes along with increased proteasome activity (Bossola *et al.*, 2003); and elevated proteasome levels were also detected in ovarian carcinoma (Bazzaro *et al.*, 2006). Further, in a gene module map approach a 'proteasome module' was identified and associated with poor prognosis in so-called "wound-like" aggressive breast tumors (Wong *et al.*, 2008).

The knowledge that the UPS mediates ERα turnover (Nawaz *et al.*, 1999a) and is required for efficient ERα transcriptional activity (Fan *et al.*, 2004; Lonard *et al.*, 2000; Reid *et al.*, 2003) as well as the need for alternative anti-breast cancer drugs are the rationale for investigating the ubiquitin-proteasome as a pharmacological target in cancer therapy in general and in breast cancer therapy in particular (Sato *et al.*, 2008).

So far, the only clinically approved proteasome inhibitor in anticancer therapy is Bortezomib. It is an effective single anticancer agent in multiple myeloma and mantle cell lymphoma and is also used in combination therapy with other drugs, e.g. Dexamethasone and Doxorubicin for refractory and relapsed disease. Further, *in vitro* monotherapy studies with Bortezomib showed cytotoxic activity against other cancer types including non-Hodgkin's lymphoma and solid tumors. And it was further shown to sensitize cancer cells to other chemotherapeutic agents and additive or synergistic activity in combination with other agents could be shown *in vivo* and *in vitro* (Richardson *et al.*, 2006).

Thus far, Bortezomib was shown to have cytotoxic activity toward a murine mammary carcinoma system (Teicher *et al.*, 1999) but as a single anticancer agent Bortezomib failed to show clinical effects on aggressive metastatic breast cancers (Yang *et al.*, 2006).

The clinical usage of the proteasome inhibitor Bortezomib in the treatment of multiple myeloma and mantle cell lymphoma as well as its potential in combined therapies against

other tumor types were our rationale to perform our studies about the effect of the UPS in nuclear hormone receptor-regulated transcription with this proteasome inhibitor.

Initial studies conducted on the activity of Bortezomib revealed that it effectively inhibited proteolytic degradation of polyubiquitinated proteins in MCF-7 and A549 cells (Figures 5 and 30). Further, Bortezomib treatment also prevented the estrogen-induced ERα proteolysis in our MCF-7 breast cancer cell system (Figure 5B) which is contradictory to a recent study which claimed that ERα protein levels were reduced 4 h after Bortezomib treatment (Powers *et al.*, 2010). The observed activity of Bortezomib on ERα proteolysis in our studies is similar to previous studies using MG-132 and lactacystin (Nawaz *et al.*, 1999a; Tateishi *et al.*, 2004) and was also confirmed by the partial blockage of Dexamethasone-induced GR degradation in A549 cells (Figure 30B). These contradictory results in ERα stabilization after proteasome inhibition using Bortezomib can so far only be explained in MCF-7 cells deriving from diverse sources and therefore behaving differently.

In our studies, Bortezomib as a single agent dose-dependently decreased the proliferation of ERα-positive MCF-7 breast cancer cells (Figure 11). Interestingly, the combined treatment of Tamoxifen and the lower dosage of Bortezomib (5 nM) reduced the proliferative capacity of MCF-7 cells stronger than the treatment with Tamoxifen alone. This additive result in reduced breast cancer cell proliferation could be relevant in respect to combined breast cancer therapy especially in regard of the lower Bortezomib concentration. One planned experiment in our MCF-7 breast cancer cell system is the determination if the effects induced by lower (< 50 nM) Bortezomib concentrations more closely resembles the milder effects observed by siRNA-mediated knockdown of 20S subunits.

Further, this study revealed that the reason for the reduced proliferation rate after proteasome inhibition is the Bortezomib-induced blockage of the estrogen-stimulated increase of the cell fraction in S phase and the induction of a G2/M arrest in MCF-7 cells (Figure 13). One feasible mechanism could be the blocked degradation of securin after its ubiquitination by the anaphase promoting complex/cyclosome (APC/C). Under normal conditions, the proteolytic degradation of the cohesin inhibitor securin leads to the release of separase which in turn cleaves cohesin bridges and initiates sister chromatid separation (Jallepalli and Lengauer, 2001). Since Bortezomib blocks the degradation of cell cycle regulatory proteins such as securin, sister chromatid separation is prevented which leads to a G2/M arrest. Similar to our findings, a cell cycle blockade in G2/M transition induced by Bortezomib was also observed

by others in PC-3 prostate carcinoma cells (Adams *et al.*, 1999) and non-small cell lung cancer cells (Ling *et al.*, 2003).

In addition, we could show that, likely as a consequence of the arrested cell cycle, prolonged Bortezomib treatment for 48 h induces apoptosis in MCF-7 breast cancer cells (Figure 8).

The DNA microarray analysis further supports Bortezomib's potential in breast cancer therapy. Treating MCF-7 breast cancer cells with Bortezomib resulted in a downregulation of the overwhelming majority of estrogen-activated target genes. Importantly, this downregulation seems to be specific for estrogen-induced genes since Bortezomib induced or repressed the expression of almost identical numbers of genes which were unaffected or repressed by estrogen (Figure 16).

In summary, our and others' results revealed that Bortezomib shows promising cytotoxic properties in breast cancer models and although this proteasome inhibitor failed thus far in *in vivo* models as a monoagent in breast cancer therapy (Yang *et al.*, 2006), it could be a possible antitumor agent in combined breast cancer therapy with e.g. Tamoxifen. Further investigations will be necessary in order to characterize the value of Bortezomib in breast cancer therapy.

## 5.3 Proteasome-dependent 3D chromosome interaction, a conceivable mechanism of how the UPS influences NHR-regulated transcription

Transcriptional activation of genes often involves long-range interaction between distal enhancers and the proximal promoter. Over the last years different models were proposed of how these DNA regulatory elements communicate, either through direct interaction or through non-contact mechanisms: 1) In the chromatin looping model, the distal enhancer associated with transcription factors and the promoter come into close spatial proximity with the intervening chromatin fiber 'looping out'. 2) The tracking hypothesis suggests that the key transcription factors assemble on the distal enhancer and then 'track' along the chromatin till reaching the respective promoter. 3) In a facilitated tracking model, the enhancer associated with the transcription-activating complex moves along the DNA to the proximal promoter, thereby the intervening DNA fiber loops out through the enhancer-activator complex. 4) The linking hypothesis suggests that facilitator proteins binding to the intervening DNA segment between enhancer and promoter mediate transcriptional activation (Li *et al.*, 2006).

Techniques like chromosome conformation capture (3C) (Dekker *et al.*, 2002), 3C variants (ChIP-3C, 4C, 5C, 6C (Dostie *et al.*, 2006; Fullwood and Ruan, 2009; Tiwari *et al.*, 2008; Zhao *et al.*, 2006)) or RNA tagging and recovery of associated proteins (RNA TRAP) (Carter *et al.*, 2002) have proven that long-range dispersed DNA elements can indeed interact according to the chromatin looping model. The first evidence for an *in vivo* cis-interaction between a distal enhancer and the corresponding gene via looping formation was shown for the *ß-globin* locus control region (LCR) and the actively transcribed *ß-globin* gene in 2002 (Carter *et al.*, 2002; Tolhuis *et al.*, 2002). Since then, long-range intra- and also interchromosomal interactions have been shown for many different sites and nowadays, it is clear that the spatial chromosomal organization plays a crucial role in efficient transcriptional regulation.

In recent years, several chromatin immunoprecipitation (ChIP) variant techniques such as ChIP microarray (ChIP-Chip) and ChIP-sequencing (ChIP-PET and ChIP-Seq) revealed global transcription factor binding sites. Interestingly, the genome-wide identification of ERα binding sites revealed that the majority of the ERα binding sites are distant (> 5 kb apart) to gene promoters (Carroll *et al.*, 2006; Lin *et al.*, 2007; Welboren *et al.*, 2009). For coordinated transcriptional activity these remote EREs have to interact via long-range distances most likely via looping formation in order to correctly control target gene transcription. Several independent studies at different loci provided evidence that distant and proximal EREs communicate via long-range interactions and that these interactions are crucial for maximal transcriptional output (Bretschneider *et al.*, 2008; Pan *et al.*, 2008; Sun *et al.*, 2007). Recently, in a very interesting study using chromatin interaction analysis by paired-end tag sequencing (ChIA-PET), a so-called “human chromatin interactome map” was generated which displays the ERα-bound chromatin interactions in MCF-7 breast cancer cells (Fullwood *et al.*, 2009).

DNA looping was not only described in estrogen-mediated transcriptional activation but also in the repression of some gene clusters which is a transient phenomenon that seems to be deregulated in breast cancer cells leading to prolonged repression of several loci (Hsu *et al.*, 2010). Further, transcriptional activation through chromosomal looping events was also described for the glucocorticoid receptor (Hakim *et al.*, 2009), androgen receptor (Wang *et al.*, 2005) and speculated for the progesterone receptor (Magklara and Smith, 2009).

In respect to these findings and after deciphering that proteasome inhibition using Bortezomib resulted in a mostly negative effect on estrogen-activated target gene expression while there is

no apparent correlation to the ERα recruitment to these target genes, we hypothesized a Bortezomib-induced effect on the three-dimensional spatial organization of estrogen-responsive genes. In order to address this question we applied the chromosome conformation capture (3C) analysis according to (Miele and Dekker, 2009) which detects the juxtaposition frequency between long-dispersed, interacting EREs or gene promoters and distal enhancers. The interacting sites of the two tested estrogen-activated genes *GREB1* and *CXCL12* were chosen based on already positive interaction data in 3C (Pan *et al.*, 2008) and ChIA-PET analyses (Fullwood *et al.*, 2009), respectively.

Our study reveals a novel mechanism of how the proteasome influences ERα-regulated gene transcription. We demonstrate that proteasome inhibition via Bortezomib treatment blocks the estrogen-induced long-range interactions between characterized EREs on the *GREB1* and *CXCL12* loci (Figures 28 and 29). These findings imply that the UPS or the proteasome itself facilitates looping formation between the interaction sites. Accordingly, correct long-range interaction between two EREs after estrogen stimulation leads to maximal gene expression which is reflected in our gene expression analyses for *CXCL12* (Figure 21) and *GREB1* (Figure 22). In the presence of Bortezomib these long-range interactions are significantly decreased by an unknown mechanism which in turn would result in decreased gene expression which was shown for both genes. If the proteasome itself accomplishes the proper looping formation or if a "looping factor" such as a motor protein is required remains unknown so far. A recent study proposed the histone lysine demethylase 1 (LSD1) as one such looping factor in the nuclear myosin-I (NMI)-dependent organization in 'interchromatin granules' upon estrogen stimulation (Hu *et al.*, 2008).

In the future, DNA-FISH experiments are planned in order to reveal if proteasome inhibition only impairs intra- or also interchromosomal interactions as judged by two loci on different chromosomes coming together in three-dimensional space in the nucleus. DNA probes for *GREB1* (chromosome 2), *TFF1* (chromosome 21), *CXCL12* (chromosome 10) and *PGR* (chromosome 11) will be generated. Two of the genes (*TFF1* and *GREB1*) were shown to come into close proximity after estrogen treatment, a seemingly prerequisite for enhanced transcriptional activation (Hu *et al.*, 2008). But these results have to be reproduced cautiously, since in two recent studies no co-localization or 3C interaction between *GREB1* and *TFF1* after estrogen-stimulation was observed (Fullwood *et al.*, 2009; Kocanova *et al.*, 2010).

This study provides evidence that proteasome inhibition using Bortezomib blocks the estrogen-induced long-range interactions for at least two ERα target genes *GREB1* and *CXCL12*. These two estrogen-activated genes were shown to be repressed after Bortezomib treatment (Figures 21 and 22). It still remains unclear how a small subset of estrogen-activated genes such as *TFF1* is hyper-activated after prolonged Bortezomib treatment. We hypothesize a rather target gene specific role of the proteasome in mediating long-range interactions. In order to address this question, we want to perform a 3C analysis on the *TFF1* locus after 24 h of estrogen and Bortezomib treatment. At this time point we showed an enhanced *TFF1* expression after proteasome inhibition compared to the estrogen-treated samples. But as already pointed out, *TFF1* expression was not increased but decreased after 2 h and 6 h of combined estrogen and Bortezomib treatment. Therefore, in order to give a precise answer of how the proteasome influences this estrogen-responsive gene, a 3C time course analysis after 2, 6 and 24 h will likely be necessary.

### 5.3.1 Potential mechanism of UPS and ERα cofactor network

So far, we showed significantly decreased estrogen-induced long-range interactions after proteasome inhibition using Bortezomib. Next, the underlying mechanism has to be analyzed. We hypothesize that either ERα cofactors and/or other "looping factors" play a role in facilitating the formation of 3D interactions.

In a recent study using a murine embryonic stem cell system, mediator and cohesin were described as such "looping factors" which mediate looping formations between enhancers and gene promoters. It was shown that the transcriptional coactivator mediator; cohesin, the complex of proteins that holds sister chromatids together; and the cohesin-loading factor Nipbl co-occupy enhancer and core promoters of different genes, mediate DNA looping between the tested enhancers and promoters and thereby mediate gene transcription (Kagey *et al.*, 2010). Cohesin has been reported to bind to CCCTC-binding factor (CTCF) binding sites and thereby mediates transcriptional insulation (Wendt *et al.*, 2008). Importantly, an independent recent study using ChIP-Seq revealed that cohesin indeed colocalizes with the ERα on estrogen responsive genes in MCF-7 cells, in an estrogen-dependent and CTCF-independent manner. Further, combining these ChIP-Seq data with former genome-wide chromosomal ERα interaction data revealed that cohesin preferentially binds to interacting EREs which indicates to a function of cohesin in mediating long-range interactions

between distal and proximal EREs and thereby regulating target gene transcription (Schmidt *et al.*, 2010). The potential involvement of mediator and cohesin in our system as well as their regulation by proteasome activity will be examined.

Our previous work revealed two cofactors CLIM/LDB1/NLI and RLIM/RNF12 which regulate the activity of ERα. Both cofactors not only directly interact with ERα but are also present on the EREs of estrogen responsive genes. While CLIM inhibits ERα transcriptional activity, the ubiquitin ligase RLIM enhances transcription of ERα target genes (Johnsen *et al.*, 2009). Since RLIM ubiquitinates CLIM and thereby causes its degradation, we think that inhibiting the proteasome destabilizes this network. Further, CLIM has already been implicated in long-range interaction and was shown to facilitate a loop structure between the *ß-globin* locus control region (LCR) and the *ß-globin* gene (Song *et al.*, 2007). Since proteasome inhibition decreased ERα-dependent long-range interactions, we hypothesize that the effects after proteasomal inhibition on the spatial organization of ERα target genes may be due at least in part to the stabilization of CLIM. Based on this hypothesis we propose two possible models:

In model 1 (Figure 34 A), CLIM binds to the ERα dimer at the EREs, of e.g. *CXCL12* gene and thus inhibits its transcriptional activity by recruiting the distal ERα enhancer to an unknown site "locus X" and thereby preventing the long-range intrachromosomal interactions between the distal and proximal EREs/enhancers. In the presence of estrogen the E3 ligase RLIM is recruited, ubiquitinates CLIM which in turn is degraded by the proteasome. Subsequently, the cleared distal and proximal enhancers can come into close proximity via long-range interaction and thereby facilitate the expression of the *CXCL12* gene. When proteasomal activity is blocked, e.g. by Bortezomib, CLIM is not degraded and therefore stays in contact with the distal ERE (enhancer site 1). Thus, looping formation between these sites is prevented and the negative regulation of ERα-mediated transcription by CLIM is maintained.

In model 2 (Figure 34 B), CLIM does not translocate the distal enhancer to an unknown site but rather directly prevents the binding of one or rather multiple unknown "looping factors Y" such as a cohesin and/or mediator which promote long-range interactions between EREs. In the absence of proteasome inhibitor, RLIM causes the ubiquitination and degradation of CLIM and thus clears the binding sites for the "looping factor Y". Upon binding of "factor Y" intrachromosomal loopings are formed which bring the distal and proximal EREs into close proximity and thereby induce target gene transcription. In case of a blocked proteasome, the

association between CLIM and ERα at the EREs is maintained, looping formation is prevented and thus ERα transcriptional activity is inhibited.

These two hypothetical models will be tested in the near future. Initially, 3C analyses will be performed in MCF-7 cells either depleted of CLIM and RLIM (via siRNA-mediated knockdown) or by overexpressing either factor in order to examine if these two ERα cofactors are in fact involved in estrogen-induced enhancer interactions. If that is the case, we will further combine e.g. knockdown and proteasome inhibitor conditions in 3C experiments. For example, we would expect a blockage of the negative effects of Bortezomib on the formation of long-range interactions in cells depleted of CLIM which in our model is the principal protein involved in preventing estrogen-induced looping events.

Collectively, this study reveals more insight into the complex mechanism by which the ubiquitin-proteasome system regulates nuclear hormone receptor-mediated transcription. Our data demonstrate that the UPS influences ERα transcriptional activity at various layers which exceed by far the simple receptor turnover.

Most results were obtained in an ERα-positive breast cancer cell line model and studies should be extended to other nuclear hormone receptor model systems such as the GR or AR as well as to normal human mammary epithelial cells. It may also be interesting to see if these interactions display a tissue- (i.e., mammary epithelial *vs.* endometrial) or ligand- (i.e., Tamoxifen *vs.* Raloxifene) specific effects. By understanding these mechanisms better it may be possible to develop even more specific anti-ERα (or anti-AR) treatments for breast (or prostate) cancer which specifically target the looping function of the nuclear hormone receptor/s.

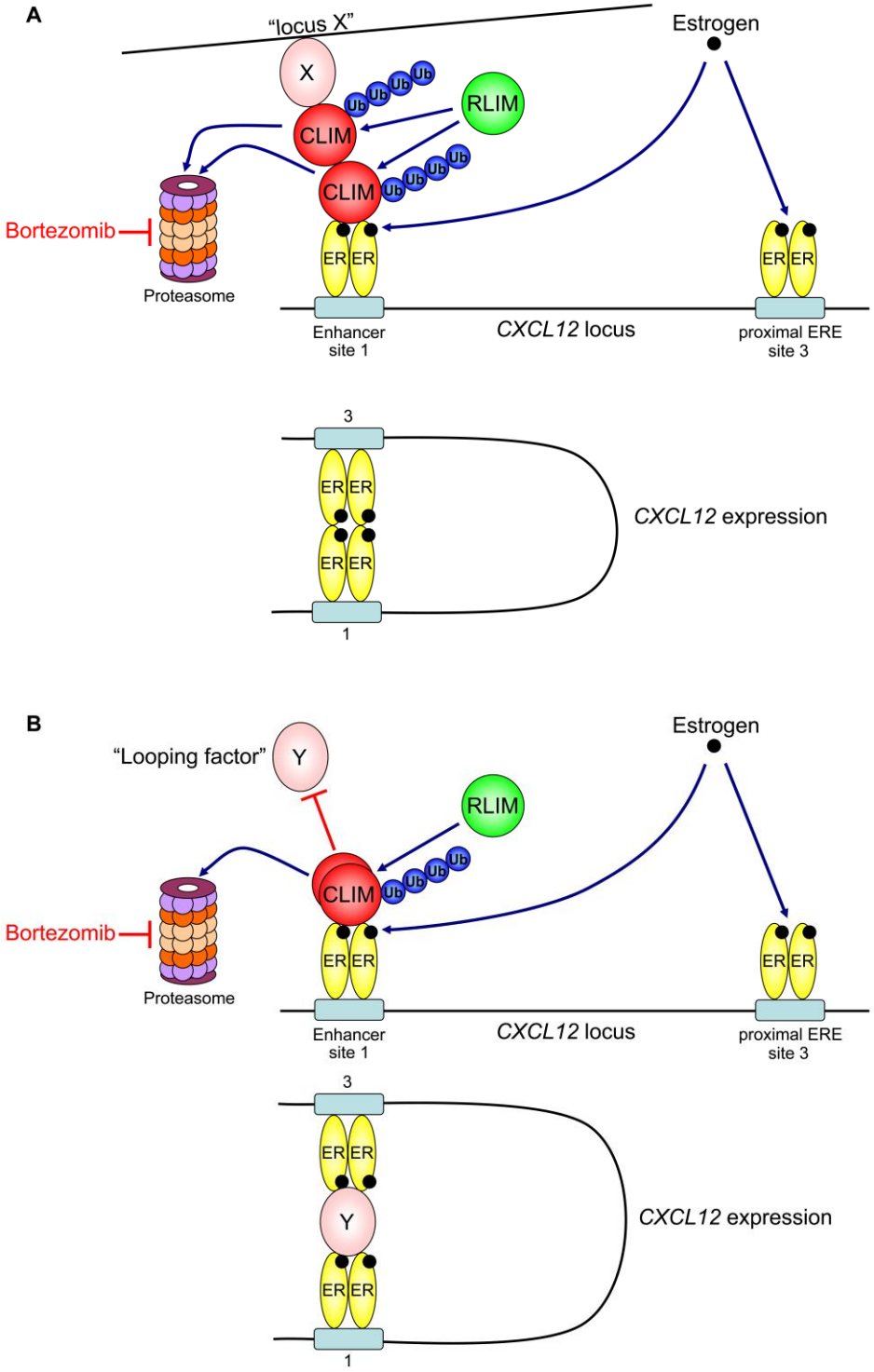


**Figure 34: Models of CLIM/RLIM-mediated long-range interactions at *CXCL12* locus.** (**A**) Model 1. CLIM binds to the ERα dimer at ERE binding sites and prevents long-range interactions between enhancer site 1 and the proximal ERE site 3 by recruiting the enhancer to a unknown locus with the help of a factor "X". ERα transcriptional activity is inhibited. In the presence of estrogen, the ubiquitin ligase RLIM ubiquitinates CLIM which in turn is proteolytically degraded. The freed distal and proximal EREs can interact via looping formation and *CXCL12* gene expression is induced. Blockade of proteasomal activity by Bortezomib inhibits the degradation of CLIM which stays associated with ERα dimer and prevents *CXCL12* transcription. For simplicity, CLIM is shown bound to only one ERE, although the mechanism may apply to both EREs. (**B**) Model 2. CLIM associates with the ERα dimer and thereby prevents the binding of a "looping factor Y" which is needed for long-range interaction formation between interaction sites 1 and 3. After estrogen induction, RLIM causes the ubiquitination and degradation of CLIM. The "looping factor Y" can bind to the ERE and induces looping formation and *CXCL12* gene expression.

# 6 Appendix

## 6.1 ChIP-ERE sites

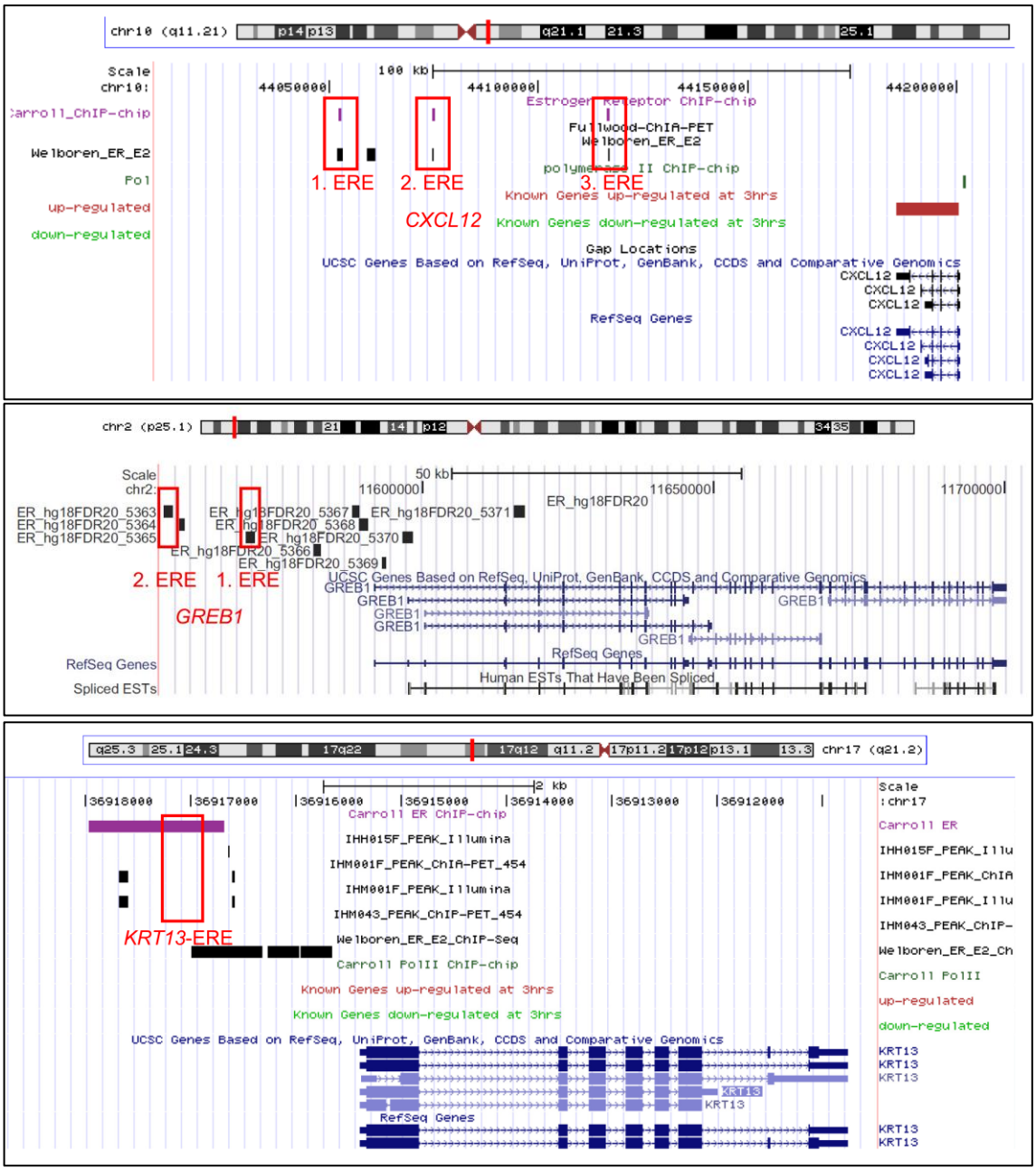

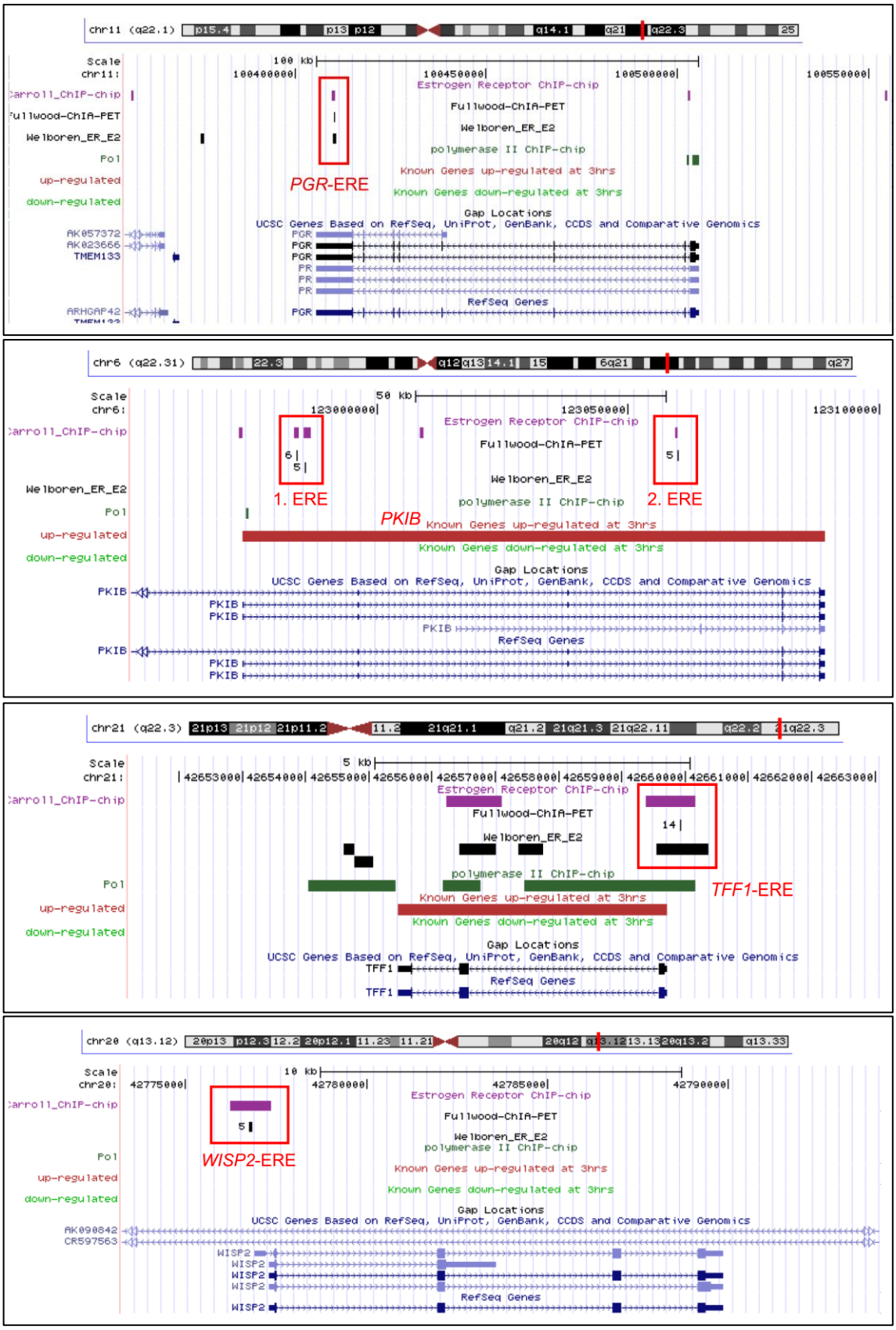


**Figure 35: Screenshots of genome browser with the chosen ChIP-ERE sites.** The respective gene together with the EREs and the RNAPII binding sites out of published ChIP-Chip (Carroll *et al.*, 2006), ChIP-Seq (Welboren *et al.*, 2009) and ChIA-PET (Fullwood *et al.*, 2009) data are shown. The red rectangles depict the chosen ChIP-ERE sites used in this study.

## 6.2 Chromatin conformation capture analysis

In order to compare 3C signal intensities in a quantitative manner, *CXCL12* and *GREB1* BAC clones were digested with BtgI restriction enzyme and ligated in accordance with the 3C templates. The serial dilution of the BAC clone DNA served as standard curves (Figure 36 and 37) in the PCR analysis.

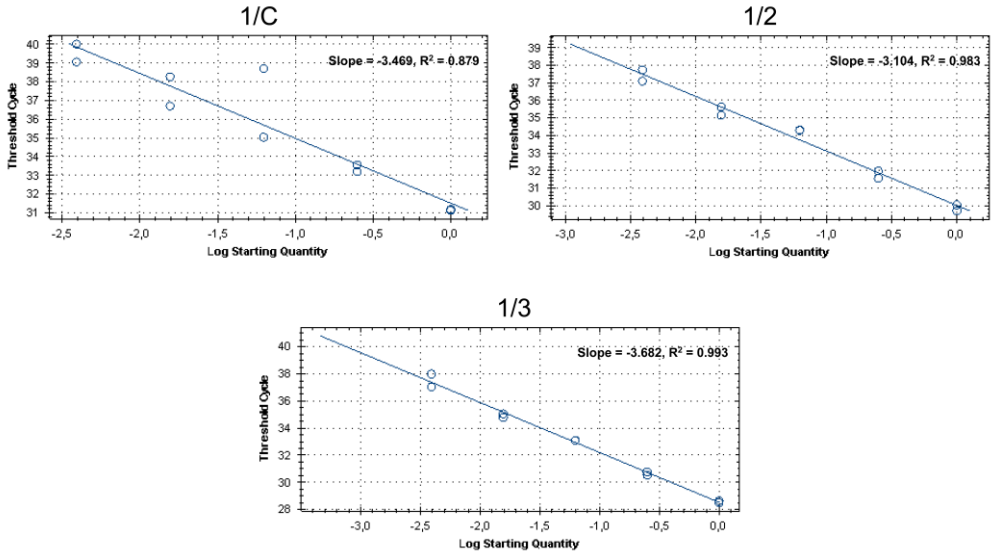


**Figure 36: *CXCL12* BAC clone standard dilution curves.** *CXCL12* BAC clone was digested with BtgI and ligated according to the 3C template DNA. The ligated BAC clone DNA was diluted to 400 ng/µl and then serial diluted (1:4; 1:16; 1:64; 1:256). The serial BAC clone DNA dilution served as standard curve in the PCR analysis using a TaqMan probe and primers specific for 1/C; 1/2 and 1/3 interaction sites on *CXCL12* locus.

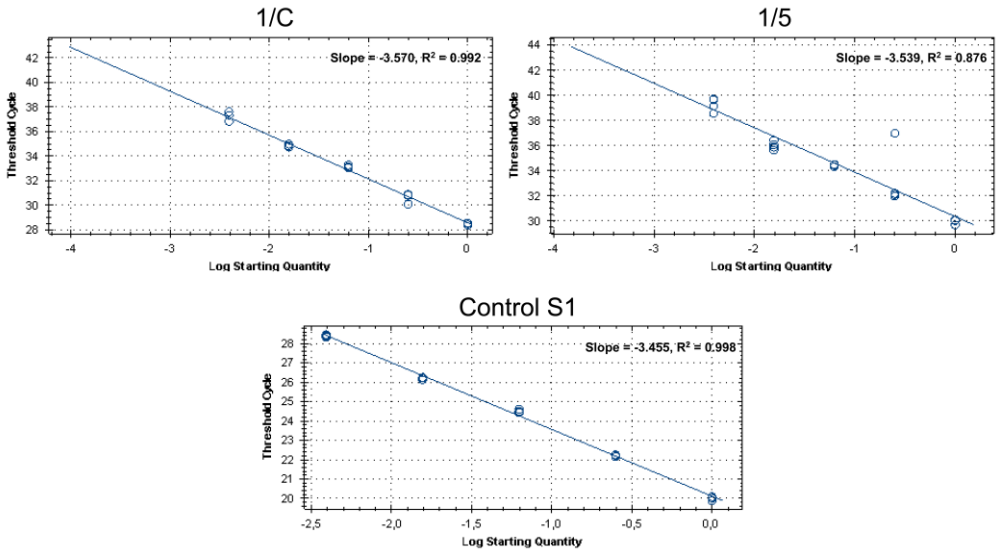


**Figure 37: *GREB1* BAC clone standard dilution curves.** *GREB1* BAC clone was digested with BtgI and ligated in accordance with the 3C template. After diluting the ligated BAC clone DNA to 400 ng/µl, it was serial diluted (1:4; 1:16; 1:64; 1:256). The serial BAC clone DNA dilution served as standard curve in the PCR analysis using a TaqMan probe and primers specific for 1/C and 1/5 interaction sites on *GREB1* locus as wells as for an internal control (S1) site that lies between BtgI sites and which was used for normalization of the *GREB1* and *CXCL12* 3C template values.

# 7 Reference List

Acconcia, F., Ascenzi, P., Bocedi, A., Spisni, E., Tomasi, V., Trentalance, A., Visca, P., and Marino, M. (2005). Palmitoylation-dependent estrogen receptor alpha membrane localization: regulation by 17beta-estradiol. Molecular biology of the cell *16*, 231-237.

Adams, J., Palombella, V.J., Sausville, E.A., Johnson, J., Destree, A., Lazarus, D.D., Maas, J., Pien, C.S., Prakash, S., and Elliott, P.J. (1999). Proteasome inhibitors: a novel class of potent and effective antitumor agents. Cancer research *59*, 2615-2622.

Agulnick, A.D., Taira, M., Breen, J.J., Tanaka, T., Dawid, I.B., and Westphal, H. (1996). Interactions of the LIM-domain-binding factor Ldb1 with LIM homeodomain proteins. Nature *384*, 270-272.

Alarid, E.T., Bakopoulos, N., and Solodin, N. (1999). Proteasome-mediated proteolysis of estrogen receptor: a novel component in autologous down-regulation. MolEndocrinol *13*, 1522-1534.

Altun, M., Galardy, P.J., Shringarpure, R., Hideshima, T., LeBlanc, R., Anderson, K.C., Ploegh, H.L., and Kessler, B.M. (2005). Effects of PS-341 on the activity and composition of proteasomes in multiple myeloma cells. Cancer research *65*, 7896-7901.

Alvarez, R.H., Valero, V., and Hortobagyi, G.N. (2010). Emerging targeted therapies for breast cancer. J Clin Oncol *28*, 3366-3379.

Arts, J., Kuiper, G.G., Janssen, J.M., Gustafsson, J.A., Lowik, C.W., Pols, H.A., and van Leeuwen, J.P. (1997). Differential expression of estrogen receptors alpha and beta mRNA during differentiation of human osteoblast SV-HFO cells. Endocrinology *138*, 5067-5070.

Arya, A.K., El-Fert, A., Devling, T., Eccles, R.M., Aslam, M.A., Rubbi, C.P., Vlatkovic, N., Fenwick, J., Lloyd, B.H., Sibson, D.R., Jones, T.M., and Boyd, M.T. (2010). Nutlin-3, the small-molecule inhibitor of MDM2, promotes senescence and radiosensitises laryngeal carcinoma cells harbouring wild-type p53. British journal of cancer *103*, 186-195.

Avenant, C., Kotitschke, A., and Hapgood, J.P. (2010). Glucocorticoid receptor phosphorylation modulates transcription efficacy through GRIP-1 recruitment. Biochemistry *49*, 972-985.

Bakir, S., Mori, T., Durand, J., Chen, Y.F., Thompson, J.A., and Oparil, S. (2000). Estrogen-induced vasoprotection is estrogen receptor dependent: evidence from the balloon-injured rat carotid artery model. Circulation *101*, 2342-2344.

Bamberger, C.M., Bamberger, A.M., de Castro, M., and Chrousos, G.P. (1995). Glucocorticoid receptor beta, a potential endogenous inhibitor of glucocorticoid action in humans. The Journal of clinical investigation *95*, 2435-2441.

Barkhem, T., Carlsson, B., Nilsson, Y., Enmark, E., Gustafsson, J., and Nilsson, S. (1998). Differential response of estrogen receptor alpha and estrogen receptor beta to partial estrogen agonists/antagonists. Molecular pharmacology *54*, 105-112.

Baumeister, W., Walz, J., Zuhl, F., and Seemuller, E. (1998). The proteasome: paradigm of a self-compartmentalizing protease. Cell *92*, 367-380.

Bazzaro, M., Lee, M.K., Zoso, A., Stirling, W.L., Santillan, A., Shih Ie, M., and Roden, R.B. (2006). Ubiquitin-proteasome system stress sensitizes ovarian cancer to proteasome inhibitor-induced apoptosis. Cancer research *66*, 3754-3763.

Beato, M. (1989). Gene regulation by steroid hormones. Cell *56*, 335-344.

Benjamini, Y., and Hochberg, Y. (1995). Controlling the false discovery rate: a practical and powerful approach to multiple testing. Journal of the Royal Statistical Society, Series B (Methodological) *57*, 289–300.

Berkers, C.R., Verdoes, M., Lichtman, E., Fiebiger, E., Kessler, B.M., Anderson, K.C., Ploegh, H.L., Ovaa, H., and Galardy, P.J. (2005). Activity probe for in vivo profiling of the specificity of proteasome inhibitor bortezomib. Nature methods *2*, 357-362.

Bolstad, B.M., Irizarry, R.A., Astrand, M., and Speed, T.P. (2003). A comparison of normalization methods for high density oligonucleotide array data based on variance and bias. Bioinformatics (Oxford, England) *19*, 185-193.

Bolzer, A., Kreth, G., Solovei, I., Koehler, D., Saracoglu, K., Fauth, C., Muller, S., Eils, R., Cremer, C., Speicher, M.R., and Cremer, T. (2005). Three-dimensional maps of all chromosomes in human male fibroblast nuclei and prometaphase rosettes. PLoS biology *3*, e157.

Bossola, M., Muscaritoli, M., Costelli, P., Grieco, G., Bonelli, G., Pacelli, F., Rossi Fanelli, F., Doglietto, G.B., and Baccino, F.M. (2003). Increased muscle proteasome activity correlates with disease severity in gastric cancer patients. Annals of surgery *237*, 384-389.

Braun, B.C., Glickman, M., Kraft, R., Dahlmann, B., Kloetzel, P.M., Finley, D., and Schmidt, M. (1999). The base of the proteasome regulatory particle exhibits chaperone-like activity. Nature cell biology *1*, 221-226.

Bretschneider, N., Kangaspeska, S., Seifert, M., Reid, G., Gannon, F., and Denger, S. (2008). E2-mediated cathepsin D (CTSD) activation involves looping of distal enhancer elements. Molecular oncology *2*, 182-190.

Bross, P.F., Kane, R., Farrell, A.T., Abraham, S., Benson, K., Brower, M.E., Bradley, S., Gobburu, J.V., Goheer, A., Lee, S.L., Leighton, J., Liang, C.Y., Lostritto, R.T., McGuinn, W.D., Morse, D.E., Rahman, A., Rosario, L.A., Verbois, S.L., Williams, G., *et al.* (2004). Approval summary for bortezomib for injection in the treatment of multiple myeloma. Clin Cancer Res *10*, 3954-3964.

Brueggemeier, R.W., Hackett, J.C., and Diaz-Cruz, E.S. (2005). Aromatase inhibitors in the treatment of breast cancer. Endocrine reviews *26*, 331-345.

Brzozowski, A.M., Pike, A.C., Dauter, Z., Hubbard, R.E., Bonn, T., Engstrom, O., Ohman, L., Greene, G.L., Gustafsson, J.A., and Carlquist, M. (1997). Molecular basis of agonism and antagonism in the oestrogen receptor. Nature *389*, 753-758.

Buckingham, J.C. (2006). Glucocorticoids: exemplars of multi-tasking. British journal of pharmacology *147 Suppl 1*, S258-268.

Bunone, G., Briand, P.A., Miksicek, R.J., and Picard, D. (1996). Activation of the unliganded estrogen receptor by EGF involves the MAP kinase pathway and direct phosphorylation. The EMBO journal *15*, 2174-2183.

Cardoso, F., Durbecq, V., Laes, J.F., Badran, B., Lagneaux, L., Bex, F., Desmedt, C., Willard-Gallo, K., Ross, J.S., Burny, A., Piccart, M., and Sotiriou, C. (2006). Bortezomib (PS-341, Velcade) increases the efficacy of trastuzumab (Herceptin) in HER-2-positive breast cancer cells in a synergistic manner. Molecular cancer therapeutics *5*, 3042-3051.

Cardoso, F., Ross, J.S., Picart, M.J., Sotiriou, C., and Durbecq, V. (2004). Targeting the ubiquitin-proteasome pathway in breast cancer. Clinical breast cancer *5*, 148-157.

Carey, L.A., Perou, C.M., Livasy, C.A., Dressler, L.G., Cowan, D., Conway, K., Karaca, G., Troester, M.A., Tse, C.K., Edmiston, S., Deming, S.L., Geradts, J., Cheang, M.C., Nielsen, T.O., Moorman, P.G., Earp, H.S., and Millikan, R.C. (2006). Race, breast cancer subtypes, and survival in the Carolina Breast Cancer Study. Jama *295*, 2492-2502.

Carroll, J.S., Liu, X.S., Brodsky, A.S., Li, W., Meyer, C.A., Szary, A.J., Eeckhoute, J., Shao, W., Hestermann, E.V., Geistlinger, T.R., Fox, E.A., Silver, P.A., and Brown, M. (2005). Chromosome-wide mapping of estrogen receptor binding reveals long-range regulation requiring the forkhead protein FoxA1. Cell *122*, 33-43.

Carroll, J.S., Meyer, C.A., Song, J., Li, W., Geistlinger, T.R., Eeckhoute, J., Brodsky, A.S., Keeton, E.K., Fertuck, K.C., Hall, G.F., Wang, Q., Bekiranov, S., Sementchenko, V., Fox, E.A., Silver, P.A., Gingeras, T.R., Liu, X.S., and Brown, M. (2006). Genome-wide analysis of estrogen receptor binding sites. NatGenet *38*, 1289-1297.

Carter, D., Chakalova, L., Osborne, C.S., Dai, Y.F., and Fraser, P. (2002). Long-range chromatin regulatory interactions in vivo. Nature genetics *32*, 623-626.

Chapman, R.D., Heidemann, M., Albert, T.K., Mailhammer, R., Flatley, A., Meisterernst, M., Kremmer, E., and Eick, D. (2007). Transcribing RNA polymerase II is phosphorylated at CTD residue serine-7. Science *318*, 1780-1782.

Chau, V., Tobias, J.W., Bachmair, A., Marriott, D., Ecker, D.J., Gonda, D.K., and Varshavsky, A. (1989). A multiubiquitin chain is confined to specific lysine in a targeted short-lived protein. Science *243*, 1576-1583.

Chen, J.D., and Evans, R.M. (1995). A transcriptional co-repressor that interacts with nuclear hormone receptors. Nature *377*, 454-457.

Chen, L., and Madura, K. (2005). Increased proteasome activity, ubiquitin-conjugating enzymes, and eEF1A translation factor detected in breast cancer tissue. Cancer research *65*, 5599-5606.

Cheskis, B.J., Greger, J.G., Nagpal, S., and Freedman, L.P. (2007). Signaling by estrogens. Journal of cellular physiology *213*, 610-617.

Clarke, R., Leonessa, F., Welch, J.N., and Skaar, T.C. (2001). Cellular and molecular pharmacology of antiestrogen action and resistance. PharmacolRev *53*, 25-71.

Collins, G.A., and Tansey, W.P. (2006). The proteasome: a utility tool for transcription? CurrOpinGenetDev *16*, 197-202.

Committee, N.R.N. (1999). A unified nomenclature system for the nuclear receptor superfamily. Cell *97*, 161-163.

Coser, K.R., Chesnes, J., Hur, J., Ray, S., Isselbacher, K.J., and Shioda, T. (2003). Global analysis of ligand sensitivity of estrogen inducible and suppressible genes in MCF7/BUS breast cancer cells by DNA microarray. Proceedings of the National Academy of Sciences of the United States of America *100*, 13994-13999.

Couse, J.F., Curtis Hewitt, S., and Korach, K.S. (2000). Receptor null mice reveal contrasting roles for estrogen receptor alpha and beta in reproductive tissues. The Journal of steroid biochemistry and molecular biology *74*, 287-296.

Couse, J.F., Hewitt, S.C., Bunch, D.O., Sar, M., Walker, V.R., Davis, B.J., and Korach, K.S. (1999). Postnatal sex reversal of the ovaries in mice lacking estrogen receptors alpha and beta. Science *286*, 2328-2331.

Curtis Hewitt, S., Couse, J.F., and Korach, K.S. (2000). Estrogen receptor transcription and transactivation: Estrogen receptor knockout mice: what their phenotypes reveal about mechanisms of estrogen action. Breast Cancer Res *2*, 345-352.

Cuzick, J., Powles, T., Veronesi, U., Forbes, J., Edwards, R., Ashley, S., and Boyle, P. (2003). Overview of the main outcomes in breast-cancer prevention trials. Lancet *361*, 296-300.

Dauvois, S., White, R., and Parker, M.G. (1993). The antiestrogen ICI 182780 disrupts estrogen receptor nucleocytoplasmic shuttling. Journal of cell science *106 ( Pt 4)*, 1377-1388.

Dekker, J., Rippe, K., Dekker, M., and Kleckner, N. (2002). Capturing chromosome conformation. Science *295*, 1306-1311.

Dennis, A.P., Lonard, D.M., Nawaz, Z., and O'Malley, B.W. (2005). Inhibition of the 26S proteasome blocks progesterone receptor-dependent transcription through failed recruitment of RNA polymerase II. The Journal of steroid biochemistry and molecular biology *94*, 337-346.

Denton, R.R., Koszewski, N.J., and Notides, A.C. (1992). Estrogen receptor phosphorylation. Hormonal dependence and consequence on specific DNA binding. The Journal of biological chemistry *267*, 7263-7268.

Deroo, B.J., Rentsch, C., Sampath, S., Young, J., DeFranco, D.B., and Archer, T.K. (2002). Proteasomal inhibition enhances glucocorticoid receptor transactivation and alters its subnuclear trafficking. Molecular and cellular biology *22*, 4113-4123.

Deveraux, Q., Ustrell, V., Pickart, C., and Rechsteiner, M. (1994). A 26 S protease subunit that binds ubiquitin conjugates. The Journal of biological chemistry *269*, 7059-7061.

Dostie, J., Richmond, T.A., Arnaout, R.A., Selzer, R.R., Lee, W.L., Honan, T.A., Rubio, E.D., Krumm, A., Lamb, J., Nusbaum, C., Green, R.D., and Dekker, J. (2006). Chromosome Conformation Capture Carbon Copy (5C): a massively parallel solution for mapping interactions between genomic elements. Genome research *16*, 1299-1309.

Driscoll, M.D., Sathya, G., Muyan, M., Klinge, C.M., Hilf, R., and Bambara, R.A. (1998). Sequence requirements for estrogen receptor binding to estrogen response elements. The Journal of biological chemistry *273*, 29321-29330.

Drissen, R., Palstra, R.J., Gillemans, N., Splinter, E., Grosveld, F., Philipsen, S., and de Laat, W. (2004). The active spatial organization of the beta-globin locus requires the transcription factor EKLF. Genes Dev *18*, 2485-2490.

Egloff, S., O'Reilly, D., Chapman, R.D., Taylor, A., Tanzhaus, K., Pitts, L., Eick, D., and Murphy, S. (2007). Serine-7 of the RNA polymerase II CTD is specifically required for snRNA gene expression. Science 1777-1779.

El Khissiin, A., and Leclercq, G. (1999). Implication of proteasome in estrogen receptor degradation. FEBS Lett *448*, 160-166.

Elsasser, S., Chandler-Militello, D., Muller, B., Hanna, J., and Finley, D. (2004). Rad23 and Rpn10 serve as alternative ubiquitin receptors for the proteasome. The Journal of biological chemistry *279*, 26817-26822.

Emmen, J.M., and Korach, K.S. (2003). Estrogen receptor knockout mice: phenotypes in the female reproductive tract. Gynecol Endocrinol *17*, 169-176.

Encio, I.J., and Detera-Wadleigh, S.D. (1991). The genomic structure of the human glucocorticoid receptor. The Journal of biological chemistry *266*, 7182-7188.

Endoh, H., Maruyama, K., Masuhiro, Y., Kobayashi, Y., Goto, M., Tai, H., Yanagisawa, J., Metzger, D., Hashimoto, S., and Kato, S. (1999). Purification and identification of p68 RNA helicase acting as a transcriptional coactivator specific for the activation function 1 of human estrogen receptor alpha. Molecular and cellular biology *19*, 5363-5372.

Ezhkova, E., and Tansey, W.P. (2004). Proteasomal ATPases link ubiquitylation of histone H2B to methylation of histone H3. Molecular cell *13*, 435-442.

Fan, M., Nakshatri, H., and Nephew, K.P. (2004). Inhibiting proteasomal proteolysis sustains estrogen receptor-alpha activation. MolEndocrinol *18*, 2603-2615.

Faus, H., and Haendler, B. (2006). Post-translational modifications of steroid receptors. Biomedicine & pharmacotherapy = Biomedecine & pharmacotherapie *60*, 520-528.

Feng, W., Ribeiro, R.C., Wagner, R.L., Nguyen, H., Apriletti, J.W., Fletterick, R.J., Baxter, J.D., Kushner, P.J., and West, B.L. (1998). Hormone-dependent coactivator binding to a hydrophobic cleft on nuclear receptors. Science *280*, 1747-1749.

Fenteany, G., Standaert, R.F., Lane, W.S., Choi, S., Corey, E.J., and Schreiber, S.L. (1995). Inhibition of proteasome activities and subunit-specific amino-terminal threonine modification by lactacystin. Science *268*, 726-731.

Ferdous, A., Gonzalez, F., Sun, L., Kodadek, T., and Johnston, S.A. (2001). The 19S regulatory particle of the proteasome is required for efficient transcription elongation by RNA polymerase II. MolCell *7*, 981-991.

Finley, D. (2009). Recognition and processing of ubiquitin-protein conjugates by the proteasome. Annual review of biochemistry *78*, 477-513.

Finley, D., Sadis, S., Monia, B.P., Boucher, P., Ecker, D.J., Crooke, S.T., and Chau, V. (1994). Inhibition of proteolysis and cell cycle progression in a multiubiquitination-deficient yeast mutant. Molecular and cellular biology *14*, 5501-5509.

Fisher, B., Costantino, J.P., Wickerham, D.L., Cecchini, R.S., Cronin, W.M., Robidoux, A., Bevers, T.B., Kavanah, M.T., Atkins, J.N., Margolese, R.G., Runowicz, C.D., James, J.M., Ford, L.G., and Wolmark, N. (2005). Tamoxifen for the prevention of breast cancer: current status of the National Surgical Adjuvant Breast and Bowel Project P-1 study. Journal of the National Cancer Institute *97*, 1652-1662.

Frasor, J., Danes, J.M., Komm, B., Chang, K.C., Lyttle, C.R., and Katzenellenbogen, B.S. (2003). Profiling of estrogen up- and down-regulated gene expression in human breast cancer cells: insights into gene networks and pathways underlying estrogenic control of proliferation and cell phenotype. Endocrinology *144*, 4562-4574.

Fritah, A., Saucier, C., Mester, J., Redeuilh, G., and Sabbah, M. (2005). p21WAF1/CIP1 selectively controls the transcriptional activity of estrogen receptor alpha. MolCell Biol *25*, 2419-2430.

Fullwood, M.J., Liu, M.H., Pan, Y.F., Liu, J., Xu, H., Mohamed, Y.B., Orlov, Y.L., Velkov, S., Ho, A., Mei, P.H., Chew, E.G., Huang, P.Y., Welboren, W.J., Han, Y., Ooi, H.S., Ariyaratne, P.N., Vega, V.B., Luo, Y., Tan, P.Y., *et al*. (2009). An oestrogen-receptor-alpha-bound human chromatin interactome. Nature *462*, 58-64.

Fullwood, M.J., and Ruan, Y. (2009). ChIP-based methods for the identification of long-range chromatin interactions. Journal of cellular biochemistry *107*, 30-39.

Galan, J.M., and Haguenauer-Tsapis, R. (1997). Ubiquitin lys63 is involved in ubiquitination of a yeast plasma membrane protein. The EMBO journal *16*, 5847-5854.

Galigniana, M.D., Scruggs, J.L., Herrington, J., Welsh, M.J., Carter-Su, C., Housley, P.R., and Pratt, W.B. (1998). Heat shock protein 90-dependent (geldanamycin-inhibited) movement of the glucocorticoid receptor through the cytoplasm to the nucleus requires intact cytoskeleton. Molecular endocrinology *12*, 1903-1913.

Galon, J., Franchimont, D., Hiroi, N., Frey, G., Boettner, A., Ehrhart-Bornstein, M., O'Shea, J.J., Chrousos, G.P., and Bornstein, S.R. (2002). Gene profiling reveals unknown enhancing and suppressive actions of glucocorticoids on immune cells. Faseb J *16*, 61-71.

Germain, P., Staels, B., Dacquet, C., Spedding, M., and Laudet, V. (2006). Overview of nomenclature of nuclear receptors. Pharmacological reviews *58*, 685-704.

Giguere, V., Yang, N., Segui, P., and Evans, R.M. (1988). Identification of a new class of steroid hormone receptors. Nature *331*, 91-94.

Gonzalez, F., Delahodde, A., Kodadek, T., and Johnston, S.A. (2002). Recruitment of a 19S proteasome subcomplex to an activated promoter. Science *296*, 548-550.

Gottardis, M.M., Robinson, S.P., Satyaswaroop, P.G., and Jordan, V.C. (1988). Contrasting actions of tamoxifen on endometrial and breast tumor growth in the athymic mouse. Cancer research *48*, 812-815.

Hafezi-Moghadam, A., Simoncini, T., Yang, Z., Limbourg, F.P., Plumier, J.C., Rebsamen, M.C., Hsieh, C.M., Chui, D.S., Thomas, K.L., Prorock, A.J., Laubach, V.E., Moskowitz, M.A., French, B.A., Ley, K., and Liao, J.K. (2002). Acute cardiovascular protective effects of corticosteroids are mediated by non-transcriptional activation of endothelial nitric oxide synthase. Nature medicine *8*, 473-479.

Hakim, O., John, S., Ling, J.Q., Biddie, S.C., Hoffman, A.R., and Hager, G.L. (2009). Glucocorticoid receptor activation of the Ciz1-Lcn2 locus by long range interactions. The Journal of biological chemistry *284*, 6048-6052.

Hall, J.M., and McDonnell, D.P. (1999). The estrogen receptor beta-isoform (ERbeta) of the human estrogen receptor modulates ERalpha transcriptional activity and is a key regulator of the cellular response to estrogens and antiestrogens. Endocrinology *140*, 5566-5578.

Hatakeyama, S., Yada, M., Matsumoto, M., Ishida, N., and Nakayama, K.I. (2001). U box proteins as a new family of ubiquitin-protein ligases. The Journal of biological chemistry *276*, 33111-33120.

Heck, S., Kullmann, M., Gast, A., Ponta, H., Rahmsdorf, H.J., Herrlich, P., and Cato, A.C. (1994). A distinct modulating domain in glucocorticoid receptor monomers in the repression of activity of the transcription factor AP-1. The EMBO journal *13*, 4087-4095.

Heery, D.M., Kalkhoven, E., Hoare, S., and Parker, M.G. (1997). A signature motif in transcriptional co-activators mediates binding to nuclear receptors. Nature *387*, 733-736.

Henderson, B.E., Ross, R., and Bernstein, L. (1988). Estrogens as a cause of human cancer: the Richard and Hinda Rosenthal Foundation award lecture. Cancer research *48*, 246-253.

Hewitt, S.C., and Korach, K.S. (2003). Oestrogen receptor knockout mice: roles for oestrogen receptors alpha and beta in reproductive tissues. Reproduction (Cambridge, England) *125*, 143-149.

Hochstrasser, M. (1996). Ubiquitin-dependent protein degradation. Annual review of genetics *30*, 405-439.

Hollenberg, S.M., Weinberger, C., Ong, E.S., Cerelli, G., Oro, A., Lebo, R., Thompson, E.B., Rosenfeld, M.G., and Evans, R.M. (1985). Primary structure and expression of a functional human glucocorticoid receptor cDNA. Nature *318*, 635-641.

Horlein, A.J., Naar, A.M., Heinzel, T., Torchia, J., Gloss, B., Kurokawa, R., Ryan, A., Kamei, Y., Soderstrom, M., Glass, C.K., and et al. (1995). Ligand-independent repression by the thyroid hormone receptor mediated by a nuclear receptor co-repressor. Nature *377*, 397-404.

Horowitz, M.C. (1993). Cytokines and estrogen in bone: anti-osteoporotic effects. Science *260*, 626-627.

Hsu, P.Y., Hsu, H.K., Singer, G.A., Yan, P.S., Rodriguez, B.A., Liu, J.C., Weng, Y.I., Deatherage, D.E., Chen, Z., Pereira, J.S., Lopez, R., Russo, J., Wang, Q., Lamartiniere, C.A., Nephew, K.P., and Huang, T.H. (2010). Estrogen-mediated epigenetic repression of large chromosomal regions through DNA looping. Genome research *20*, 733-744.

Hu, Q., Kwon, Y.S., Nunez, E., Cardamone, M.D., Hutt, K.R., Ohgi, K.A., Garcia-Bassets, I., Rose, D.W., Glass, C.K., Rosenfeld, M.G., and Fu, X.D. (2008). Enhancing nuclear receptor-induced transcription requires nuclear motor and LSD1-dependent gene networking in interchromatin granules. Proceedings of the National Academy of Sciences of the United States of America *105*, 19199-19204.

Husnjak, K., Elsasser, S., Zhang, N., Chen, X., Randles, L., Shi, Y., Hofmann, K., Walters, K.J., Finley, D., and Dikic, I. (2008). Proteasome subunit Rpn13 is a novel ubiquitin receptor. Nature *453*, 481-488.

Ito, K., Yamamura, S., Essilfie-Quaye, S., Cosio, B., Ito, M., Barnes, P.J., and Adcock, I.M. (2006). Histone deacetylase 2-mediated deacetylation of the glucocorticoid receptor enables NF-kappaB suppression. The Journal of experimental medicine *203*, 7-13.

Jakacka, M., Ito, M., Weiss, J., Chien, P.Y., Gehm, B.D., and Jameson, J.L. (2001). Estrogen receptor binding to DNA is not required for its activity through the nonclassical AP1 pathway. The Journal of biological chemistry *276*, 13615-13621.

Jallepalli, P.V., and Lengauer, C. (2001). Chromosome segregation and cancer: cutting through the mystery. Nat Rev Cancer *1*, 109-117.

Jemal, A., Siegel, R., Xu, J., and Ward, E. (2010). Cancer Statistics, 2010. CA: a cancer journal for clinicians.

Joel, P.B., Traish, A.M., and Lannigan, D.A. (1995). Estradiol and phorbol ester cause phosphorylation of serine 118 in the human estrogen receptor. Molecular endocrinology *9*, 1041-1052.

Johnsen, S.A., Güngör, C., Prenzel, T., Riethdorf, S., Riethdorf, L., Taniguchi-Ishigaki, N., Rau, T., Tursun, B., Furlow, J.D., Sauter, G., Scheffner, M., Pantel, K., Gannon, F., and Bach, I. (2009). Regulation of estrogen-dependent transcription by the LIM cofactors CLIM and RLIM in breast cancer. Cancer Res *69*, 128-136.

Jonat, C., Rahmsdorf, H.J., Park, K.K., Cato, A.C., Gebel, S., Ponta, H., and Herrlich, P. (1990). Antitumor promotion and antiinflammation: down-modulation of AP-1 (Fos/Jun) activity by glucocorticoid hormone. Cell *62*, 1189-1204.

Jordan, V.C. (2001). Selective estrogen receptor modulation: a personal perspective. Cancer research *61*, 5683-5687.

Kagey, M.H., Newman, J.J., Bilodeau, S., Zhan, Y., Orlando, D.A., van Berkum, N.L., Ebmeier, C.C., Goossens, J., Rahl, P.B., Levine, S.S., Taatjes, D.J., Dekker, J., and Young, R.A. (2010). Mediator and cohesin connect gene expression and chromatin architecture. Nature.

Kane, R.C., Farrell, A.T., Sridhara, R., and Pazdur, R. (2006). United States Food and Drug Administration approval summary: bortezomib for the treatment of progressive multiple myeloma after one prior therapy. Clin Cancer Res *12*, 2955-2960.

Kang, L., Zhang, X., Xie, Y., Tu, Y., Wang, D., Liu, Z., and Wang, Z.Y. (2010). Involvement of estrogen receptor variant ER-alpha36, not GPR30, in nongenomic estrogen signaling. Molecular endocrinology *24*, 709-721.

Kang, Z., Pirskanen, A., Janne, O.A., and Palvimo, J.J. (2002). Involvement of proteasome in the dynamic assembly of the androgen receptor transcription complex. JBiolChem *277*, 48366-48371.

Kato, S., Endoh, H., Masuhiro, Y., Kitamoto, T., Uchiyama, S., Sasaki, H., Masushige, S., Gotoh, Y., Nishida, E., Kawashima, H., Metzger, D., and Chambon, P. (1995). Activation of the estrogen receptor through phosphorylation by mitogen-activated protein kinase. Science *270*, 1491-1494.

Keeton, E.K., and Brown, M. (2005). Cell cycle progression stimulated by tamoxifen-bound estrogen receptor-alpha and promoter-specific effects in breast cancer cells deficient in N-CoR and SMRT. Molecular endocrinology *19*, 1543-1554.

Kelsey, J.L., Gammon, M.D., and John, E.M. (1993). Reproductive factors and breast cancer. Epidemiologic reviews *15*, 36-47.

Kim, I., Mi, K., and Rao, H. (2004). Multiple interactions of rad23 suggest a mechanism for ubiquitylated substrate delivery important in proteolysis. Molecular biology of the cell *15*, 3357-3365.

Kim, J., Hake, S.B., and Roeder, R.G. (2005). The human homolog of yeast BRE1 functions as a transcriptional coactivator through direct activator interactions. Molecular cell *20*, 759-770.

Kim, M.Y., Woo, E.M., Chong, Y.T., Homenko, D.R., and Kraus, W.L. (2006). Acetylation of estrogen receptor alpha by p300 at lysines 266 and 268 enhances the deoxyribonucleic acid binding and transactivation activities of the receptor. Molecular endocrinology *20*, 1479-1493.

Kininis, M., Isaacs, G.D., Core, L.J., Hah, N., and Kraus, W.L. (2009). Postrecruitment regulation of RNA polymerase II directs rapid signaling responses at the promoters of estrogen target genes. Molecular and cellular biology *29*, 1123-1133.

Kinyamu, H.K., and Archer, T.K. (2007). Proteasome activity modulates chromatin modifications and RNA polymerase II phosphorylation to enhance glucocorticoid receptor-mediated transcription. Molecular and cellular biology *27*, 4891-4904.

Kinyamu, H.K., Collins, J.B., Grissom, S.F., Hebbar, P.B., and Archer, T.K. (2008). Genome wide transcriptional profiling in breast cancer cells reveals distinct changes in hormone receptor target genes and chromatin modifying enzymes after proteasome inhibition. Molecular carcinogenesis *47*, 845-885.

Kisselev, A.F., Akopian, T.N., Woo, K.M., and Goldberg, A.L. (1999). The sizes of peptides generated from protein by mammalian 26 and 20 S proteasomes. Implications for understanding the degradative mechanism and antigen presentation. The Journal of biological chemistry *274*, 3363-3371.

Klinge, C.M. (2000). Estrogen receptor interaction with co-activators and co-repressors. Steroids *65*, 227-251.

Kocanova, S., Kerr, E.A., Rafique, S., Boyle, S., Katz, E., Caze-Subra, S., Bickmore, W.A., and Bystricky, K. (2010). Activation of estrogen-responsive genes does not require their nuclear co-localization. PLoS genetics *6*, e1000922.

Koegl, M., Hoppe, T., Schlenker, S., Ulrich, H.D., Mayer, T.U., and Jentsch, S. (1999). A novel ubiquitination factor, E4, is involved in multiubiquitin chain assembly. Cell *96*, 635-644.

Koh, S.S., Chen, D., Lee, Y.H., and Stallcup, M.R. (2001). Synergistic enhancement of nuclear receptor function by p160 coactivators and two coactivators with protein methyltransferase activities. The Journal of biological chemistry *276*, 1089-1098.

Kousteni, S., Bellido, T., Plotkin, L.I., O'Brien, C.A., Bodenner, D.L., Han, L., Han, K., DiGregorio, G.B., Katzenellenbogen, J.A., Katzenellenbogen, B.S., Roberson, P.K., Weinstein, R.S., Jilka, R.L., and Manolagas, S.C. (2001). Nongenotropic, sex-nonspecific signaling through the estrogen or androgen receptors: dissociation from transcriptional activity. Cell *104*, 719-730.

Kumar, R., and Thompson, E.B. (1999). The structure of the nuclear hormone receptors. Steroids *64*, 310-319.

Kumatori, A., Tanaka, K., Inamura, N., Sone, S., Ogura, T., Matsumoto, T., Tachikawa, T., Shin, S., and Ichihara, A. (1990). Abnormally high expression of proteasomes in human leukemic cells. Proceedings of the National Academy of Sciences of the United States of America *87*, 7071-7075.

Kushner, P.J., Agard, D.A., Greene, G.L., Scanlan, T.S., Shiau, A.K., Uht, R.M., and Webb, P. (2000). Estrogen receptor pathways to AP-1. The Journal of steroid biochemistry and molecular biology *74*, 311-317.

Laemmli, U.K. (1970). Cleavage of structural proteins during the assembly of the head of bacteriophage T4. Nature *227*, 680-685.

Lam, Y.A., Lawson, T.G., Velayutham, M., Zweier, J.L., and Pickart, C.M. (2002). A proteasomal ATPase subunit recognizes the polyubiquitin degradation signal. Nature *416*, 763-767.

Lannigan, D.A. (2003). Estrogen receptor phosphorylation. Steroids *68*, 1-9.

Lassot, I., Latreille, D., Rousset, E., Sourisseau, M., Linares, L.K., Chable-Bessia, C., Coux, O., Benkirane, M., and Kiernan, R.E. (2007). The proteasome regulates HIV-1 transcription by both proteolytic and nonproteolytic mechanisms. MolCell *25*, 369-383.

Le Drean, Y., Mincheneau, N., Le Goff, P., and Michel, D. (2002). Potentiation of glucocorticoid receptor transcriptional activity by sumoylation. Endocrinology *143*, 3482-3489.

Le Romancer, M., Treilleux, I., Leconte, N., Robin-Lespinasse, Y., Sentis, S., Bouchekioua-Bouzaghou, K., Goddard, S., Gobert-Gosse, S., and Corbo, L. (2008). Regulation of estrogen rapid signaling through arginine methylation by PRMT1. Molecular cell *31*, 212-221.

Li, Q., Barkess, G., and Qian, H. (2006). Chromatin looping and the probability of transcription. Trends Genet *22*, 197-202.

Li, X., Huang, J., Yi, P., Bambara, R.A., Hilf, R., and Muyan, M. (2004). Single-chain estrogen receptors (ERs) reveal that the ERalpha/beta heterodimer emulates functions of the ERalpha dimer in genomic estrogen signaling pathways. Molecular and cellular biology *24*, 7681-7694.

Lightcap, E.S., McCormack, T.A., Pien, C.S., Chau, V., Adams, J., and Elliott, P.J. (2000). Proteasome inhibition measurements: clinical application. Clinical chemistry *46*, 673-683.

Lin, C.Y., Vega, V.B., Thomsen, J.S., Zhang, T., Kong, S.L., Xie, M., Chiu, K.P., Lipovich, L., Barnett, D.H., Stossi, F., Yeo, A., George, J., Kuznetsov, V.A., Lee, Y.K., Charn, T.H., Palanisamy, N., Miller, L.D., Cheung, E., Katzenellenbogen, B.S., *et al.* (2007). Whole-genome cartography of estrogen receptor alpha binding sites. PLoS genetics *3*, e87.

Lin, H.K., Altuwaijri, S., Lin, W.J., Kan, P.Y., Collins, L.L., and Chang, C. (2002). Proteasome activity is required for androgen receptor transcriptional activity via regulation of androgen receptor nuclear translocation and interaction with coregulators in prostate cancer cells. The Journal of biological chemistry *277*, 36570-36576.

Ling, Y.H., Liebes, L., Jiang, J.D., Holland, J.F., Elliott, P.J., Adams, J., Muggia, F.M., and Perez-Soler, R. (2003). Mechanisms of proteasome inhibitor PS-341-induced G(2)-M-phase arrest and apoptosis in human non-small cell lung cancer cell lines. Clin Cancer Res *9*, 1145-1154.

Lonard, D.M., Nawaz, Z., Smith, C.L., and O'Malley, B.W. (2000). The 26S proteasome is required for estrogen receptor-alpha and coactivator turnover and for efficient estrogen receptor-alpha transactivation. MolCell *5*, 939-948.

Love, R.R., Mazess, R.B., Barden, H.S., Epstein, S., Newcomb, P.A., Jordan, V.C., Carbone, P.P., and DeMets, D.L. (1992). Effects of tamoxifen on bone mineral density in postmenopausal women with breast cancer. The New England journal of medicine *326*, 852-856.

Lu, D., Kiriyama, Y., Lee, K.Y., and Giguere, V. (2001). Transcriptional regulation of the estrogen-inducible pS2 breast cancer marker gene by the ERR family of orphan nuclear receptors. Cancer research *61*, 6755-6761.

Lu, Q., Pallas, D.C., Surks, H.K., Baur, W.E., Mendelsohn, M.E., and Karas, R.H. (2004). Striatin assembles a membrane signaling complex necessary for rapid, nongenomic activation of endothelial NO synthase by estrogen receptor alpha. Proceedings of the National Academy of Sciences of the United States of America *101*, 17126-17131.

Magklara, A., and Smith, C.L. (2009). A composite intronic element directs dynamic binding of the progesterone receptor and GATA-2. Molecular endocrinology *23*, 61-73.

Maier, C., Runzler, D., Schindelar, J., Grabner, G., Waldhausl, W., Kohler, G., and Luger, A. (2005). G-protein-coupled glucocorticoid receptors on the pituitary cell membrane. Journal of cell science *118*, 3353-3361.

Mangelsdorf, D.J., Thummel, C., Beato, M., Herrlich, P., Schutz, G., Umesono, K., Blumberg, B., Kastner, P., Mark, M., Chambon, P., and Evans, R.M. (1995). The nuclear receptor superfamily: the second decade. Cell *83*, 835-839.

Massarweh, S., Osborne, C.K., Creighton, C.J., Qin, L., Tsimelzon, A., Huang, S., Weiss, H., Rimawi, M., and Schiff, R. (2008). Tamoxifen resistance in breast tumors is driven by growth factor receptor signaling with repression of classic estrogen receptor genomic function. Cancer research *68*, 826-833.

McKay, L.I., and Cidlowski, J.A. (1998). Cross-talk between nuclear factor-kappa B and the steroid hormone receptors: mechanisms of mutual antagonism. Molecular endocrinology *12*, 45-56.

Meng, L., Mohan, R., Kwok, B.H., Elofsson, M., Sin, N., and Crews, C.M. (1999). Epoxomicin, a potent and selective proteasome inhibitor, exhibits in vivo antiinflammatory activity. Proceedings of the National Academy of Sciences of the United States of America *96*, 10403-10408.

Metivier, R., Penot, G., Hubner, M.R., Reid, G., Brand, H., Kos, M., and Gannon, F. (2003). Estrogen receptor-alpha directs ordered, cyclical, and combinatorial recruitment of cofactors on a natural target promoter. Cell *115*, 751-763.

Metivier, R., Reid, G., and Gannon, F. (2006). Transcription in four dimensions: nuclear receptor-directed initiation of gene expression. EMBO Rep *7*, 161-167.

Miele, A., and Dekker, J. (2009). Mapping cis- and trans- chromatin interaction networks using chromosome conformation capture (3C). Methods in molecular biology *464*, 105-121.

Migliaccio, A., Di Domenico, M., Castoria, G., de Falco, A., Bontempo, P., Nola, E., and Auricchio, F. (1996). Tyrosine kinase/p21ras/MAP-kinase pathway activation by estradiol-receptor complex in MCF-7 cells. The EMBO journal *15*, 1292-1300.

Mitsiades, N., Mitsiades, C.S., Poulaki, V., Chauhan, D., Fanourakis, G., Gu, X., Bailey, C., Joseph, M., Libermann, T.A., Treon, S.P., Munshi, N.C., Richardson, P.G., Hideshima, T., and Anderson, K.C. (2002). Molecular sequelae of proteasome inhibition in human multiple myeloma cells. Proceedings of the National Academy of Sciences of the United States of America *99*, 14374-14379.

Monroe, D.G., Getz, B.J., Johnsen, S.A., Riggs, B.L., Khosla, S., and Spelsberg, T.C. (2003a). Estrogen receptor isoform-specific regulation of endogenous gene expression in human osteoblastic cell lines expressing either ERalpha or ERbeta. JCell Biochem *90*, 315-326.

Monroe, D.G., Johnsen, S.A., Subramaniam, M., Getz, B.J., Khosla, S., Riggs, B.L., and Spelsberg, T.C. (2003b). Mutual antagonism of estrogen receptors alpha and beta and their preferred interactions with steroid receptor coactivators in human osteoblastic cell lines. JEndocrinol *176*, 349-357.

Monroe, D.G., Secreto, F.J., Subramaniam, M., Getz, B.J., Khosla, S., and Spelsberg, T.C. (2005). Estrogen receptor alpha and beta heterodimers exert unique effects on estrogen- and tamoxifen-dependent gene expression in human U2OS osteosarcoma cells. Molecular endocrinology *19*, 1555-1568.

Moore, B.S., Eustaquio, A.S., and McGlinchey, R.P. (2008). Advances in and applications of proteasome inhibitors. Current opinion in chemical biology *12*, 434-440.

Naar, A.M., Lemon, B.D., and Tjian, R. (2001). Transcriptional coactivator complexes. Annual review of biochemistry *70*, 475-501.

Nawaz, Z., Lonard, D.M., Dennis, A.P., Smith, C.L., and O'Malley, B.W. (1999a). Proteasome-dependent degradation of the human estrogen receptor. ProcNatlAcadSciUSA *96*, 1858-1862.

Nawaz, Z., Lonard, D.M., Smith, C.L., Lev-Lehman, E., Tsai, S.Y., Tsai, M.J., and O'Malley, B.W. (1999b). The Angelman syndrome-associated protein, E6-AP, is a coactivator for the nuclear hormone receptor superfamily. MolCell Biol *19*, 1182-1189.

Nelson, J.D., Denisenko, O., and Bomsztyk, K. (2006). Protocol for the fast chromatin immunoprecipitation (ChIP) method. Nature protocols *1*, 179-185.

Nijman, S.M., Luna-Vargas, M.P., Velds, A., Brummelkamp, T.R., Dirac, A.M., Sixma, T.K., and Bernards, R. (2005). A genomic and functional inventory of deubiquitinating enzymes. Cell *123*, 773-786.

Nirmala, P.B., and Thampan, R.V. (1995). Ubiquitination of the rat uterine estrogen receptor: dependence on estradiol. BiochemBiophysResCommun *213*, 24-31.

Noordermeer, D., and de Laat, W. (2008). Joining the loops: beta-globin gene regulation. IUBMB life *60*, 824-833.

Nunez, E., Fu, X.D., and Rosenfeld, M.G. (2009). Nuclear organization in the 3D space of the nucleus - cause or consequence? Current opinion in genetics & development *19*, 424-436.

Oakley, R.H., Jewell, C.M., Yudt, M.R., Bofetiado, D.M., and Cidlowski, J.A. (1999). The dominant negative activity of the human glucocorticoid receptor beta isoform. Specificity and mechanisms of action. The Journal of biological chemistry *274*, 27857-27866.

Orlowski, R.Z., and Kuhn, D.J. (2008). Proteasome inhibitors in cancer therapy: lessons from the first decade. Clin Cancer Res *14*, 1649-1657.

Orphanides, G., and Reinberg, D. (2002). A unified theory of gene expression. Cell *108*, 439-451.

Osborne, C.S., Chakalova, L., Brown, K.E., Carter, D., Horton, A., Debrand, E., Goyenechea, B., Mitchell, J.A., Lopes, S., Reik, W., and Fraser, P. (2004). Active genes dynamically colocalize to shared sites of ongoing transcription. Nature genetics *36*, 1065-1071.

Ostrowska, H., Wojcik, C., Omura, S., and Worowski, K. (1997). Lactacystin, a specific inhibitor of the proteasome, inhibits human platelet lysosomal cathepsin A-like enzyme. Biochemical and biophysical research communications *234*, 729-732.

Palombella, V.J., Rando, O.J., Goldberg, A.L., and Maniatis, T. (1994). The ubiquitin-proteasome pathway is required for processing the NF-kappa B1 precursor protein and the activation of NF-kappa B. Cell *78*, 773-785.

Palstra, R.J., Tolhuis, B., Splinter, E., Nijmeijer, R., Grosveld, F., and de Laat, W. (2003). The beta-globin nuclear compartment in development and erythroid differentiation. Nature genetics *35*, 190-194.

Pan, Y.F., Wansa, K.D., Liu, M.H., Zhao, B., Hong, S.Z., Tan, P.Y., Lim, K.S., Bourque, G., Liu, E.T., and Cheung, E. (2008). Regulation of estrogen receptor-mediated long range transcription via evolutionarily conserved distal response elements. The Journal of biological chemistry *283*, 32977-32988.

Parada, L., and Misteli, T. (2002). Chromosome positioning in the interphase nucleus. Trends in cell biology *12*, 425-432.

Park, K.J., Krishnan, V., O'Malley, B.W., Yamamoto, Y., and Gaynor, R.B. (2005). Formation of an IKKalpha-dependent transcription complex is required for estrogen receptor-mediated gene activation. MolCell *18*, 71-82.

Park, W.C., and Jordan, V.C. (2002). Selective estrogen receptor modulators (SERMS) and their roles in breast cancer prevention. Trends in molecular medicine *8*, 82-88.

Pearce, S.T., and Jordan, V.C. (2004). The biological role of estrogen receptors alpha and beta in cancer. Critical reviews in oncology/hematology *50*, 3-22.

Peterson, J.E., Kulik, G., Jelinek, T., Reuter, C.W., Shannon, J.A., and Weber, M.J. (1996). Src phosphorylates the insulin-like growth factor type I receptor on the autophosphorylation sites. Requirement for transformation by src. The Journal of biological chemistry *271*, 31562-31571.

Picard, D., and Yamamoto, K.R. (1987). Two signals mediate hormone-dependent nuclear localization of the glucocorticoid receptor. The EMBO journal *6*, 3333-3340.

Pike, C.J., Carroll, J.C., Rosario, E.R., and Barron, A.M. (2009). Protective actions of sex steroid hormones in Alzheimer's disease. Frontiers in neuroendocrinology *30*, 239-258.

Powers, G.L., Ellison-Zelski, S.J., Casa, A.J., Lee, A.V., and Alarid, E.T. (2010). Proteasome inhibition represses ERalpha gene expression in ER+ cells: a new link between proteasome activity and estrogen signaling in breast cancer. Oncogene *29*, 1509-1518.

Pratt, W.B., and Toft, D.O. (1997). Steroid receptor interactions with heat shock protein and immunophilin chaperones. Endocrine reviews *18*, 306-360.

Ray, A., and Prefontaine, K.E. (1994). Physical association and functional antagonism between the p65 subunit of transcription factor NF-kappa B and the glucocorticoid receptor. Proceedings of the National Academy of Sciences of the United States of America *91*, 752-756.

Razandi, M., Oh, P., Pedram, A., Schnitzer, J., and Levin, E.R. (2002). ERs associate with and regulate the production of caveolin: implications for signaling and cellular actions. Molecular endocrinology *16*, 100-115.

Reichardt, H.M., Kaestner, K.H., Tuckermann, J., Kretz, O., Wessely, O., Bock, R., Gass, P., Schmid, W., Herrlich, P., Angel, P., and Schutz, G. (1998). DNA binding of the glucocorticoid receptor is not essential for survival. Cell *93*, 531-541.

Reid, G., Hubner, M.R., Metivier, R., Brand, H., Denger, S., Manu, D., Beaudouin, J., Ellenberg, J., and Gannon, F. (2003). Cyclic, proteasome-mediated turnover of unliganded and liganded ERalpha on responsive promoters is an integral feature of estrogen signaling. MolCell *11*, 695-707.

Richardson, P.G., Mitsiades, C., Hideshima, T., and Anderson, K.C. (2006). Bortezomib: proteasome inhibition as an effective anticancer therapy. Annual review of medicine *57*, 33-47.

Rock, K.L., Gramm, C., Rothstein, L., Clark, K., Stein, R., Dick, L., Hwang, D., and Goldberg, A.L. (1994). Inhibitors of the proteasome block the degradation of most cell proteins and the generation of peptides presented on MHC class I molecules. Cell *78*, 761-771.

Rogatsky, I., Wang, J.C., Derynck, M.K., Nonaka, D.F., Khodabakhsh, D.B., Haqq, C.M., Darimont, B.D., Garabedian, M.J., and Yamamoto, K.R. (2003). Target-specific utilization of transcriptional regulatory surfaces by the glucocorticoid receptor. Proceedings of the National Academy of Sciences of the United States of America *100*, 13845-13850.

Rose, P.G. (1996). Endometrial carcinoma. The New England journal of medicine *335*, 640-649.

Ross, J.S. (2009). Multigene classifiers, prognostic factors, and predictors of breast cancer clinical outcome. Advances in anatomic pathology *16*, 204-215.

Russo, J., Moral, R., Balogh, G.A., Mailo, D., and Russo, I.H. (2005). The protective role of pregnancy in breast cancer. Breast Cancer Res *7*, 131-142.

Saji, S., Okumura, N., Eguchi, H., Nakashima, S., Suzuki, A., Toi, M., Nozawa, Y., Saji, S., and Hayashi, S. (2001). MDM2 enhances the function of estrogen receptor alpha in human breast cancer cells. BiochemBiophysResCommun *281*, 259-265.

Sanchez, E.R., Toft, D.O., Schlesinger, M.J., and Pratt, W.B. (1985). Evidence that the 90-kDa phosphoprotein associated with the untransformed L-cell glucocorticoid receptor is a murine heat shock protein. The Journal of biological chemistry *260*, 12398-12401.

Sapolsky, R.M., Romero, L.M., and Munck, A.U. (2000). How do glucocorticoids influence stress responses? Integrating permissive, suppressive, stimulatory, and preparative actions. Endocrine reviews *21*, 55-89.

Sato, K., Rajendra, E., and Ohta, T. (2008). The UPS: a promising target for breast cancer treatment. BMCBiochem *9 Suppl 1*, S2.

Satyaswaroop, P.G., Zaino, R.J., and Mortel, R. (1984). Estrogen-like effects of tamoxifen on human endometrial carcinoma transplanted into nude mice. Cancer research *44*, 4006-4010.

Scheffner, M., Nuber, U., and Huibregtse, J.M. (1995). Protein ubiquitination involving an E1-E2-E3 enzyme ubiquitin thioester cascade. Nature *373*, 81-83.

Scheinman, R.I., Gualberto, A., Jewell, C.M., Cidlowski, J.A., and Baldwin, A.S., Jr. (1995). Characterization of mechanisms involved in transrepression of NF-kappa B by activated glucocorticoid receptors. Molecular and cellular biology *15*, 943-953.

Schmidt, D., Schwalie, P.C., Ross-Innes, C.S., Hurtado, A., Brown, G.D., Carroll, J.S., Flicek, P., and Odom, D.T. (2010). A CTCF-independent role for cohesin in tissue-specific transcription. Genome research *20*, 578-588.

Schule, R., Rangarajan, P., Kliewer, S., Ransone, L.J., Bolado, J., Yang, N., Verma, I.M., and Evans, R.M. (1990). Functional antagonism between oncoprotein c-Jun and the glucocorticoid receptor. Cell *62*, 1217-1226.

Seeler, J.S., and Dejean, A. (2003). Nuclear and unclear functions of SUMO. Nature reviews *4*, 690-699.

Sentis, S., Le Romancer, M., Bianchin, C., Rostan, M.C., and Corbo, L. (2005). Sumoylation of the estrogen receptor alpha hinge region regulates its transcriptional activity. Molecular endocrinology *19*, 2671-2684.

Shaaban, A.M., Sloane, J.P., West, C.R., and Foster, C.S. (2002). Breast cancer risk in usual ductal hyperplasia is defined by estrogen receptor-alpha and Ki-67 expression. The American journal of pathology *160*, 597-604.

Shang, Y., Hu, X., DiRenzo, J., Lazar, M.A., and Brown, M. (2000). Cofactor dynamics and sufficiency in estrogen receptor-regulated transcription. Cell *103*, 843-852.

Shiau, A.K., Barstad, D., Loria, P.M., Cheng, L., Kushner, P.J., Agard, D.A., and Greene, G.L. (1998). The structural basis of estrogen receptor/coactivator recognition and the antagonism of this interaction by tamoxifen. Cell *95*, 927-937.

Shih, S.C., Sloper-Mould, K.E., and Hicke, L. (2000). Monoubiquitin carries a novel internalization signal that is appended to activated receptors. The EMBO journal *19*, 187-198.

Simonis, M., Klous, P., Splinter, E., Moshkin, Y., Willemsen, R., de Wit, E., van Steensel, B., and de Laat, W. (2006). Nuclear organization of active and inactive chromatin domains uncovered by chromosome conformation capture-on-chip (4C). Nature genetics *38*, 1348-1354.

Slamon, D.J., Leyland-Jones, B., Shak, S., Fuchs, H., Paton, V., Bajamonde, A., Fleming, T., Eiermann, W., Wolter, J., Pegram, M., Baselga, J., and Norton, L. (2001). Use of chemotherapy plus a monoclonal antibody against HER2 for metastatic breast cancer that overexpresses HER2. The New England journal of medicine *344*, 783-792.

Smyth, G.K. (2004). Linear models and empirical bayes methods for assessing differential expression in microarray experiments. Statistical applications in genetics and molecular biology *3*, Article3.

So, A.Y., Chaivorapol, C., Bolton, E.C., Li, H., and Yamamoto, K.R. (2007). Determinants of cell- and gene-specific transcriptional regulation by the glucocorticoid receptor. PLoSGenet *3*, e94.

Song, R.X., Barnes, C.J., Zhang, Z., Bao, Y., Kumar, R., and Santen, R.J. (2004). The role of Shc and insulin-like growth factor 1 receptor in mediating the translocation of estrogen receptor alpha to the plasma membrane. Proceedings of the National Academy of Sciences of the United States of America *101*, 2076-2081.

Song, R.X., Fan, P., Yue, W., Chen, Y., and Santen, R.J. (2006). Role of receptor complexes in the extranuclear actions of estrogen receptor alpha in breast cancer. Endocrine-related cancer *13 Suppl 1*, S3-13.

Song, S.H., Hou, C., and Dean, A. (2007). A positive role for NLI/Ldb1 in long-range beta-globin locus control region function. Molecular cell *28*, 810-822.

Sorlie, T., Perou, C.M., Tibshirani, R., Aas, T., Geisler, S., Johnsen, H., Hastie, T., Eisen, M.B., van de, R.M., Jeffrey, S.S., Thorsen, T., Quist, H., Matese, J.C., Brown, P.O., Botstein, D., Eystein, L.P., and Borresen-Dale, A.L. (2001). Gene expression patterns of breast carcinomas distinguish tumor subclasses with clinical implications. ProcNatlAcadSciUSA *98*, 10869-10874.

Spence, J., Sadis, S., Haas, A.L., and Finley, D. (1995). A ubiquitin mutant with specific defects in DNA repair and multiubiquitination. Molecular and cellular biology *15*, 1265-1273.

Spilianakis, C.G., Lalioti, M.D., Town, T., Lee, G.R., and Flavell, R.A. (2005). Interchromosomal associations between alternatively expressed loci. Nature *435*, 637-645.

Stender, J.D., Frasor, J., Komm, B., Chang, K.C., Kraus, W.L., and Katzenellenbogen, B.S. (2007). Estrogen-regulated gene networks in human breast cancer cells: involvement of E2F1 in the regulation of cell proliferation. Molecular endocrinology *21*, 2112-2123.

Stenoien, D.L., Patel, K., Mancini, M.G., Dutertre, M., Smith, C.L., O'Malley, B.W., and Mancini, M.A. (2001). FRAP reveals that mobility of oestrogen receptor-alpha is ligand- and proteasome-dependent. Nature cell biology *3*, 15-23.

Subramanian, K., Jia, D., Kapoor-Vazirani, P., Powell, D.R., Collins, R.E., Sharma, D., Peng, J., Cheng, X., and Vertino, P.M. (2008). Regulation of estrogen receptor alpha by the SET7 lysine methyltransferase. Molecular cell *30*, 336-347.

Sun, J., Nawaz, Z., and Slingerland, J.M. (2007). Long-range activation of GREB1 by estrogen receptor via three distal consensus estrogen-responsive elements in breast cancer cells. Molecular endocrinology *21*, 2651-2662.

Sunwoo, J.B., Chen, Z., Dong, G., Yeh, N., Crowl Bancroft, C., Sausville, E., Adams, J., Elliott, P., and Van Waes, C. (2001). Novel proteasome inhibitor PS-341 inhibits activation of nuclear factor-kappa B, cell survival, tumor growth, and angiogenesis in squamous cell carcinoma. Clin Cancer Res *7*, 1419-1428.

Tanaka, K. (2009). The proteasome: overview of structure and functions. Proceedings of the Japan Academy *85*, 12-36.

Tateishi, Y., Kawabe, Y., Chiba, T., Murata, S., Ichikawa, K., Murayama, A., Tanaka, K., Baba, T., Kato, S., and Yanagisawa, J. (2004). Ligand-dependent switching of ubiquitin-proteasome pathways for estrogen receptor. EMBO J *23*, 4813-4823.

Taylor, A.H., and Al-Azzawi, F. (2000). Immunolocalisation of oestrogen receptor beta in human tissues. Journal of molecular endocrinology *24*, 145-155.

Teicher, B.A., Ara, G., Herbst, R., Palombella, V.J., and Adams, J. (1999). The proteasome inhibitor PS-341 in cancer therapy. ClinCancer Res *5*, 2638-2645.

Terrell, J., Shih, S., Dunn, R., and Hicke, L. (1998). A function for monoubiquitination in the internalization of a G protein-coupled receptor. Molecular cell *1*, 193-202.

Teyssier, C., Bianco, S., Lanvin, O., and Vanacker, J.M. (2008). The orphan receptor ERRalpha interferes with steroid signaling. Nucleic acids research *36*, 5350-5361.

Thrower, J.S., Hoffman, L., Rechsteiner, M., and Pickart, C.M. (2000). Recognition of the polyubiquitin proteolytic signal. The EMBO journal *19*, 94-102.

Tian, S., Poukka, H., Palvimo, J.J., and Janne, O.A. (2002). Small ubiquitin-related modifier-1 (SUMO-1) modification of the glucocorticoid receptor. The Biochemical journal *367*, 907-911.

Tiwari, V.K., Cope, L., McGarvey, K.M., Ohm, J.E., and Baylin, S.B. (2008). A novel 6C assay uncovers Polycomb-mediated higher order chromatin conformations. Genome research *18*, 1171-1179.

Tolhuis, B., Palstra, R.J., Splinter, E., Grosveld, F., and de Laat, W. (2002). Looping and interaction between hypersensitive sites in the active beta-globin locus. Molecular cell *10*, 1453-1465.

Towbin, H., Staehelin, T., and Gordon, J. (1979). Electrophoretic transfer of proteins from polyacrylamide gels to nitrocellulose sheets: procedure and some applications. Proceedings of the National Academy of Sciences of the United States of America *76*, 4350-4354.

Tsubuki, S., Saito, Y., Tomioka, M., Ito, H., and Kawashima, S. (1996). Differential inhibition of calpain and proteasome activities by peptidyl aldehydes of di-leucine and tri-leucine. Journal of biochemistry *119*, 572-576.

Vakoc, C.R., Letting, D.L., Gheldof, N., Sawado, T., Bender, M.A., Groudine, M., Weiss, M.J., Dekker, J., and Blobel, G.A. (2005). Proximity among distant regulatory elements at the beta-globin locus requires GATA-1 and FOG-1. Molecular cell *17*, 453-462.

Valley, C.C., Metivier, R., Solodin, N.M., Fowler, A.M., Mashek, M.T., Hill, L., and Alarid, E.T. (2005). Differential regulation of estrogen-inducible proteolysis and transcription by the estrogen receptor alpha N terminus. MolCell Biol *25*, 5417-5428.

Vassilev, L.T. (2007). MDM2 inhibitors for cancer therapy. Trends in molecular medicine *13*, 23-31.

Vogel, C.L., Cobleigh, M.A., Tripathy, D., Gutheil, J.C., Harris, L.N., Fehrenbacher, L., Slamon, D.J., Murphy, M., Novotny, W.F., Burchmore, M., Shak, S., Stewart, S.J., and Press, M. (2002). Efficacy and safety of trastuzumab as a single agent in first-line treatment of HER2-overexpressing metastatic breast cancer. J Clin Oncol *20*, 719-726.

Wakeling, A.E., Dukes, M., and Bowler, J. (1991). A potent specific pure antiestrogen with clinical potential. Cancer research *51*, 3867-3873.

Wallace, A.D., and Cidlowski, J.A. (2001). Proteasome-mediated glucocorticoid receptor degradation restricts transcriptional signaling by glucocorticoids. The Journal of biological chemistry *276*, 42714-42721.

Wang, C., Fu, M., Angeletti, R.H., Siconolfi-Baez, L., Reutens, A.T., Albanese, C., Lisanti, M.P., Katzenellenbogen, B.S., Kato, S., Hopp, T., Fuqua, S.A., Lopez, G.N., Kushner, P.J., and Pestell, R.G. (2001). Direct acetylation of the estrogen receptor alpha hinge region by p300 regulates transactivation and hormone sensitivity. The Journal of biological chemistry *276*, 18375-18383.

Wang, F., Hoivik, D., Pollenz, R., and Safe, S. (1998). Functional and physical interactions between the estrogen receptor Sp1 and nuclear aryl hydrocarbon receptor complexes. Nucleic acids research *26*, 3044-3052.

Wang, J.C., Derynck, M.K., Nonaka, D.F., Khodabakhsh, D.B., Haqq, C., and Yamamoto, K.R. (2004). Chromatin immunoprecipitation (ChIP) scanning identifies primary glucocorticoid receptor target genes. ProcNatlAcadSciUSA *101*, 15603-15608.

Wang, Q., Carroll, J.S., and Brown, M. (2005). Spatial and temporal recruitment of androgen receptor and its coactivators involves chromosomal looping and polymerase tracking. Molecular cell *19*, 631-642.

Wang, Z., Chen, W., Kono, E., Dang, T., and Garabedian, M.J. (2007). Modulation of glucocorticoid receptor phosphorylation and transcriptional activity by a C-terminal-associated protein phosphatase. Molecular endocrinology *21*, 625-634.

Wang, Z., Frederick, J., and Garabedian, M.J. (2002). Deciphering the phosphorylation "code" of the glucocorticoid receptor in vivo. The Journal of biological chemistry *277*, 26573-26580.

Watanabe, T., Inoue, S., Ogawa, S., Ishii, Y., Hiroi, H., Ikeda, K., Orimo, A., and Muramatsu, M. (1997). Agonistic effect of tamoxifen is dependent on cell type, ERE-promoter context, and estrogen receptor subtype: functional difference between estrogen receptors alpha and beta. Biochemical and biophysical research communications *236*, 140-145.

Webster, J.C., Jewell, C.M., Bodwell, J.E., Munck, A., Sar, M., and Cidlowski, J.A. (1997). Mouse glucocorticoid receptor phosphorylation status influences multiple functions of the receptor protein. The Journal of biological chemistry *272*, 9287-9293.

Weigel, M.T., and Dowsett, M. (2010). Current and emerging biomarkers in breast cancer: prognosis and prediction. Endocrine-related cancer.

Welboren, W.J., van Driel, M.A., Janssen-Megens, E.M., van Heeringen, S.J., Sweep, F.C., Span, P.N., and Stunnenberg, H.G. (2009). ChIP-Seq of ERalpha and RNA polymerase II defines genes differentially responding to ligands. The EMBO journal *28*, 1418-1428.

Wendt, K.S., Yoshida, K., Itoh, T., Bando, M., Koch, B., Schirghuber, E., Tsutsumi, S., Nagae, G., Ishihara, K., Mishiro, T., Yahata, K., Imamoto, F., Aburatani, H., Nakao, M., Imamoto, N., Maeshima, K., Shirahige, K., and Peters, J.M. (2008). Cohesin mediates transcriptional insulation by CCCTC-binding factor. Nature *451*, 796-801.

Wijayaratne, A.L., and McDonnell, D.P. (2001). The human estrogen receptor-alpha is a ubiquitinated protein whose stability is affected differentially by agonists, antagonists, and selective estrogen receptor modulators. JBiolChem *276*, 35684-35692.

Wijayaratne, A.L., Nagel, S.C., Paige, L.A., Christensen, D.J., Norris, J.D., Fowlkes, D.M., and McDonnell, D.P. (1999). Comparative analyses of mechanistic differences among antiestrogens. Endocrinology *140*, 5828-5840.

Wilkinson, C.R., Seeger, M., Hartmann-Petersen, R., Stone, M., Wallace, M., Semple, C., and Gordon, C. (2001). Proteins containing the UBA domain are able to bind to multi-ubiquitin chains. Nature cell biology *3*, 939-943.

Wong, D.J., Nuyten, D.S., Regev, A., Lin, M., Adler, A.S., Segal, E., van de Vijver, M.J., and Chang, H.Y. (2008). Revealing targeted therapy for human cancer by gene module maps. Cancer research *68*, 369-378.

Wu, W.K., Cho, C.H., Lee, C.W., Wu, K., Fan, D., Yu, J., and Sung, J.J. (2010). Proteasome inhibition: a new therapeutic strategy to cancer treatment. Cancer letters *293*, 15-22.

Xing, D., Nozell, S., Chen, Y.F., Hage, F., and Oparil, S. (2009). Estrogen and mechanisms of vascular protection. Arteriosclerosis, thrombosis, and vascular biology *29*, 289-295.

Yang, C.H., Gonzalez-Angulo, A.M., Reuben, J.M., Booser, D.J., Pusztai, L., Krishnamurthy, S., Esseltine, D., Stec, J., Broglio, K.R., Islam, R., Hortobagyi, G.N., and Cristofanilli, M. (2006). Bortezomib (VELCADE) in metastatic breast cancer: pharmacodynamics, biological effects, and prediction of clinical benefits. Ann Oncol *17*, 813-817.

Yang, Y., Kitagaki, J., Dai, R.M., Tsai, Y.C., Lorick, K.L., Ludwig, R.L., Pierre, S.A., Jensen, J.P., Davydov, I.V., Oberoi, P., Li, C.C., Kenten, J.H., Beutler, J.A., Vousden, K.H., and Weissman, A.M. (2007). Inhibitors of ubiquitin-activating enzyme (E1), a new class of potential cancer therapeutics. Cancer research *67*, 9472-9481.

Yao, T., and Cohen, R.E. (2002). A cryptic protease couples deubiquitination and degradation by the proteasome. Nature *419*, 403-407.

Yoshikawa, N., Nagasaki, M., Sano, M., Tokudome, S., Ueno, K., Shimizu, N., Imoto, S., Miyano, S., Suematsu, M., Fukuda, K., Morimoto, C., and Tanaka, H. (2009). Ligand-based gene expression profiling reveals novel roles of glucocorticoid receptor in cardiac metabolism. American journal of physiology *296*, E1363-1373.

Zhang, H., Sun, L., Liang, J., Yu, W., Zhang, Y., Wang, Y., Chen, Y., Li, R., Sun, X., and Shang, Y. (2006). The catalytic subunit of the proteasome is engaged in the entire process of estrogen receptor-regulated transcription. The EMBO journal *25*, 4223-4233.

Zhao, Z., Tavoosidana, G., Sjolinder, M., Gondor, A., Mariano, P., Wang, S., Kanduri, C., Lezcano, M., Sandhu, K.S., Singh, U., Pant, V., Tiwari, V., Kurukuti, S., and Ohlsson, R. (2006). Circular chromosome conformation capture (4C) uncovers extensive networks of epigenetically regulated intra- and interchromosomal interactions. Nature genetics *38*, 1341-1347.

Zheng, N., Wang, P., Jeffrey, P.D., and Pavletich, N.P. (2000). Structure of a c-Cbl-UbcH7 complex: RING domain function in ubiquitin-protein ligases. Cell *102*, 533-539.

# 8 Acknowledgements

My profound gratitude goes to Prof. Dr. Steven A. Johnsen for making this thesis work possible. I highly appreciate the trust you put in me as well as the foresight, guidance and general support you provided. It was always good to know that your door is open at all times and I could count on scientific advice whenever needed.

I thank my thesis committee members Prof. Dr. Holger Reichardt and Dr. Tobias Pukrop for the inspiring discussions and their support and help throughout the thesis work. In addition, I appreciate Prof. Dr. Holger Reichardt for being the thesis second reviewer.

Further, I would like to thank Prof. Dr. Mikael Simons for collaborating and giving me the opportunity to work in his laboratory. Many thanks go to Dr. Chieh Hsu who kindly helped me with the FRAP analyses and spent long nights in the lab for that.
For the practical performance and the initial analyses of the microarray data, I thank Dr. Gabriela Salinas-Riester, Susanne Luthin and Lennart Opitz. For the valuable statistical analyses I am very appreciative of Prof. Dr. Tim Beißbarth and Frank Kramer.
Thank also goes to Prof. Dr. Martin Scheffner at the University of Konstanz for providing laboratory space and helpful guidance in order to perform our ERα ubiquitination assays.

Thanks to all the current and former members of the Department of Molecular Oncology for a nice and helpful working atmosphere. In particular, I would like to thank Prof. Dr. Matthias Dobbelstein for giving me the opportunity to carry out my thesis work in his department and for scientific advices. Further, I am thankful to Antje Dickmanns and Cathrin Hippel for technical assistance and support in building up a new lab. Special thanks also go to my colleagues and friends Ulli Beyer, Isa Drewelus, Theresa Gorsler and Judith Pirngruber and all group members from the Johnsen group.

My heartfelt thanks go to my parents Waltraud and Siegfried as well as to my siblings Antje, Milan and Tino. Thanks for your everlasting love, support and trust. I am grateful to each of you.
I thank you, Torben, for all your help and advice, for bearing my crises of confidence and especially for never doubting.

# 9 Curriculum Vitae

For reasons of data protection the CV is not included in the online version.

Der Lebenslauf ist in der Online-Version aus Gründen des Datenschutzes nicht enthalten.